Organic-inorganic hybrid functional materials by nitroxide-mediated polymerization

Emmanuel Beyou, Elodie Bourgeat-Lami

Organic–inorganic hybrid functional materials by nitroxide-mediated polymerization

Emmanuel Beyou [1,*] and Elodie Bourgeat-Lami [2,*]

[1] Univ Lyon, Université Lyon 1, UMR CNRS 5223, Ingénierie des Matériaux Polymères, F-69622, Lyon, France

[2] Univ Lyon, Université Claude Bernard Lyon 1, CPE Lyon, CNRS UMR 5265, Chemistry, Catalysis, Polymers and Processes (C2P2), 43 Bvd. du 11 Novembre 1918, F-69616 Villeurbanne, France

* Correspondence: emmanuel.beyou@univ-lyon1.fr (E.B); elodie.bourgeat-lami@univ-lyon1.fr (E.B-L)

Abstract: Hybrid materials formed by the combination of inorganic components with organic polymers have emerged as a rapidly expanding and internationally competitive field of research in polymer science. These materials show great promise in many important applications where the control of the surface properties, as well as the structure and interfacial interactions between the two primary components, are determinant. In this paper, we present a review of literature on the synthesis of functional organic-inorganic hybrid materials through nitroxide-mediated polymerization (NMP), focusing on both their academic development and their potential industrial applications. After a brief overview of the main polymer grafting techniques and the benefits of using NMP, the surface modification of silica-based materials (oxidized silicon wafers or spherical silica particles), phyllosilicates, metallic substrates and metal oxide nanoparticles are discussed. NMP not only allows fine control over polymer chain length, composition and topology, but has also proven to be an efficient tool for surface and interface engineering. The corresponding nanostructured materials exhibit tailored properties in terms of dispersion, wettability, stimuli-responsive, gas barrier and viscoelastic behaviour for applications in the field of reinforced polymer-based materials, optical or biological sensors, microfluidics, membranes and supported catalysis.

Keywords: functional hybrid materials; polymer grafting; reversible-deactivation radical polymerization; nitroxide-mediated polymerization; practical applications

Abbreviations

AFM	atomic force microscopy
AIBN	azobis isobutyronitrile
APTES	3-acryloxypropyl triethoxysilane
APTMS	3-acryloxypropyl trimethoxysilane
ATRP	atom transfer radical Polymerization
BMA	butyl methacrylate
BPO	benzoyl peroxide
BSA	bovine serum albumin
$CHCl_3$	chloroform
ε-CL	epsilon caprolactone
CLRP	controlled/living radical polymerization
CPB	concentrated polymer brush
CpPOSS	octacyclopentyl POSS
D	distance between two anchored polymer chains
DMAEA	2-(dimethylamino)ethyl acrylate
DEPN	N-tert-butyl-N-[1-diethylphosphono-(2,2-dimethylpropyl)] nitroxide
DPPC	L-α-dipalmitoyl-phosphatidylcholine
f	molar fraction
h	film thickness
K	equilibrium constant
kc	combinaison constant
kd	dissociation constant
kp	propagation constant
HFIPA	1,1,1,3,3,3-hexafluoroisopropyl acrylate
KPS	potassium persulfate
LB	Langmuir-Blodgett
LCST	lower critical solution temperature
M	monomer
MAMA-DEPN	2-methyl-2-[N-tert-butyl-N-(1-diethoxyphosphoryl-2,dimethyl propyl) aminooxy]propionic acid
mM	milimol L^{-1}
M_n	molar mass
MAA	methacrylic acid
MMA	methyl methacrylate
MMT	montmorillonite
N	chain length
NIPAAm	N-isopropylacrylamide
NMP	nitroxide-mediated polymerization
NP	nanoparticle

OMS	ordered mesoporous silicas
OVE	7-octenylvinyl ether
P	poly (prefix)
P3VP	poly(3-vinylpyridine)
P4VP	poly(4-vinylpyridine)
P•	active specie/macroradical
PAA	poly(acrylic acid)
PBA	poly(*n*-butyl acrylate)
PE	polyethylene
PEG	poly(ethylene glycol)
PEO	poly(ethylene oxide)
PEOMA	poly(ethylene oxide) methyl ether methacrylate
PISA	polymerization-induced self-assembly
PL-QY	photoluminescence quantum yield
PMMA	poly(methyl methacrylate)
POSS	polyhedral oligomeric silsesquioxanes
PRE	persistent radical effect
PS	polystyrene
P(S-*co*-A)	statistical random copolymers of styrene and alizarin
PSMA	poly(styrene-*co*-maleic anhydride)
P(S-*co*-MMA)	statistical random copolymers of styrene and methyl methacrylate
PS-*b*-PPFS	block copolymer of styrene and pentafluorostyrene
PS-*b*-PVP	block copolymer of styrene and vinylpyridine
P*t*BA	poly(*tert*-butyl acrylate)
PVBIm-PF_6	poly[1-(4-vinylbenzyl)-3-butyl imidazolium hexafluoro phosphate]
PVP	polyvinylpyridine
P-X	dormant specie
RAFT	reversible addition-fragmentation chain transfer
RDRP	reversible deactivation radical polymerization
Rg	radius of gyration of an undisturbed chain
R6G	rhodamine G
R_1R_2NO•	persistant nitroxide radical
R_1R_2NO-P	(macro)alkoxyamine
ROP	ring opening metathesis
σ	chain grafting density
SEC	steric exclusion chromatography
SANS	small angle neutron scattering
SCS	sulfur-carbon-sulfur
SDPB	semidilute polymer brush
SIP	surface-initiated polymerization
SI-NMP	surface-initiated NMP
SPR	surface plasmon resonance

S	styrene
STEM	scanning transmission electronic microscopy
T-AuNPs	thiolate-stabilized gold nanoparticles
TEM	transmission electronic microscopy
TEMPO	2,2,6,6-tetramethyl-1-piperidinyloxy
TEMPOL	4-hydroxy-2,2,6,6-tetramethylpiperidine-N-oxyl
Tg	glass transition temperature
THF	tetrahydrofurane
TIPNO	N-tert-butyl-N-[1-phenyl- 2-(methyl propyl)] Nitroxide
UV	ultraviolet
VBA	4-vinylboronic acid
VBTMACl	vinylbenzyl trimethylammonium chloride
VOC	volatile organic compounds
4VP	4-vinyl pyridine
X	persistant specie

Table of Contents

1. Introduction

Owing to their remarkable properties, hybrid materials occupy an increasingly important place in our daily life and can find applications in various domains including construction, aerospace, automobile, biomedical or coating industries. According to Ashby and Bréchet [1], hybrid materials can be defined as resulting from the « combination of two or more components (usually organic and inorganic) in a predetermined geometry or scale, optimally serving a specific engineering purpose». The combination of materials with markedly different chemical and physical properties not only enables the properties of the raw components to be merged, but also confers new synergetic effects resulting from the creation of interfaces, most often leading to properties far superior to those of the individual elements [2]. Hybrid materials are usually classified according to the nature and the strength of the interaction between the organic and inorganic phases, and can be divided in two families [3]: class I corresponds to materials exhibiting weak interfacial interactions such as van der Waals, hydrogen bonding or electrostatic interactions, while class II corresponds to materials exhibiting covalent or iono-covalent bonds between the two phases.

A particular class of hybrid materials is that resulting from the combination of polymers and inorganic components. A large variety of different methods have been reported for the preparation of polymer/inorganic hybrid materials in solution, in bulk or in heterogeneous media using either preformed polymers or *in situ* polymerization techniques [4-6]. Among them, the coating of inorganic surfaces with polymers by physical adsorption is experimentally simple and quick, but the corresponding surface most often exhibits weak interactions with the bottom substrate which may lead to poor thermal or mechanical properties. In contrast, the formation of strong chemical bonds at the organic/inorganic interface allows the formation of firmly attached polymer layers. The grafting of polymer chains on inorganic surfaces is of major importance in many technical applications and has been reported as early as the 1960s as briefly reviewed by Kroker and Hamann [7]. Although surface-tethered polymer chains can be conceptually produced by a variety of techniques including anionic, cationic and ring-opening polymerizations [8], reversible deactivation radical polymerization (RDRP), formally known as controlled/living radical polymerization (CLRP) [9], has quicky become the preferred method. Indeed RDRP techniques have witnessed major progress over the past 30 years, providing polymer chemists with very efficients tools to tailor the structure and properties of polymeric materials and design a range of functional hybrid materials as described in several reviews [10-18]. Covalent modifications of inorganic materials with well-defined polymers not only allows the control of their surface properties and design robust non-reconstructing surfaces, but also improves the dispersion of inorganic particles in organic solvents and prevent their aggregation in polymeric matrices. Inorganic particles

surrounded by a hairy polymer shell also enable to access self-supported, one-component hybrids with unique self-assembly behavior, expanding the range of potential applications of the resulting nanostructured materials [12, 19, 20].

Among the various RDRP methods, nitroxide-mediated polymerization (NMP) has revealed to be a promising technique for accessing a wide range of polymer architectures and organic/inorganic hybrids due to its simplicity, absence of toxicity and robustness. In light of the abundant literature on the use of RDRP processes for the preparation of hybrid materials, and the ever-increasing breadth in the field, the aim of this review article is not to provide a complete overview of all available synthetic methods but rather to highlight the use of NMP for the preparation of organic-inorganic materials, focusing on their properties and applications. Indeed, to the best of our knowledge, and apart from a general review on NMP that comprises a section on this topic [21], there are only three review articles dedicated to the elaboration of organic/inorganic hybrids by this technique. The first one dates back to 2009 [22] and describes the formation of polymer brushes on both flat and nanoparticle surfaces. The review is organized according to the method used to immobilize the alkoxyamine initiator (unimolecular, bimolecular initiation or direct initiator synthesis, *vide infra*) and also includes a short section on the elaboration of structured polymer brushes and the design of advanced materials. Ghannam et al. [23] also wrote a mini-review a few years earlier dedicated to silica particles, focusing mainly on synthetic aspects. Lastly, more recently, Phan et al. completed a thorough review of synthetic strategies toward the elaboration of functional surfaces by NMP including both inorganic and organic substrates [24].

The present review is an update and extension of these previous reports focusing essentially on material properties and recent developments. After some general considerations on end-tethered polymer chains and RDRP mechanisms, the subsequent sections will review the use of NMP as a tool to introduce polymers onto flat and/or nanoparticle substrates, and elaborate functional materials. Recent advances in the synthesis of waterborne colloidal nanocomposites with controlled morphologies using NMP in aqueous dispersed media and the concept of polymerization-induced self-assembly (PISA), will also be briefly discussed.

2. Chemical Modification of Inorganic Surfaces with Polymers

The surface modification of inorganic materials (in the form of nanoparticles or planar surfaces) with a polymer layer is commonly used to modulate their properties, ensuring better performances in terms of dispersibility in organic media, protection against corrosion, lubrification or biocompatibility, with applications in the field of colloidal stabilization, tribology or microlithography [25-31]. As already mentioned, there are two main approaches to functionalize a surface by polymers : in either a non-covalent way by physisorption of the

polymer chains or in a covalent way by creating chemical bonds between the polymer chains and the surface of the substrate. The latter approach is usually prefered to avoid desorption phenomena and consequently a modification of the properties of the corresponding material. The past few decades have witnessed a growing interest for the grafting of polymer chains to inorganic surfaces and the production of functional polymer brush materials.

Three main strategies are reported for the covalent grafting of polymer chains onto a substrate [8, 10, 32, 33]: (i) the « grafting onto » method, where end-functionalized polymers react with appropriate surface sites, (ii) the « grafting from », where chains grow *in situ* from preformed surface-grafted initiators, and (iii) surface copolymerization through a covalently linked monomer (« grafting through ») (Figure 1) [34]. These methods are briefly presented below.

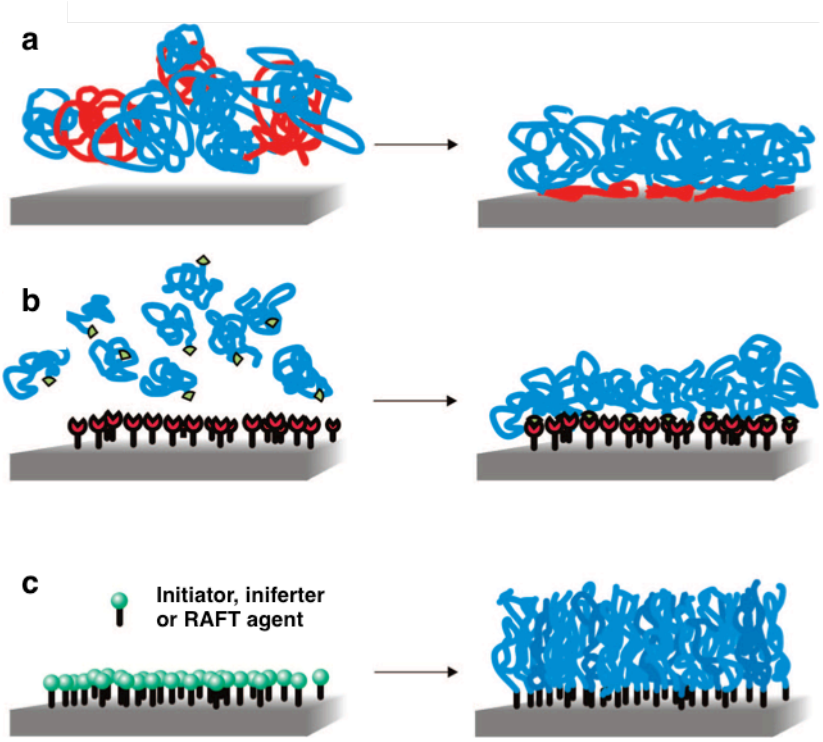

Figure 1. Schematic illustration of the three main techniques used to attach polymer chains on inorganic substrates. a) Grafting onto, b) grafting through and c) grafting from. [13], Copyright 2009. Reproduced with permission from the American Chemical Society.

2.1. Grafting onto

The « grafting onto » technique (Figure 1a) is based on the formation of a covalent bond between a end-functionalized polymer with a complementary reactive group located on the surface [35-38]. The amount of polymer that can be immobilized is highly dependent on the reaction conditions and in particular on the concentration of the polymer in solution and its molar mass [39]. Indeed,

polymer chain diffusion is a major limitation of this technique : polymer chain motion is constrained by entanglement with surrounding molecules and increasing chain length slows down polymer diffusion. Moreover, during the polymer grafting reaction, the free functional groups on the surface become less and less accessible and the polymer chains have to face an increasingly unfavourable concentration gradient so that it is difficult to achieve high grafting densities by this technique. The polymer grafting density is usually lower than 0.05 chain/nm^2 and may reach 0.3 chain/nm^2 under optimized experimental conditions [40].

2.2. Grafting through

The « grafting through » technique involves copolymerization of free monomers in solution with polymerizable groups covalently attached to the surface [41]. As illustrated in Figure 1b, the presence of a conventional initiator in solution means that the polymerization can take place both in the continuous phase and at the surface leading to the formation of free polymer chains and surface-attached polymer. As discussed by Henze et al. [41], although this grafting process is also limited by steric hindrance, it leads to a slow increase of the grafting density during polymerization contrary to the « grafting onto » technique, resulting in polymer grafting densities up to 0.06 chain/nm^2.

2.3. Grafting from

The « grafting from » technique (also called Surface-Initiated Polymerization, SIP, *vide infra*) has aroused great interest for the formation of polymer films on inorganic surfaces [11, 42-44] The process involves two steps. First, a suitable initiator is attached to the substrate and then polymer chains are grown directly from the tethered initiating groups. In this route, diffusion of the monomer molecules towards the surface according to the concentration gradient ensures the growth of the chains. The grafting density of the initiator may reach 1 to 5 molecule/nm^2 [45], allowing the formation of polymer films with a higher graft density and a higher thickness than the grafting onto or the grafting through techniques, which is a clear advantage of this process even if the initiation efficiency is often low, varying from typically 5 to 30%. Although grafting from is experimentally less straighforward than the two other techniques, it remains the most preferred method as it may lead to the formation of polymer brushes.

The term polymer brush refers to polymer chains that are attached by one end to a surface or an interface. In the absence of chain–surface interactions, the conformation of surface-tethered polymer chains (pancake, mushroom or brush-like) is predominantly determined by excluded volume interactions between adjacent chains that, in turn, depend on the distance, D, between the chains, and hence on the grafting density (i.e., on the number of chains per unit area) [46]. Depending on the ratio between D and the radius of gyration of an undisturbed chain (R_g), several cases can be distinguished: if $D > 2\ R_g$, the chains are isolated

and tend to spread out over the surface (mushroom regime). In contrast, when D is smaller than $2R_g$, the system moves into the brush regime leading to moderately to highly dense brushes depending on the chain density [47]. In the high-density regime, chain conformation is also affected by solvent quality. Steric repulsion between the chains forces the polymer chains to stretch away from the surface and adopt an extended conformation, the thickness of the polymer layer being dependent on both the molar mass of the polymer and the nature of the solvent (Figure 2).

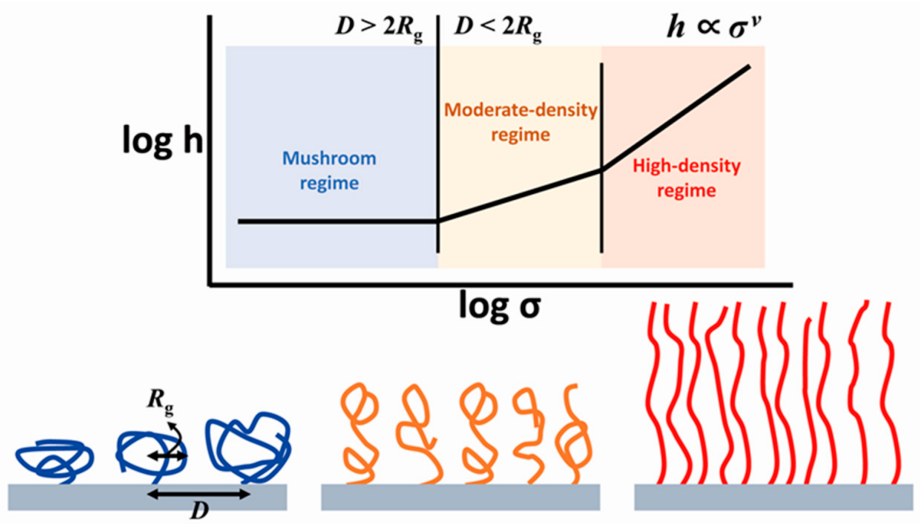

Figure 2. Schematic illustration of the three different types of conformations of surface-attached polymers in the case of planar substrates. For D > 2 R_g, the thickness of the film, h, correlates with the chain density, σ, through the scaling law: $h \propto \sigma^{\nu}$, with the exponent, ν, varying with the grafting density and the solvent quality [47].

It should be noted that the above classification into distinct and unique conformational regimes based on the grafting density only applies to flat surfaces. Indeed, in the case of curved interfaces (e.g. (nano)particles), the polymer chains, although also possibly stretched at the interface, adopt a different conformation as they extend away from the surface. The effective grafting density significantly decreases in this case as the radial distance from the spherical surface increases, and the polymer grafts consequently adopt a relaxed conformation [48]. This also holds true for nanostructured surfaces whose topographical features are comparable to the polymer chain dimensions. These conformational transitions in spherical polymer brushes are all the more relevant as the particle size decreases and have been shown to strongly influence the structure, formation, interaction, as well as dynamic properties of particle brush materials [49, 50].

Controlling the molecular weight and molecular weight distribution, architecture and density of the grafted polymer chains is therefore essential to the

properties and performance of the resulting materials, as these parameters dictate the conformation and uniformity of the polymer layer. This can be achieved by using living polymerization techniques such as anionic [45, 51-53], cationic [51, 53], ring opening metathesis (ROP) [54, 55] or RDRP. In this respect RDRP has appeared to be particularly well suited for the synthesis of a wide range of structurally advanced and well-defined macromolecular structures that were until now inaccessible by non living radical polymerization techniques. RDRP processes are now well-established in polymer chemistry and have been extensively reviewed [56-61]. A common feature of all RDRP systems is the establishement of a dynamic equilibrium between propagating radicals and dormant species as depicted in Figure 3.

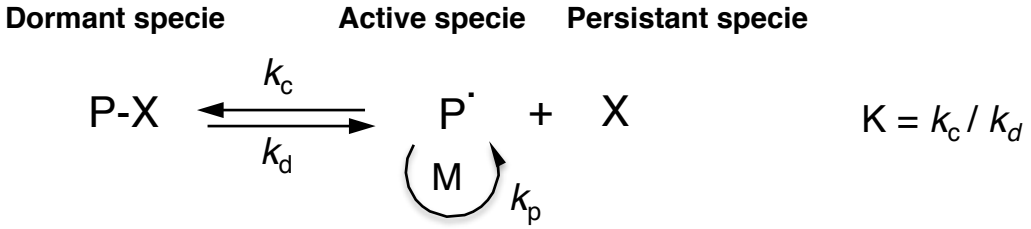

Figure 3. Dynamic equilibrium between dormant and active species, k_d = dissociation constant, k_c = combinaison constant and k_p = propagation constant.

Two main categories can be distinguished depending on the nature of the deactivation process [56, 57, 59]. The first category includes the well-known atom transfer radical polymerization (ATRP) and nitroxide-mediated polymerization (NMP) techniques, and operates based on the persistent radical effect (PRE, *vide infra*). In the second category, the activation-deactivation process involves a degenerative transfer between chain transfer agents and growing radicals. There are several radical polymerization processes that obey this last mechanism [62], the most famous of which being the Reversible Addition-Fragmentation chain Transfer (RAFT) technique. All three methods have attracted great attention for the synthesis of polymer/inorganic hybrid materials. In particular, RAFT [63-68] and ATRP [69-71] have been extensively explored. RDRP techniques not only allow fine control of the architecture of polymer-tethered particles but also enable to introduce specific groups providing the resulting products with potentially enhanced functionalities [72]. Polymers synthesized by RDRP are used in a wide range of applications like adhesives and coatings, drug delivery, memory devices, surface functionalization and composite manufactoring, as selected examples. To this regards and despite its inherent limitations, NMP has attracted increasing attention for its simplicity, absence of toxicity and robustness, and has revealed to be a method of choice for accessing a wide range of polymer architectures and organic/inorganic hybrids under industrially relevant conditions, especially in

dispersed media. In the following, the general concepts, the mechanisms and benefits of NMP are briefly introduced.

2.4. Nitroxide-Mediated Polymerization (NMP)

In 1986, Solomon and Rizzardo [73, 74] were the pioneers to use stable nitroxyl radicals that can act as reversible terminators for free radical species. These persistent radicals allow the reversible termination of the radical growing species via the formation of C-ON-linked alkoxyamine groups. The control of the polymerization is based on a thermo-reversible equilibrium between a dormant specie (the alkoxyamine) and an active specie (the alkyl radical) (Figure 4).

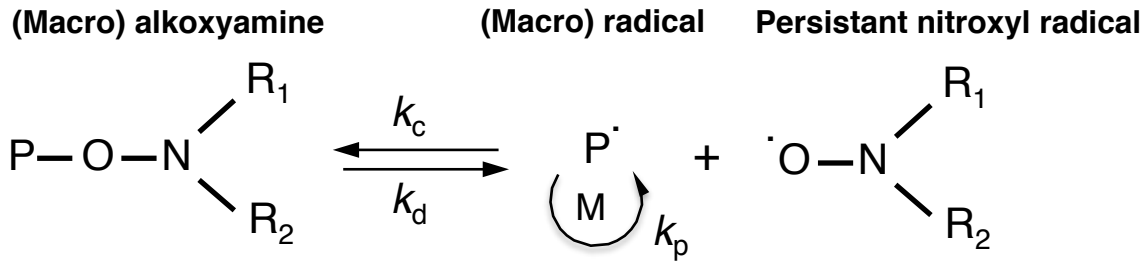

Figure 4. Mechanism of NMP.

The chemical nature of the alkoxyamine moiety strongly influences the polymerization kinetics and the range of polymerizable monomers. The stability of the C-ON bond depends on the nature of the substituents on both the nitroxyl and carbon radicals. For example, alkoxyamines based on 2,2,6,6-tetramethyl-1-piperidinyloxy (TEMPO) behave more as inhibitors than as control agents due to the high thermal stability of the corresponding alkoxyamine bond, and the corresponding reactions are therefore limited to styrenic derivatives and bulk processes [75]. In addition, high temperatures are required to achieve reasonable conversions. Therefore, new alkoxyamines have been developed from the well-known N-tert-butyl-N-[1-diethyl phosphono- (2,2-dimethylpropyl)] nitroxide (DEPN) and N-tert-butyl-N-[1-phenyl- 2-(methyl propyl)] nitroxide (TIPNO) (Figure 5) [76-78].

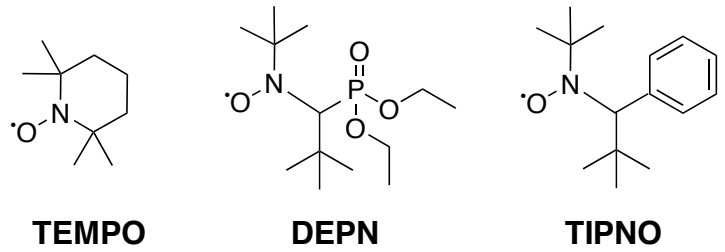

Figure 5. Main nitroxyl radicals used in NMP.

The corresponding alkoxyamines have been shown to effectively control the polymerization of styrenic monomers, acrylic esters, acrylates, acrylonitrile, acrylic acid, vinylpyridine, dimethylacrylamide and dienes in bulk or in solution [21, 79-84]. However, controlling the free radical polymerization of methacrylic esters such as methyl methacrylate (MMA) or its derivatives by NMP has long represented a challenge in the field, due to side reactions and/or slow recombination of the polymeric radicals with most common nitroxides [85]. In the early 2000's, drastic improvements were nevertheless made by Charleux et al. [86-88] who demonstrated that the addition of a small amount of a comonomer with a low activation-deactivation equilibrium constant $<K> = K_d/K_c$, such as styrene, strongly improved the DEPN-mediated polymerization of MMA. The method was later successfully extended to 4-vinyl pyridine (4VP) [89] and various styrenic compounds [90-92]. The role of these *controlling* comonomers is to reduce the activation-deactivation rate constant, leading to a diminution of the concentration of propagating radicals, and hence to a better control. More recently, new nitroxides that could mediate the polymerization of MMA [93, 94] and of both styrene and methacrylates [95-97] have been developed, extending the range of monomers that can be homo- or copolymerized by NMP, making this technique a method of choice for accessing a wide range of polymer architectures under industrially relevant conditions.

This review article focuses on the use of NMP to engineer the surface, interfacial and bulk properties of polymer-functionalized hybrid materials. After a brief description of the methods used to attach alkoxyamine initiators onto inorganic surfaces and the need for sacrificial initiators, the different approaches undertaken to finely control the structure and properties of the resulting hybrid materials will be presented and critically analyzed. As will be shown in the review, the combination of NMP with inorganic components allows access to a range of functional materials with unique topologies, microstructures and physicochemical behaviours depending on the intrinsic characteristics and properties of both the polymer chains and the inorganic substrate. The article will also briefly discuss recent advances in the design of colloidal nanocomposites using NMP in heterogeneous dispersed media.

3. NMP synthesis of organic/inorganic hybrid materials

3.1. Surface-Initiated NMP (SI-NMP): general considerations

The synthesis of polymer brush materials with precisely controlled structures and compositions has been the focus of intense research. Among the different grafting processes, surface-initiated NMP (SI-NMP) has received great attention. SI-NMP involves the growth of polymer chains directly from the inorganic surface and requires covalent attachement of the controlling agent : i.e., the alkoxyamine initiator in the present case. Three main strategies have been reported [22]. In a

first method, called bimolecular NMP, a conventional initiator (AIBN, BPO) is previously attached to the surface, and used to generate *in situ,* in the presence of a nitroxide and a monomer, an alkoxyamine polymer (dormant polymer) (Figure 6a). The second method is based on a two steps procedure. First, the inorganic surface is chemically modified by an alkoxyamine carrying a functional group that allows its attachment to the surface. Radical polymerization is then initiated from the tethered alkoxyamine in the presence of a monomer (Figure 6b). In a last method, the alkoxyamine is formed *in situ* by reacting a conventional initiator (like for instance AIBN) with double bonds previously attached to the inorganic surface in the presence of a nitroxyl radical, followed by polymer chain growth as in route b (Figure 6c).

As mentioned above, NMP relies on the persistent radical effect (PRE). PRE occurs when two radicals are generated at a similar rate and one is more persistent than the other [98]. In the early stages of polymerization, the transient propagating radicals can either be reversibly trapped by the deactivating agent (i.e, the persistent nitroxyl radical) or undergo an irreversible termination reaction. However, the persistent radicals do not self-terminate and can only react by cross-coupling with the propagating radicals. The result is an accumulation of excess deactivating agent in the reaction medium with increasing time, leading to a shift of the activation-deactivation equilibrium toward the dormant side, and thus a significant reduction in both the propagation and termination rates. However, in SI-NMP the amount of attached initiator is most often too low for the PRE to effectively operate. Furthermore, diffusion of the persistent radical away from the surface may also be unfavorable as reversible capping would be less efficient in this case, leading to a diminution of the concentration of deactivator. Therefore, to obtain an accurate control of the polymerization occuring at the inorganic surface, it is necessary to add a sacrificial alkoxyamine-based initiator in the polymerization medium to ensure a sufficiently high concentration of nitroxyl radicals with respect to the monomer concentration and garantee a controlled reaction. Consequently, polymer chains are growing both on the inorganic surface and in the bulk. The free polymer chains can be however removed from the polymer grafted brushes by washing with a good solvent, and used to estimate the molar mass and the dispersity of the tethered polymer chains. Indeed, it was shown by Husemann [99] and many others that the free polymer chains produced in solution by the sacrificial initiator have similar characteristics as the ones attached to the surface. Although this has been more rarely reported in the literature, an alternative approach to the use of sacrifical initiator is the direct addition of free controller (i.e., the stable nitroxyl radical) [100]. This strategy not only allows a fairly good control of the length of the tethered polymer chains, but also has the tremendous advantage of avoiding the formation of free polymer chains giving acccess to one-component, matrix-free particle brush composite materials.

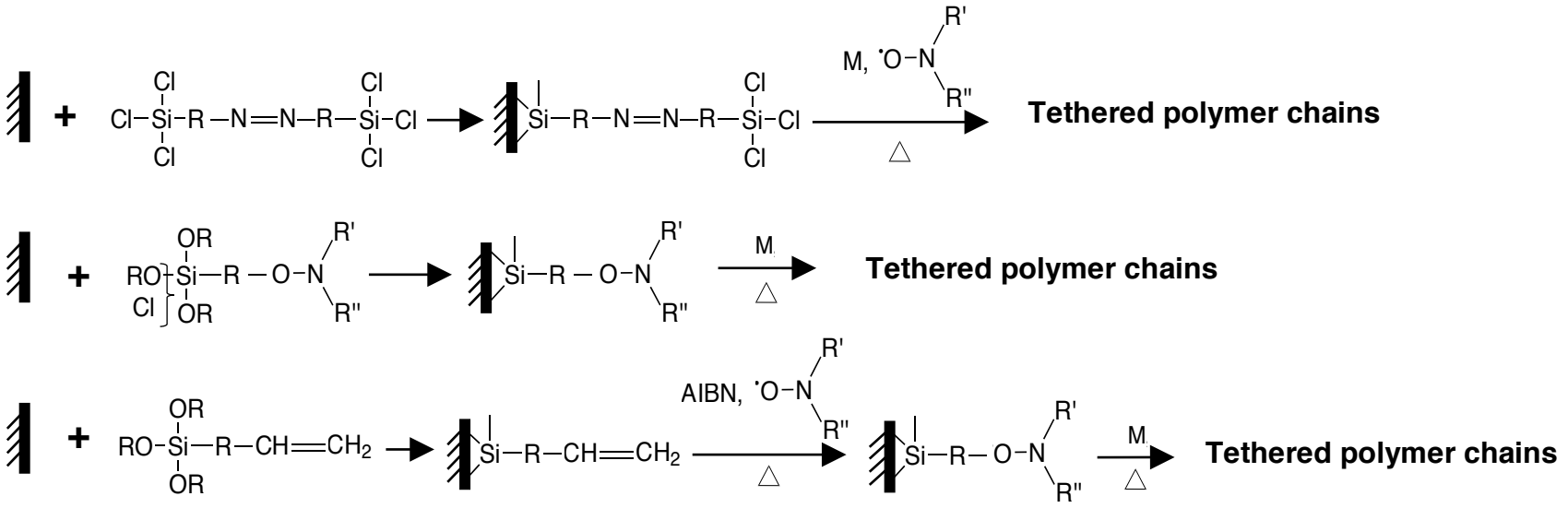

Figure 6. Scheme illustrating the growth of polymer chains from inorganic surfaces by SI-NMP using a) a bimolecular or b) a unimolecular initiating system. In scheme c), the alkoxyamine is formed *in situ* by spin trapping radicals produced at the particle surface with a nitroxide.

SI-NMP has been applied to grow polymer brushes from a wide variety of different substrates of various topologies such as planar surfaces (silicon wafers, glass, mica), nanoparticles or mesoporous structures, and produce diverse functional organic/inorganic materials. The next sections present an overview of the research in this area, with emphasis being placed on the control of the physicochemical properties of the resulting polymer brush materials.

3.2. Surface modification of flat silicon oxide surfaces

Mastering the physicochemical properties of chemically-modified inorganic surfaces is of fundamental importance for diverse applications [101-104]. Grafting of polymers onto planar surfaces using NMP allows precise control of properties such as hydrophilicity and roughness which can be accomplished by varying the nature and/or composition of the (co)polymers, the grafting density, the chain length and the thickness of the grafted layer. In addition, the formation of tethered polymer brushes also offers the possibility to form cohesive surfaces preventing dewetting or depression from the substrate, create complex 2D structures using micro/nanoscale patterning techniques and elaborate bioactive surfaces.

3.2.1. Control of the surface energy and wetting properties of functionalized silicon wafers

The grafting of polymeric chains to inorganic surfaces has revealed to be an efficient tool to engineer the properties of material interfaces and a great deal of research effort has been thus dedicated to modifying the surface behavior of a variety of substrates by the incorporation of well-defined (co)polymers. Hawker et al. were the first ones to report the use of NMP and the grafting onto method to control the wetting behavior of silicon wafers [105]. Hydroxyl end-functionalized statistical random copolymers of styrene (S) and methyl methacrylate (MMA) (P(S-*co*-MMA)) with a styrene molar fraction, f, varying from 0 to 1 and molar masses close to 10 000 g mol^{-1}, were firstly synthesized (Figure 7a), and subsequently grafted onto a silicon wafer by heating at 140 °C to ensure the reaction of the terminal OH groups with the silanols located on the native oxide surface. Random copolymer brushes about 5 nanometers thick were obtained with a grafting density of 0.3 chain/nm^2. PS and PMMA homopolymers were then spin-coated on the functionalized surface, and their wetting behavior assessed by contact angle measurements. As shown in Figure 7b, the lower the degree of chemical mistmach between the homopolymers and the grafted random copolymers, the lower was the interfacial energy (as determined from contact angle measurements), and the greater was consequently the polymer chains wetting ability.

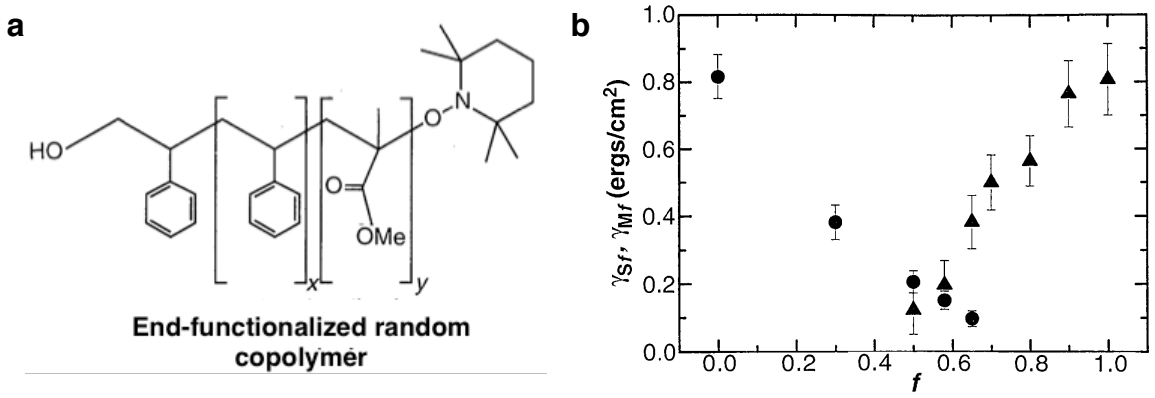

Figure 7. a) Structure of the end-functionalized P(S-*co*-MMA) random copolymers used to modify the surface of silicon wafers by the grafting onto technique and control the wetting behaviour of polymers spin-coated on that surface. b) Interfacial tensions between the PS (circles) or the PMMA (triangles) homopolymers and the random copolymer brush as a function of the styrene molar fraction, f [105], Copyright 1997. Reproduced with permission from AAAS.

As said above, aside from this early work, the most common method for the synthesis of polymeric brushes onto flat silicon oxide surfaces is based on the use of the grafting from technique [99, 106-120].

One of the first reports along this line was published by Husseman et al. [99] who grafted styrene homopolymer and copolymer chains from oxidized silicon wafers using a TEMPO-based alkoxyamine carrying a trichlorosilyl end group. The authors reported a linear increase of the film thickness with both the molar mass and the conversion indicating the effective controlled character of the radical polymerization occuring at the inorganic surface. Besides, the authors showed that polymer chains with molar masses higher than 20 000 g mol^{-1} were quite stretched at the surface with a cross-sectional area per chain of, in average, 200 $Å^2$ (i.e., corresponding to around 0.8 chains/nm^2). Similar linear increase of brush thichness with molar mass were reported by Devaux et al. [106, 112] and others [107, 108, 110, 113-119]. In the former case, the polymer brushes were prepared by NMP of styrene initiated by trialkoxysilyl-terminated alkoxyamines previously deposited on the wafer surface using the Langmuir-Blodgett (LB) technique to enable the formation of very dense brushes. The chain length was varied by adjusting the amount of sacrificial initiator in the bulk while the grafting density was controlled by the surface pressure during LB deposition, allowing the conformation of the polymer brushes to be finely tuned from the collapsed to the highly stretched state (Figure 8).

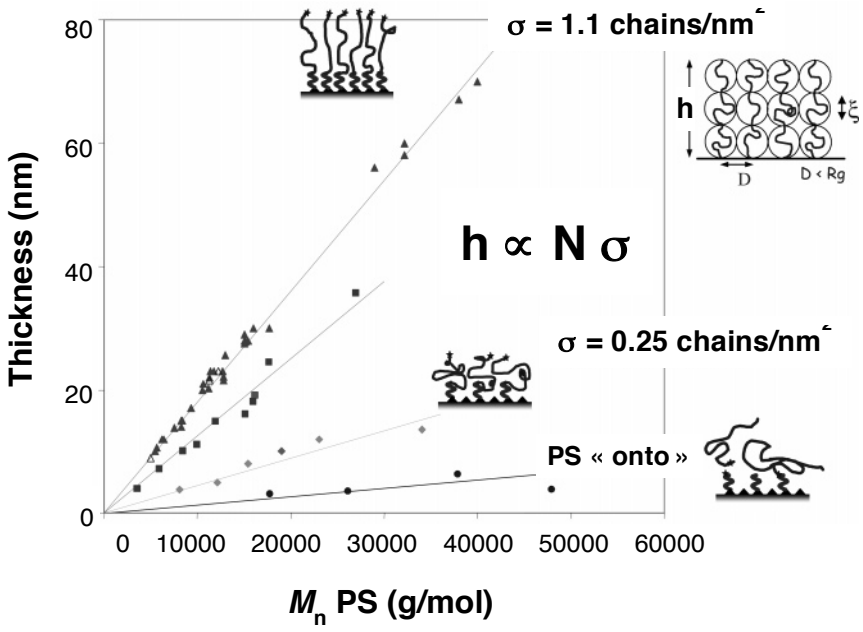

Figure 8. Brush thickness measured by ellipsometry in air as a function of the molar mass, M_n (or chain length N), of PS chains grafted from a native silicon oxide surface for different polymer chains grafting densities. An example of grafting onto is also given for comparison [112], Copyright 2005. Reproduced with permission from the American Chemical Society.

The highly dense brushes with extended conformation were shown to exhibit a very low swelling capacity in good solvents, as attested by neutron reflectivity measurements. This unsual swelling behavior was attributed to polymer-polymer chain interactions and was shown to significantly deviate from predicted scaling laws of neutral polymer brushes [112]. In a subsequent paper, the same group determined that the degree of stretching was also dependent on the chemical nature of the alkoxyamine (i.e, on its behaviour at the air/water interface during LB deposition) (Figure 9). Indeed the less amphiphilic compounds (structures 1 and 2 in Figure 9a) led to the lowest grafting densities and hence to the lowest stretching values and film thicknesses (Figure 9b) [116].

In addition to film thickness, SI-NMP also allows controlling the surface roughness and topology which may have strong implication on film properties such as wetting or adhesion. As a rule of thumb, the surface roughness decreases with increasing the grafting density and/or the polymerization time (i.e. with increasing film thickness). For instance, Zhou et al. [119] reported the grafting of PS-*b*-PVP block copolymers by Si-NMP and showed that the roughness decreased from 1.73 to 0.34 nm with time (i.e., upon increasing the length of the second block), providing at the end of the reaction a relatively smooth film consistent with the relatively high grafting density As expected, the surface wettability was influenced by the roughness and increased with increasing the evenness of the coating as indicated by the decrease of the contact angle, θ, from 89 to 78°.

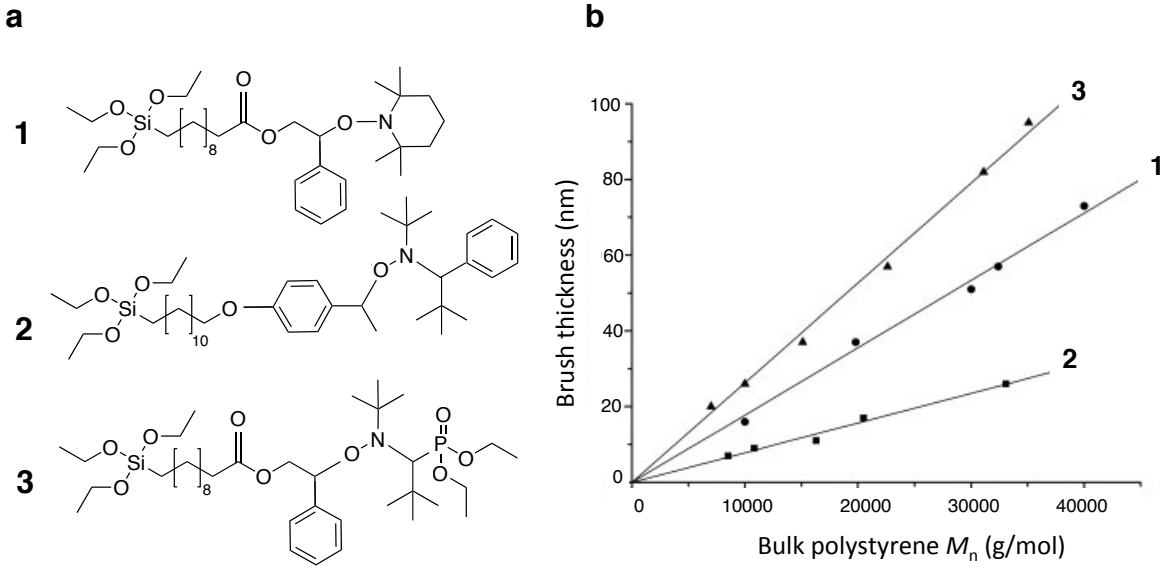

Figure 9. a) Chemical formula of the triethoxysilane-terminated alkoxyamines and b) thickness of PS brushes grafted from alkoxyamines 1–3 deposited onto oxidized silicon wafers by the LB technique versus M_n of the corresponding bulk polystyrenes [116], Copyright 2008. Adapted with permission from Wiley Periodicals, Inc.

In a similar vein, Lewis and Cohen [115] reported the grafting of polystyrene chains from the surface of silicon wafers previously activated using an atmospheric pressure plasma in order to form highly dense and uniform films. The generated surface radicals were spin trapped with TEMPO resulting, after styrene polymerization, in polymer films with very low surface roughness (Figure 10). The root-mean-square (rms) roughness, R_{rms}, decreased with increasing the amount of TEMPO indicating that a minimum concentration of counter radicals was required to achieve a good control and form homogeneous brushes. The resulting polymer-grafted surfaces were compared to films obtained by plasma-induced conventional radical polymerization. While the surface roughness (i.e., around 0.36 nm for 28.5 nm thick brushes) and the feature height distribution of the controlled polymer films were similar to that of the native silicon substrate indicating the formation of a smooth polymer layer, the films synthesized by conventional polymerization exhibited a significantly higher, temperature-dependent, surface roughness with an asymmetric height distribution (see Figure 10b). Distribution enlargement was attributed to the grafting of un-controlled polymer chains formed by thermal polymerization in solution, resulting in a broader range of polymer chain lengths.

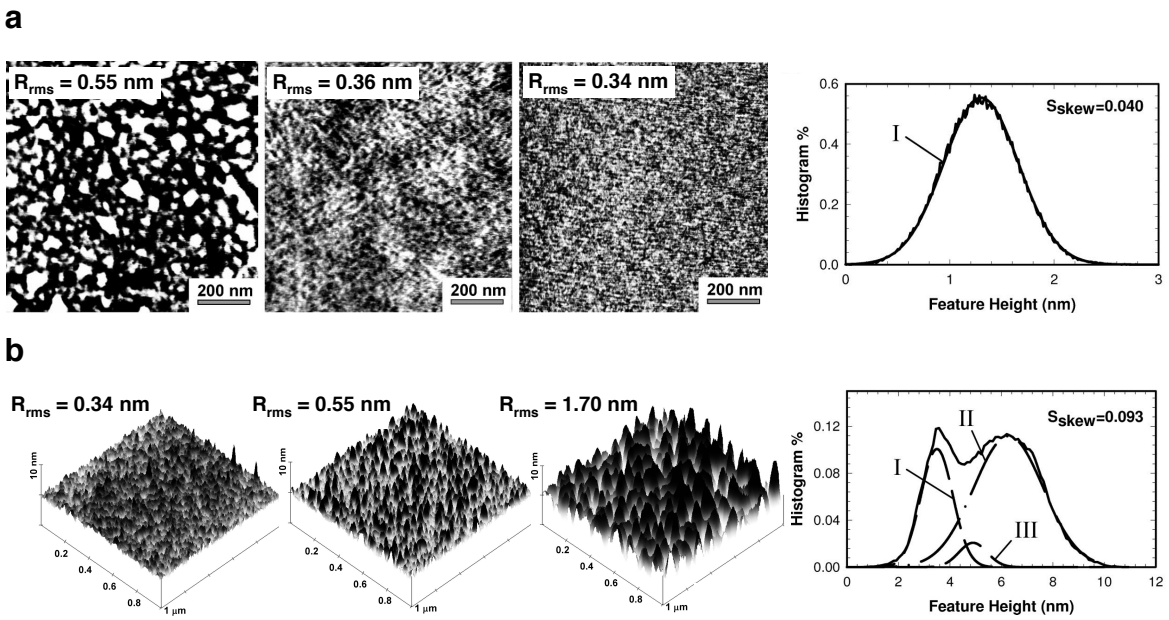

Figure 10. a) Tapping mode AFM images of PS-grafted silicon wafers obtained by NMP of styrene under plasma activation at 120 °C for 60 h in the presence of TEMPO (from left to right : [TEMPO] = 5, 10 and 15 mM) and b) AFM surface images of PS-grafted silicon by conventional radical polymerization (from left to right : T = 70, 85 and 100 °C). The right side images show the corresponding polymer feature height histograms with fitted Gaussian distributions [115], Copyright 2008. Adapted with permission from the American Chemical Society.

The production of robust, defect-free polymer films is of high importance in many technological applications and is particularly problematic in thin films [121]. Compared to physisorbed polymer films, polymer brushes based on covalently attached polymer chains are generally considered more stable. Instability of adsorbed polymer films often manifests itself when the polymer layer can undergo swelling or has enough mobility to phase separate from the substrate leading to film desorption and/or dewetting. Parvole et al. [114] reported the grafting of soft poly(*n*-butyl acrylate) (PBA) brushes from silicon wafers by SI-NMP, and showed that the formation of a thick layer (30 nm) of long and crowded surface-tethered polymer chains (M_n = 86 000 g mol^{-1}) stabilized the film towards dewetting. Moreover, the formation of dense and highly stretched copolymer brushes also enables to better control the extreme film surface properties and stabilize the film toward surface reconstruction when exposed to different environments. Indeed, the outermost block completely covers the surface regardless of its surface energy which is of particular interest for designing marine antifouling coatings as shown by Andruzzi et al. [109]. In this work, a series of styrene-based block copolymers bearing semifluorinated alkyl side groups of different chain lengths $(PS)_p$-*b*-$(PF_n)_m$ (n = 6 or 8) were grown from the surface of silicon wafers (Figure 11a), and further exposed to water for 1 week. It was found that the polymer brushes with the longer length of the fluorocarbon side chain substituent formed a prefered

orientation at the polymer film/air interface and were more stable toward surface reconstruction than those with shorter fluorinated side groups (Figure 11b). This behaviour was only observed for thicknesses higher than 40 nm and was attributed to the formation of densely packed CF_3 groups on the extreme surface.

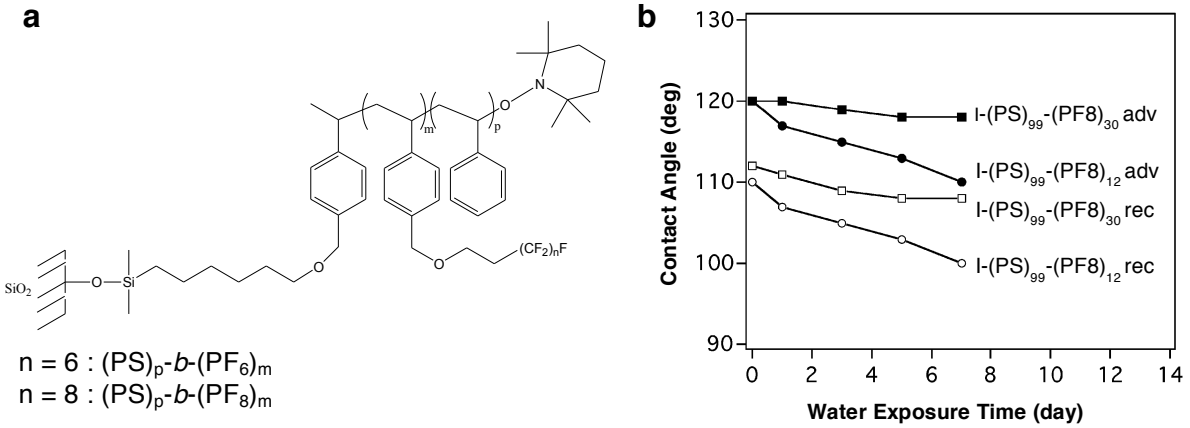

Figure 11. a) Chemical formulae of the fluorinated copolymer-grafted silicon oxide wafer and b) advancing (filled symbols) and receding (open symbols) water contact angles of $(PS)_{99}$-*b*-$(PF_8)_{12}$ and $(PS)_{99}$-*b*-$(PF_8)_{30}$ brushes as a function of immersion time [109], Copyright 2004. Adapted with permission from the American Chemical Society.

Si-NMP has also been used to prepare stimuli-responsive brushes. Indeed, the design of polymer layers that can undergo reversible change in conformation and structure upon exposure to external stimuli, such as changes in pH, temperature, solvent or chemical environment, can bring added-value to hybrid materials and have attracted particular attention. For example, poly(ionic liquid) brushes with tunable wettability were successfully grafted from silicon wafers [117] and copper oxide (CuO) sheets [120] by NMP using a multistep procedure. In the case of CuO sheets, the surface was modified by poly[1-(4-vinylbenzyl)-3-butyl imidazolium hexafluoro phosphate] (PVBIm-PF_6) using a bimolecular NMP process involving surface immobilized peroxide groups, the ionic liquid monomer (VBIm-PF_6) and TEMPO as mediator (Figure 12a). Subsequent sequential exchange of the hydrophobic PF_6^- with the hydrophilic Cl^- counter anion induced reversible switching between hydrophobic and hydrophilic surface properties as attested by contact angle measurements (Figure 12b).

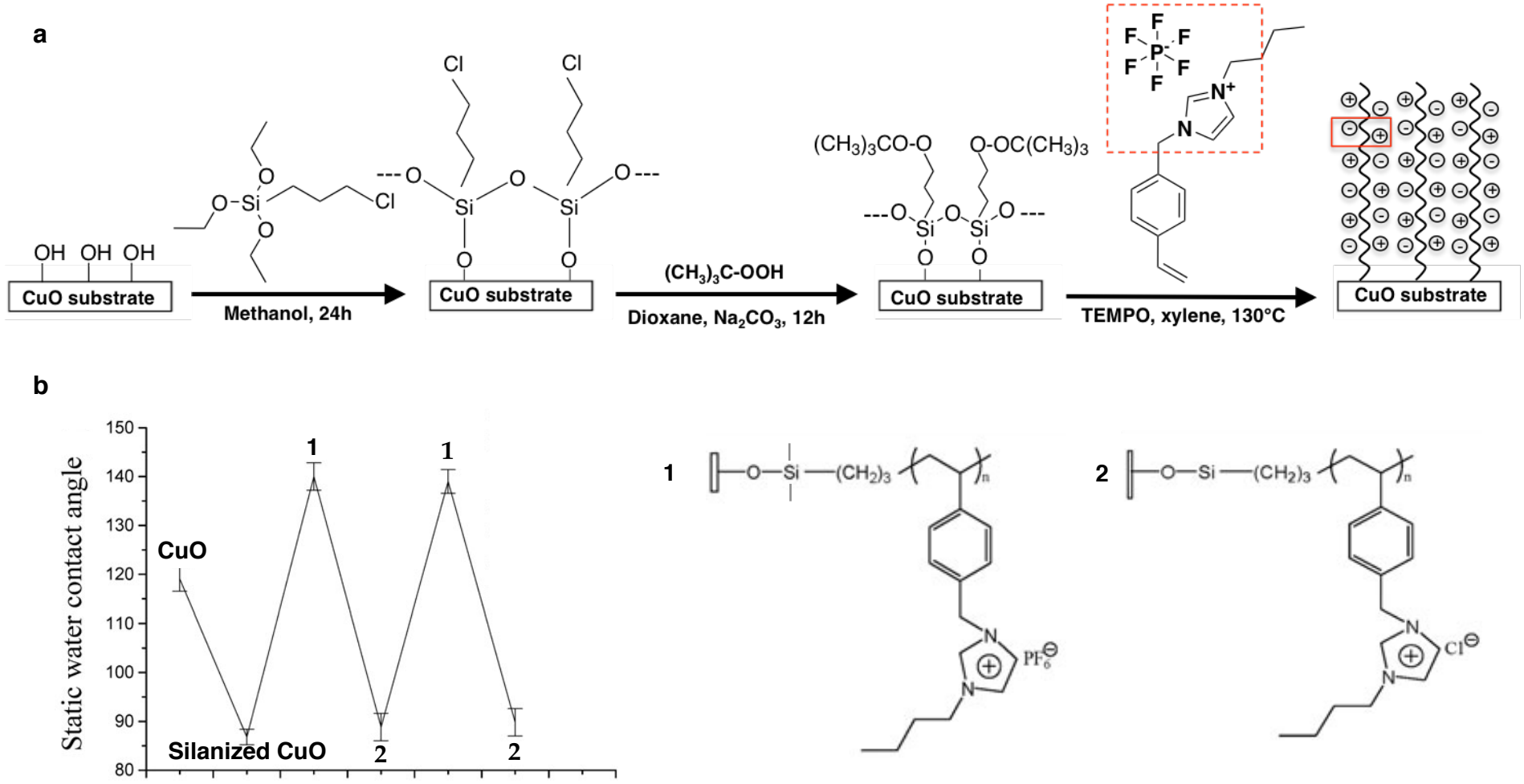

Figure 12. a) Synthetic procedure for modifying CuO with a poly(ionic liquid). b) Changes of static water contact angles corresponding to various surfaces of copper sheets [120], Copyright 2012. Adapted with permission from Wiley Periodicals, Inc.

In another example, Li et al. [113] reported an innovative surface-initiated vapor deposition method to control the polymerization of *N*-isopropylacrylamide (NIPAAm) which is not efficient via the NMP method in bulk. Poly(NIPAAm) exhibits a lower critical solution temperature (LCST) of about 32 °C in aqueous solution, and the thickness of the corresponding thermal responsive coating decreased from 200 nm to around 50 nm with increasing the temperature from 22 to 50 °C.

Another strategy to control the morphology and properties of surface-tethered polymer chains is to randomly graft different kinds of homopolymers on a surface [107, 108, 110, 111, 118]. Such binary brushes have been extensively investigated both theoretically and experimentally and have been shown to behave differently from block copolymer brushes. Exposure of the mixed brush to a specific solvent triggers a selective swelling of one of the components of the brush and at the same time a collapse of the other polymer chains, leading to a phase separation and the formation of nanoscale surface patterns. In a typical strategy, a mixture of two different orthogonally active initiators (in for instance ATRP and NMP) is grafted on the inorganic surface, and used to induce chain growth as reported by Zhao et al. [107]. However, this strategy does not allow precise control over the ratio and distribution of the two polymer brushes. Therefore, the same group later described the synthesis of bifunctional initiators containing an alkyl bromide for ATRP and an alkoxyamine for NMP, leading to Y-shaped PMMA/PS mixed brushes (Figure 13) [108, 110, 122].

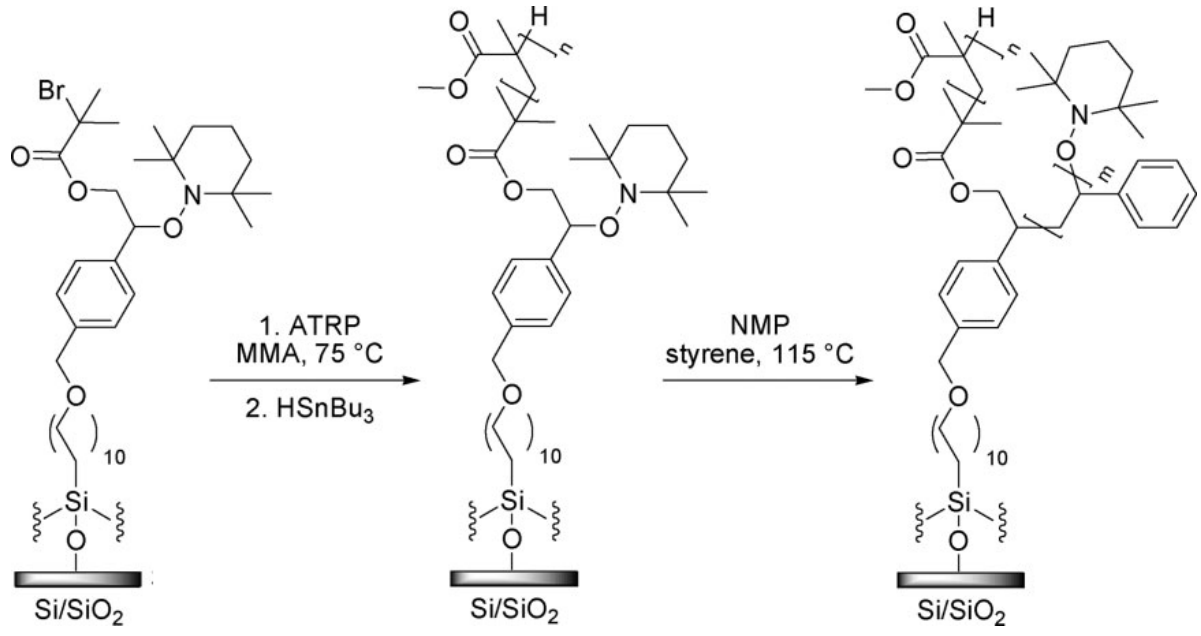

Figure 13. Synthetic strategy used to graft mixed Y-shaped PMMA/PS brushes from a self-assembled monolayer of asymmetric bifunctional initiator [110], Copyright 2004. Adapted with permission from the American Chemical Society.

These binary brushes showed solvent-induced nanophase separation with the formation of a rough surface composed of ordered nanoscale domains of PMMA after treatment with glacial acetic acid, and a smooth surface morphology with extended conformation when the sample was treated with cyclohexane, a selective solvent for PS. In the later case, the wetting behavior of the mixed brush was dominated by the presence of the PS chains that assumed a more extended conformation than PMMA, leading to a PS-enriched outermost surface while the PMMA chains were burried inside the brush to minimize the total free energy. This process was shown to be reversible.

More recently, Thiessen et al. [118] employed a similar dual initiator strategy to grow mixed binary PS/poly(4-vinylpyrine) (P4VP) polymer brushes on silicon wafers by successive ATRP of styrene and NMP of 4VP. The resulting brushes were shown to exhibit a reversibly switching hydrophobic/hydrophilic wetting behaviour upon alternatingly dipping the susbtrate in toluene and aqueous hydrochloric acid.

Finally, some years ago a one-step orthogonal approach was devised by Wang et al. [123] for the synthesis of mixed brushes via the simultaneous combination of SI-NMP and surface-initiated living cationic ring-opening polymerization of 2-phenyl-2- oxazoline, following an earlier report from Weimer et al. [124]. The resulting brushes were again shown to exhibit a switchable behavior as a function of the solvent exposed. For more details on the synthesis and properties of mixed polymer brushes, the reader is directed to a recent review by Li et al. [125] which provides a good overview on the topic.

3.2.2. Combining lithographic techniques and NMP for the design of well-defined patterned SiO_2 surfaces for microfluidic and biosensing applications

Lithographic techniques and microcontact printing allow for the selective chemical modification of inorganic substrates with various hydrophilic and hydrophobic polymers and molecular recognition sites in micro or nanoscale patterns, and have been extensively explored to create functional surfaces [104, 126]. Not only can ATRP or RAFT be used for this purpose, but NMP has also been reported to be an efficient method for the preparation of patterned polymer brushes. For example, Husemann et al. [127] described the top-down patterning of poly(*tert*-butyl acrylate) (P*t*BA) brushes using a combination of NMP and photolithography (Figure 14). The polymer brushes were spin-coated with a photoresist layer containing an acid generator leading to well-defined hydrophobic (P*t*BA) and hydrophilic poly(acrylic acid) (PAA) domains after exposure to radiation through a mask (Figure 14a). As expected, the film thickness decreased from 130 to 80 nm after deprotection of the *t*BA groups due to shrinkage of the formed PAA brushes. Moreover, after exposing the PAA to a solution of trimethylamine, the corresponding carboxylated domains became hydrophilic and

were essentially wetted by water, which can be of potential interest to microfluidic devices for controlling and directing fluid flow (Figure 14c). A similar photoresist procedure was used by Xu et al. [128] to fabricate micropatterned polymer brushes of different chemical natures on silicon wafers by the successive use of NMP and ATRP methods.

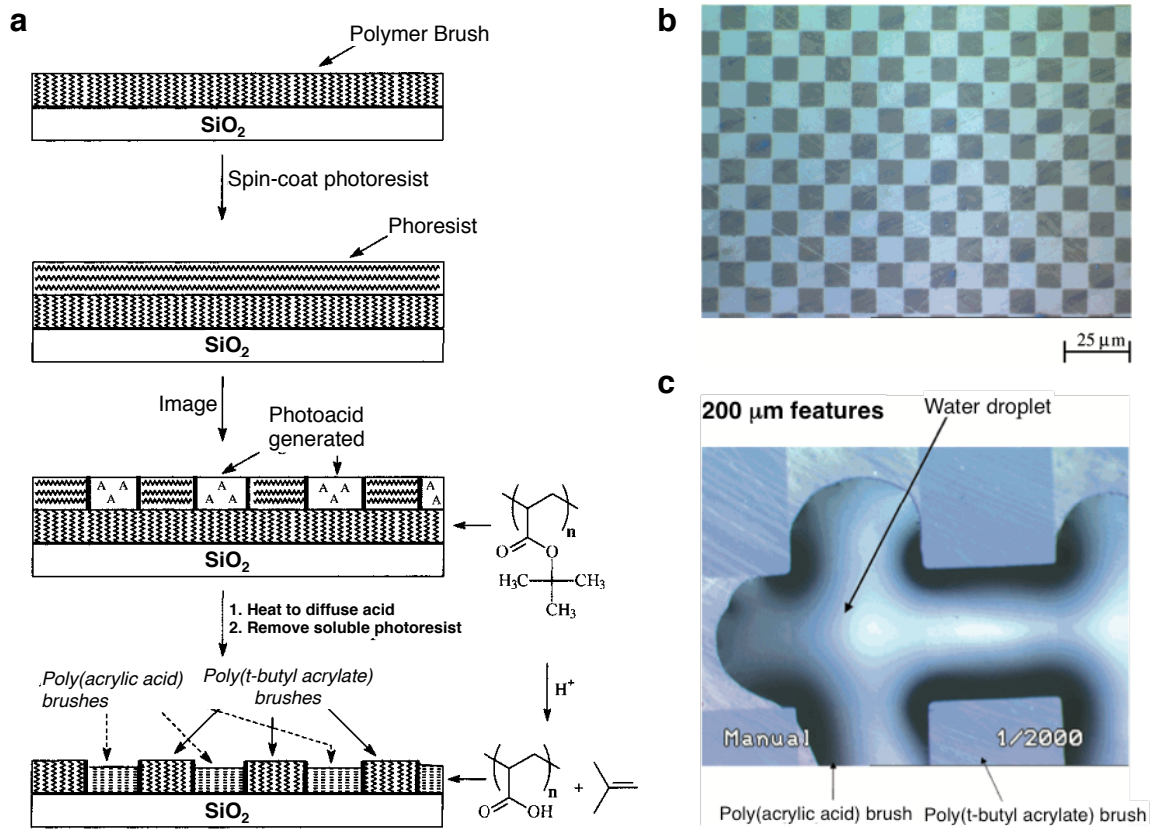

Figure 14. a) Strategy for patterning of a polymer brush using a sacrificial photoresist layer and lithography imaging. b) Optical micrograph of 10 µm features in a continuous polymer brush showing regions of P*t*BA (blue dark) and poly(acrylic acid) (PAA) (blue light) polymers and c) interaction of a water droplet with 200 µm features showing an unusual wetting profile and preferential interaction with the PAA brush domains [127], Copyright 2000. Adapted with permission from the American Chemical Society.

Later, a bottom-up approach that combined lithography and Langmuir-Blodgett (LB) deposition (so-called LB-lithography) was reported by Brinks et al. [129]. In this work, a mixture of L-α-dipalmitoyl-phosphatidylcholine (DPPC) and a triethoxysilyl-terminated alkoxyamine initiator was deposited on an oxidized wafer surface by the LB technique and subsequently used to initiate SI-NMP of styrene or BA. Substrate-induced DPPC condensation promoted microphase separation of the DPPC and the alkoxyamine initiator upon LB

transfer, leading after polymerization to the formation of regular stripe patterns of PS or PBA brushes with submicrometer scale lateral dimensions. The width and the height of the stripes were controlled by the experimental conditions and in particular by the initiator concentration in the mixed monolayer.

In addition, several authors were interested in the elaboration of biosensors by combining photolithography or microcontact printing and NMP [130-135]. Indeed metal impurities are undesirable for biological applications and NMP is particularly well-suited in this case as it does not require the use of any metal catalyst contrary to ATRP. Taking advantage of the ability of oligo(ethylene glycol) surfaces to resist protein and cell fouling, Andruzzi et al. [130] reported the coating of silicon oxide wafers by biocompatible homopolymers and copolymers based on styrenic monomers containing oligo (ethylene glycol) moieties. Due to their high surface coverage and high molar masses, the PS_y-*b*-P(STY-PEG_n)$_x$ grafted copolymers were shown to be highly resistant to protein adsorption. After a photolithographic treatment, patterned surfaces with feature sizes varying between 10 and 90 nm initially incubated with a dinitrophenyl derivatized bovine serum albumin (BSA) and then exposed to anti-dinitrophenyl IgE antibodies sensitized RBL cells, showed specific cell localization on the BSA regions.

Following a related approach, Mardyukov et al. [133] selectively immobilized streptavidin on a functionalized PS-based brush containing a biotin-conjugated nitroxide as an acyl radical trapping reagent. A styrene derivative bearing a photoreactive α-hydroxyalkyl–ketone group was first polymerized from an alkoxamine-functionalized silicon wafer and then photochemically postmodified with a TEMPO-derived nitroxide bearing biotin in presence of a photomask to ensure the formation of a patterned SiO_2 surface. Fluorescence microscopy revealed that the resulting functionalized patterned wafer was efficient for selective protein immobilization on the biotin-functionalized silicon oxide surface.

In another approach, Hirtz and co-workers reported the formation of structured PS, PNIPAAm and PBA brushes by mechanical nanoscratching with AFM lithography [131]. In brief, the method consists of using the mechanical properties of the atomic force microscope's tip in order to create lithographic patterns through nano indentation. The structures obtained after AFM scratching were highly stable allowing a second writing over the existing scratched lines (perpendicular to the first scratched directions) resulting in pilllar structures. In a first paper, the authors used this technique to pattern PS brushes and demonstrated that the brushes exhibited selective dye adsorption to the polymer covered regions or to the scratched areas depending on dye polarity [131]. The technique was further exploited to generate protein biochips [132]. Highly dense and thick (40 nm) protein repellent PS and PBA brushes were first grafted on the surface. Subsequent AFM lithography on the grafted brushes allowed for nanoscale site-selective protein adsorption on the hydrophilic scratched-out areas of the wafer substrate.

A similar brush thickness-dependent site-specific protein adsorption on patterned glass-supported PS brushes was also reported by Roling et al. [134] using microcontact thiol-ene click chemistry. The glass surface was coated with a monolayer of alkene groups and brought into contact with an elastomeric stamp impregnated with a thiol-terminated alkoxyamine forming a patterned layer of covalently bound initiator after exposure to UV light and click reaction. The brush thickness was controlled by the addition of free alkoxyamine and only the thicker brushes (40 nm or larger) showed protein repellence while brushes below 15 nm thickness revealed protein adhesive properties. Functional groups were further introduced in the brush layer and used to immobilize silica nanoparticles and liposomes by host-guest chemistry.

More recently, Buhl et al. [135] reported the synthesis of polymer brushes and their post-polymerization modification through again microcontact printing onto glass and silicon wafer substrates (Figure 15). Successive Si-NMP of 1,1,1,3,3,3-hexafluoroisopropyl acrylate (HFIPA) and 7-octenylvinyl ether (OVE) led to the formation of alternating polymer brushes allowing the successful side-by-side orthogonal immobilization of mannose-NH_2 and biotin-SH as bioactive ligands for the recognition of proteins. Indeed, the alkene functionality of OVE was post-modified with biotin-SH through a photoinitiated thiol-ene reaction while the fluorinated ester groups of HFIPA were converted into amide groups in presence of mannose-NH_2. Finally, the surface was incubated with solutions of fluorescein isothiocyanate-modified Concanavalin A and rhodamine B-functionalized streptavidin. Fluorescence microscopy analysis highlighted the specific binding of the respective proteins to their ligands biotin and mannose.

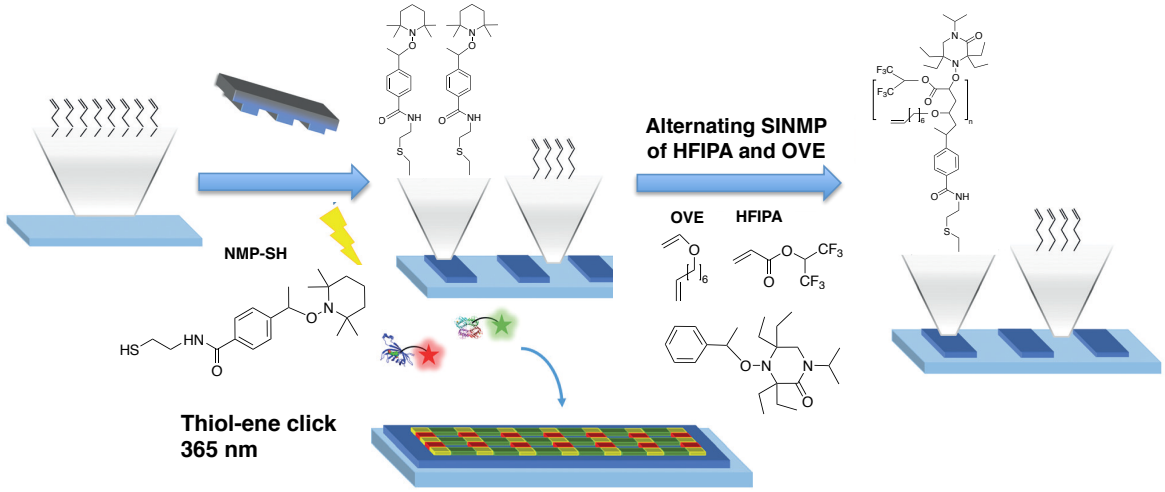

Figure 15. Synthetic scheme for the preparation of biochips by using microcontact printing combined with NMP [135], Copyright 2017. Adapted with permission from John Wiley & Sons Inc.

3.3. Silica-based hybrid materials

Silica nanoparticles can be easily synthesized with a broad range of sizes using various methods and are arguably the most investigated of all inorganic compounds [136, 137]. Among the various silica particles used for the elaboration of organic-inorganic materials, fumed and colloidal silicas are the most frequently reported. Regardless of their chemical origin or their method of production, silica particles are very often functionalized with organic polymers to improve their colloidal stabilization in apolar solution, control their dispersion into polymeric matrices or synthesize so-called one-component, matrix-free composites. Silica/polymer hybrid materials can also be obtained by the sol-gel technique via the synthesis of functional copolymers incorporating hydrolytically-reactive alkoxysilyl moieties. Examples of these different approaches are reviewed below.

3.3.1. Hairy silica particles with tailored structures and properties

Nanoparticles surrounded by a layer of end-grafted polymer chains in good solvents are often refered to as 'hairy' particles. In the literature, hairy silica particles have been mostly synthesized using the grafting from technique in order to obtain high polymer grafting densities, as previously mentioned. Both bimolecular [138-141] and unimolecular [142-148] initiating systems have been reported. In the case of bimolecular initiation [141], the initiator grafting density was shown to be close to 0.9 molecule per nm^2 while the polymer grafting density varied from 0.1 to 0.2 chain per nm^2 depending on the molar mass of the polymer, which corresponds to an initiation efficiency of less than 30%. Monomolecular initiating systems on the other hand, usually involve alkoxyamine initiators carrying trichlorosilyl or triethoxysilyl end groups or formed *in situ* through atom transfer radical addition in which surface tethered carbon radicals are trapped by a stable nitroxyl radical [145-149]. Although these last two strategies do not allow to increase the NMP-initiator grafting density in comparison to bimolecular initiation, the corresponding polymer chain growth is generally improved with an initiation efficiency close to 45% [142, 147]. Indeed, in bimolecular initiating systems, two radical fragments are formed initially, one of which is attached to the inorganic substrate while the other is free to diffuse in the reaction medium leading to an increase of the concentration of un-bound radicals in the initial phase of the polymerization, which may favor termination reactions.

Among the many interesting developments of polymer-tethered silica particles, the formation of stable dispersions in organic solutions has aroused particular attention. Indeed, the grafting of densely grafted and long enough polymer chains have been shown to significantly improve colloidal stability. For instance, Bartholome et al. [145] demonstrated that the grafting of PS chains from the surface of fumed silica enabled to disperse the initial aggregates in toluene (a good solvent for polystyrene) and decrease their size to about 200 nm.

On the other hand, Chevigny and coll. [100, 150] examined the structure of PS-grafted colloidal silica particles suspended in dimethyl acetamide (DMAc) with small angle neutron scattering (SANS) using neutron contrast matching, and showed that the grafted polymer chains formed a regular corona around each silica particle. Physical parameters such as the number of chains per particle, the molar mass and the radius of gyration of the grafted polymer could be extracted from the scattering data by fitting the curves to a core-shell model, and were shown to be in good agreement with those deduced from chemical analysis. The polymer chains displayed an extended conformation at the silica surface, the brush thickness exceeding the length of the polymer chains in agreement with the results predicted from particle brush scaling laws. Such accurate characterization and control of the brush structure is essential for a better understanding of the miscibility and behavior of inorganic particles dispersed in a host polymer matrix as will be discussed in further details below (see section 3.3.3).

In addition, several authors have investigated the synthesis of core-shell nanohybrid materials with tailored surface properties by reactivating the polymer grafted chain ends by a second monomer in order to obtain block copolymer tethered particles. For example, Laruelle et al. [143] reported the controlled growth of PBA-*b*-PS block copolymer brushes from colloidal silica by SI-NMP with 80% reinitiation efficiency, in agreement with the work of Bartholome et al. [145] on the grafting from of styrene. The resulting hybrid particles exhibited a core-shell morphology with a soft PBA core and a hard PS shell.

Moreover, Wang et al. [151, 152] immobilized brush-like poly(styrene-*co*-maleic anhydride) (PSMA) copolymers onto fumed silica using the grafting onto technique and TEMPO as mediator. PSMA-coated silica particles with 53 wt% copolymer content were successfully obtained by this method. Anhydride groups were introduced in the copolymer shell to further react with alcohols, amines or polycondensates and improve silica dispersion in various polymeric matrices.

More recently, PS-*b*-polypentafluorostyrene (PS-*b*-PPFS) block copolymers were attached to the surface of fumed silica particles using the grafting through technique in presence of a well-defined PS-DEPN macroinitiator (Figure 16a) [153]. TEM and AFM analyses revealed that the silica particles were surrounded by a polymer layer (Figure 16b), with the roughness varying from 32.5 to 55.8 nm with increasing the amount of grafted polymer from 5 to 32 wt%, leading to nanohybrids with tunable hydrophobic surface properties. The hydrophobicity of the PS-*b*-PPFS grafted silica particles was controlled by both the surface roughness and the low surface energy provided by the fluorinated groups located at the extreme particle surface, resulting in a significant increase of the water contact angle (WCA) from 27.8° for the APTMS-grafted silica to 132° for the polymer functionalized particles (Figure 16c).

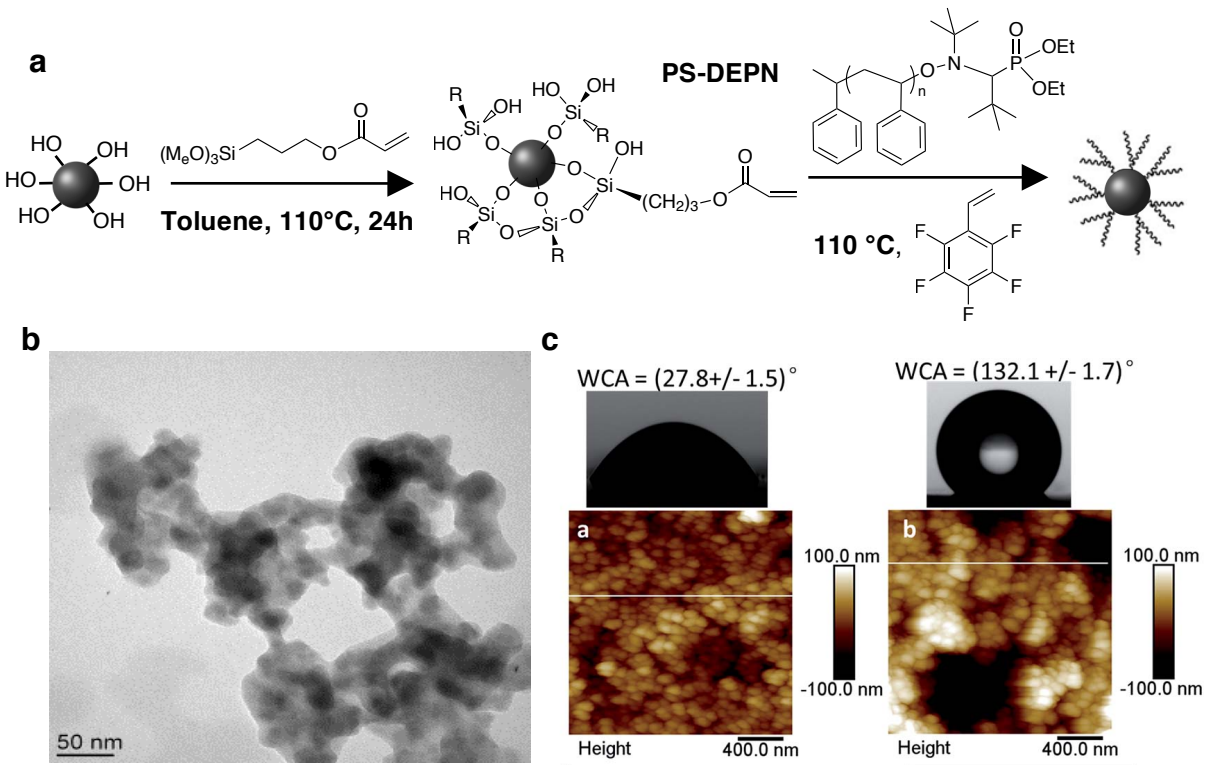

Figure 16. a) Synthetic scheme for the grafting of PPFS through the surface of APTMS-functionalized fumed silica using PS-DEPN as macroalkoxyamine initiator, b) TEM image of PS-*b*-PPFS grafted silica nanoparticles cast from a tetrahydrofuran (THF) suspension (grafted polymer content = 32 wt%), and c) AFM topographic images and wettability properties of deposited layers of APTMS-grafted silica (left) and PS-*b*-PPFS grafted silica (right) [153], Copyright 2016. Adapted with permission from the Royal Society of Chemistry.

Moreover, in a series of papers, the group of Zhao and co-workers reported the combined use of NMP and ATRP [154-160] or NMP and ring opening polymerization (ROP) [161] to graft polymer chains of different chemical natures onto colloidal silicas using asymmetric difunctional initiators, and induce microphase separation between the dissimilar polymer chains at the particle surface, as described above for planar surfaces (see section 3.1) (Figure 17a). Phase separation was shown to be dependent on the structural parameters of the Y-shaped brushes such as the chain length disparity between the two grafted polymers [156, 157], the overall grafting density [158], or the molar mass (for otherwise a fixed grafting density), and was also strongly influenced by the size and hence the curvature of the inorganic particles [159]. Figure 17b illustrates the morphology obtained in the case of mixed P*t*BA/PS brushes of similar grafting densities, σ, but increasing molar masses of each of the two polymers, grafted from 167 nm diameter silica particles. The brush samples were cast from chloroform ($CHCl_3$) dispersions (a non-selective good solvent of both polymers) and imaged by TEM after selective staining of the PS domains with RuO_4 vapor. As seen in the

Figure, the binary brushes formed rippled nanostructures composed of dark PS and bright P*t*BA nanostripes. The morphology evolved from isolated, nearly spherical PS nanodomains to bicontinuous worm-like nanostructures upon increasing the molar mass of the polymer chains (Figure 17b) [160]. The surface curvature also played an important role and truncated wedge-shaped nanodomains were observed when decreasing the silica particle size to 67 nm as revealed using conventional TEM [159] and further confirmed by electron tomography and 3D-reconstruction images [162].

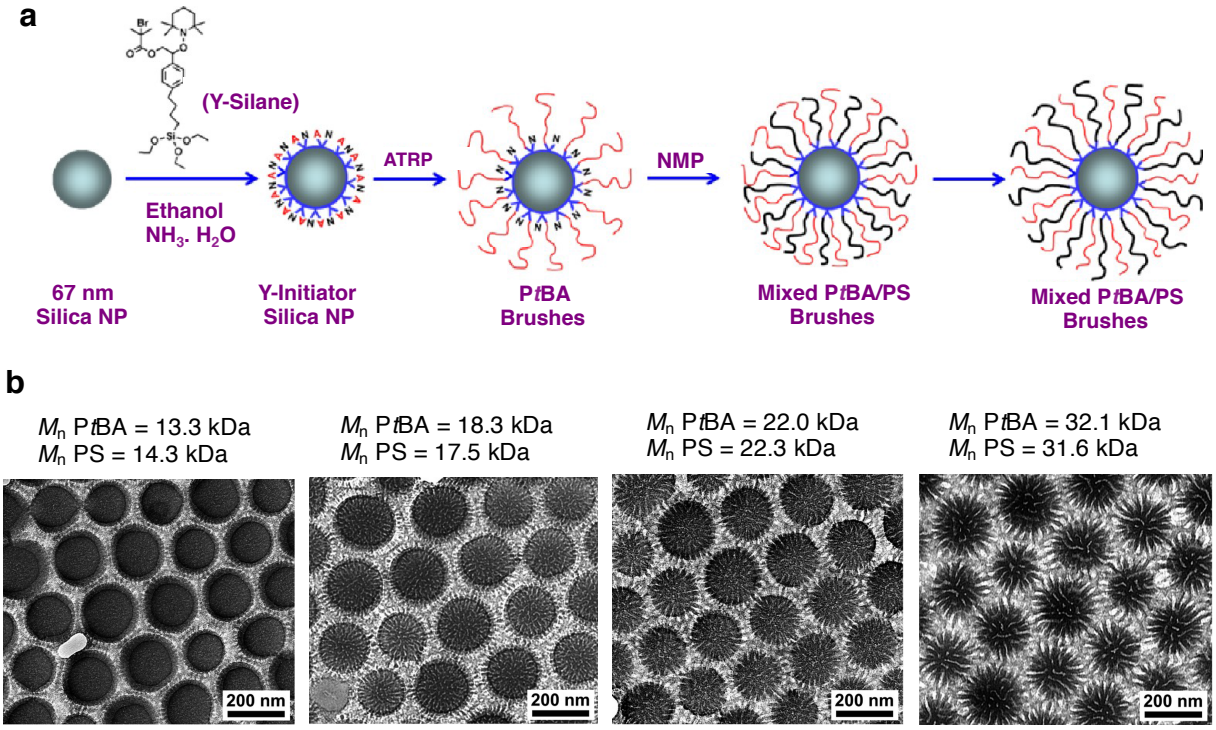

Figure 17. a) Scheme illustrating the synthesis of mixed P*t*BA/PS brushes grafted from colloidal silica particles by sequential ATRP and NMP and their lateral phase separation [159], Copyright 2012. Reproduced with permission from the American Chemical Society. Panel b) shows the evolution of particle morphology with increasing the molar mass of the PS and P*t*BA chains in the binary brush (σ ~ 0.4 chains/nm^2 and D_n Silica = 167 nm) [160], Copyright 2014. Adapted with permission from the American Chemical Society.

The approach was next extended to mixed PAA/PS brushes obtained by removal of the tertbutyl group of P*t*BA using iodotrimethylsilane. The resulting particle brushes were cast from either DMF (a non-selective solvent) or water (a selective solvent for PAA) leading to different morphologies [163]. While in DMF, the mixed PAA/PS brushes formed laterally separated microdomains, in water the PAA chains were found to completely cover the PS core domain resulting in core-shell particles as confirmed by cryo-electron tomography [164].

At last, more recently, mixed P*t*BA/PS brush-grafted silica nanoparticles were introduced in selective homolymer matrices of either the P*t*BA or PS brushes, and their morphology investigated using both TEM and electron tomogaphy [165]. The morphology of the mixed brushes was shown to strongly depend on the respective chain length of the brush and the matrix in agreement with theoretical predictions. When the molecular weight of the homopolymer matrix was much lower than that of the compatible brushes, the matrix polymer swelled the compatible grafted chains, and the immiscible grafted chains collapsed into isolated microdomains in an entropic driven process. On the other hand, the morphology of the mixed brushes was almost unperturbed in the dry-brush regime when the molar masses of the matrix chains was much larger than that of the brush.

3.3.2. Hollow polymer spheres from tethered brush silica particles

Polymeric nanocapsules have attracted increasing attention in the recent years for the encapsulation of active substances with potential applications in medecine, cosmetics, catalysis or coatings [166]. Among the many different approaches for producing hollow spheres, the use of inorganic particles as sacrificial template is the most commonly reported [167]. In this strategy, the hollow structure is obtained by selective etching of the inorganic phase from core-shell particles. Blomberg et al. [168] used this method to prepare shell cross-linked polymeric capsules. Micrometric silica beads were first modified by grafting on their surface a chlorosilane alkoxyamine initiator, and used to control the growth of copolymer chains carrying maleic anhydride functional groups for further cross-linking reactions. A diamine crosslinker was added in a subsequent step to allow interchain coupling via the formation of a bisimide. The inorganic silica template was finally removed by chemical etching (Figure 18). In an alternative strategy (not shown), styrene monomer was copolymerized with 4-vinyl benzocyclobutene, and the resulting core/shell nanocomposite particles were heated at 200 °C for thermal cross-linking affording nanocapsules with greater dimensional stability than the ones obtained by chemical cross-linking.

Another noteworthy example of porous morphology was provided by Ladmiral et al. [169]. Monodisperse zinc sulfide (ZnS) particles were first coated with a thin silica layer, and used to graft high-density PS brushes from their surface by Si-NMP. Selective dissolution of the ZnS core afforded hollow SiO_2@polymer hybrid particles. In addition, the ZnS@SiO_2-PS composite particles were shown to be highly dispersable in various organic solvents and also led to the formation of two-dimensional periodic colloidal arrays after deposition on a solid support, producing structural colors.

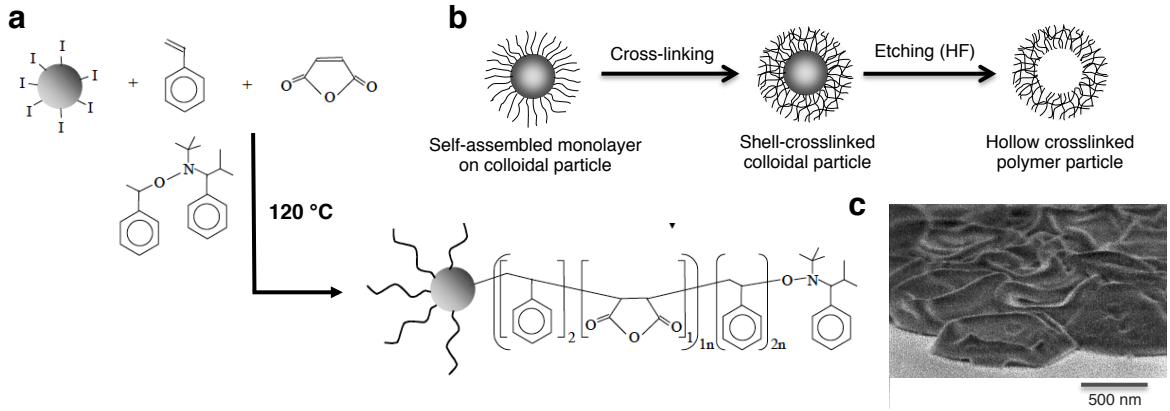

Figure 18. a) Preparation of maleic anhydride-functionalized nanoparticles, b) synthetic scheme for the preparation of hollow crosslinked polymer nanocapsules using the silica core as sacrificial template and c) FESEM image of crosslinked poly(styrene-*co*-maleic anhydride)-modified nanocapsules after removal of the silica core by chemical etching with HF [168], Copyright 2002. Adapted with permission from Wiley Periodicals, Inc.

In addition to dense silica particles, SI-NMP has also been conducted in the confined space of ordered mesoporous silicas (OMS) [170, 171]. For instance, Blas et al. [171] performed SI-NMP of styrene from OMS of various pore sizes and morphologies. Polymerization was shown to occur inside the channels and did not affect the intricate pore structure. The authors observed that mesoporous silicas with pore sizes lower than typically 5 nm in diameter suffered diffusional limitations, resulting in a non-uniform concentration of radical trap and larger molar mass distributions. The porous morphology, and in particular the pore connectivity was also shown to play an important role, the best results being obtained for mesoporous structures with open pores.

3.3.3. Structured silica particles for unraveling the mechanism of mechanical reinforcement in polymer nanocomposites

Polymer-grafted silica particles have also attracted great interest as model systems for a better understanding of the effect of surface modification and nanoparticle/polymer interfacial interactions on the viscoelastic behaviour of polymer matrix nanocomposites [172-174]. The effect of molar mass and grafting density on the structure and properties of polymer-grafted nanoparticles, has been extensively studied in the literature and is well documented [175-178]. In the case of matrix-free systems, inorganic particles with a high graft density of short unentangled chains have been reported to behave like colloidal soft glasses in the concentrated polymer brush regime. With increasing chain length, interactions with chains on neighboring particles are favored and polymer-grafted nanoparticles behave like rubbery reinforced polymers [179, 180]. In the latter case,

the viscoelastic response of the material is characterized by the presence of a low-frequency plateau in the storage modulus corresponding to a solid-like behaviour beyond the liquid-solid (or sol-gel) transition [181]. This effect, known as the liquid-to-solid transition was shown to also occur for hairy nanoparticles dispersed in a homopolymer matrix, even at low loadings [182]. Mechanical properties are also strongly dependent on the nanoparticles dispersion state, albeit in a complex and sometimes controversial way as various microscopic mechanisms, such as the presence of a thin immobilized polymer layer, confinement effects or polymer/filler affinity, can influence the macroscopic rheological response. In this regards, the formation of well-defined nanocomposites with controlled polymer chain lengths and dispersion states affords a mean to tentatively decorrelate such effects.

For example, Bartholome et al. [144] studied the viscoelastic properties of blends of PS-grafted fumed silica (5% vol.) with pure polystyrene, whose molar mass, M_n = 100 000 g mol^{-1}, was larger than the critical molar mass between entanglements, M_c = 18 000 g mol^{-1}. As shown in Figure 19, the PS/fumed silica (non-functionalized) nanocomposites displayed an elastic behavior at low frequencies (Ge~3x10^4 Pa) due to silica self-aggregation by van der waals interactions leading to the formation of a particle network [183].

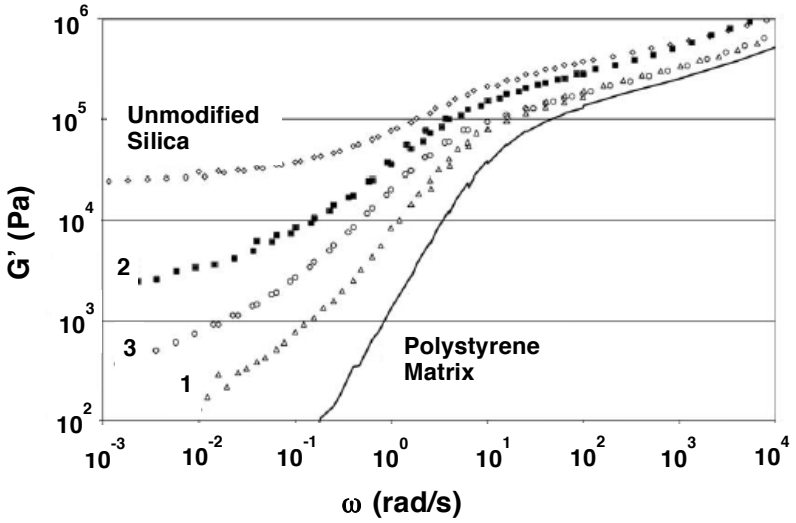

Figure 19. Storage shear modulus of blends of pure PS (M_n = 100 000 g.mol^{-1}) and PS-grafted silica with different molar masses and grafting densities (samples 1 : M_n grafted PS = 14 800 g mol^{-1} , density = 0.05 μmol/m^2 ; sample 2 : M_n grafted PS = 60 000 g mol^{-1}, density = 0.05 μmol/m^2 and sample 3 : M_n grafted PS = 60 000 g mol^{-1}, density = 0.27 μmol/m^2) [144], Copyright 2005. Reproduced with permission from Elsevier Science Ltd.

The nature of the physical network, and hence the viscoelastic response of the materials, was shown to be strongly dependent on the surface modification of the silica particles. Indeed, the grafting of polymer chains via NMP disrupted silica-silica particle interactions leading to a decrease of the storage modulus, G' (samples 1-3 in Figure 19). Even a small amount of short chains with a molar mass lower than the molar mass required for physical entanglement (sample 1), was very efficient in preventing the formation of a silica network as evidenced by the absence of a plateau in the low frequency region. However, upon increasing chain length, physical entanglement of the long grafted polymer chains with the free chains of the PS matrix favored gel formation resulting in a higher modulus and a more pronounced plateau (samples 2 and 3). Two concomittant effects were thus at stake here : a first effect related to the destruction of the percolating silica network favored by the grafting of short chains, and a second effect attributed to the diminution of the relaxation times of the chains in the matrix as a result of strong interactions with the polymer grafted inorganic particles.

A similar slowdown of low-frequency dynamics was also observed by Inoubli et al. [184] when studying the spectromechanical properties of PBA films filled with PBA-grafted Stöber silica particles (grafting density = 0.4 μmol/m^2 and M_n of grafted PBA = 33 800 g mol^{-1}). However, in this case, the silica particles were well dispersed within the matrix and the linear viscoelastic response was dominated by strongly favorable interactions between the grafted particles and the polymer matrix rather than by particle/particle interactions. It is predicted in this case that the system transits from a liquid to a gel upon increasing the amount of nanoparticles [185]. Indeed, while varying the silica content from 1.8 to 4.7 vol%, the authors showed the appearance of a secondary relaxation distinct from that of the matrix attributed to the presence of the inorganic particles. Above a critical value of 2.5 vol%, the composite material displayed a gel-like behaviour in the low frequency region consistent with the formation of a percolating network as confirmed by the observation of a structure factor in SANS experiments.

In another example, Chevigny et al. [186] studied the effect of silica nanoparticles dispersion state on the viscoelastic properties of PS-grafted silica particles dispersed in a PS matrix [187]. It was shown that the dispersion was mainly controlled by the chain length ratio, R, between the grafted and free polymer chains. Large and compact aggregates were obtained when the length of the matrix chains was significantly larger than that of the brush (i.e. for R values lower than typically 0.24) due to a collapse of the grafted polymer chains into a more entropically favorable coiled conformation on the inorganic surface, while individual nanoparticle dispersions were favored for R > 0.24. Such a transition between the formation of dense silica aggregates and individually dispersed particles upon increasing the length of the grafted polymer chains, for otherwise a fixed intermediate grafting density, was confirmed by TEM and small angle X-ray scattering (SAXS) analyses, and is in qualitative agreement with theoretical

predictions [188]. As in the two previous examples, the well-dispersed nanocomposites also displayed a solid-like behavior (as indicated by the apparition of a much longer relaxation time in the low frequency range) but at higher particle concentration (i.e. 12 wt. % silica), when two neighboring grafted silica particles could start to overlap and become indirecly connected through the grafted polymer chains, forming a percolating network. The effect was even more pronounced for the aggregates and was attributed to short-range interparticle interactions as the aggregates are not connected to each other. This behavior is similar to the observation of Inoubli et al. [149] for individually grafted silica particles at low concentration, and suggests that interpenetration between the grafted brushes would dominate over interactions between grafted and free polymers chains. Additional effects such as polymer confinement within the aggregates or the intrinsic slowing down of the relaxation dynamics of the aggregates were also invoked.

3.3.4. In situ synthesis of silicon oxide-based hybrid materials through NMP and the sol-gel process

Aside from the grafting of polymers from the surface of preformed silica colloids, NMP has also been combined with the sol-gel technique for *in situ* synthesis of silicon oxide-based hybrid materials of controlled morphologies. Indeed, as shown in several reports, unsaturated monomers containing reactive alkoxysilyl groups such as 3-acryloxypropyl triethoxysilane (APTES) can be readily homo- or copolymerized with acrylic or styrenic monomers by RDRP [189-194]. The resulting functional polymers can further undergo hydrolysis/condensation reactions or be combined with tetraethoxysilane after the polymerization step to afford organic/inorganic hybrid materials [195, 196]. Following this strategy, Gamys and coworkers reported the NMP synthesis of poly(APTES)-*b*-PS (PAPTES-*b*-PS) diblock copolymers [197] and PS-*b*-PAPTES-*b*-PS triblock copolymers [198] of various compositions and molar masses (Figure 20). The copolymers were subsequently self-assembled in a mixture of dioxane and methanol for the diblock and in bulk for the triblock, resulting respectively in the formation of spherical micelles and a lamellar structure regardless of the copolymer composition. Hydrolysis/condensation of the PAPTES block in acidic conditions was carried out to induce crosslinking and fix the morphology. In the case of the micelles, crosslinking led to a decrease of the corona diameter by around 10-15 nm due to shrinkage of the PAPTES block as evidenced by dynamic light scattering [197]. Structural characterization by SANS revealed that the core radius and aggregation number obeyed two different scaling regimes depending on the molar mass of the PAPTES corona-forming block [199]. PAPTES with molar masses lower than typically 25 000 g mol^{-1} were shown to be partially embedded inside the micellar core. SAXS analysis before and after crosslinking further

confirmed the decrease in shell thickness, the higher the PAPTES content in the block copolymer, the lower the shrinking ratio [199]. When using the triblock copolymer, it was shown that the lamellar morphology obtained by its bulk self assembly and subsequent crosslinking, was retained after calcination at 800 °C [198]. The approach was next extended to the formation of triblock copolymers with a central PS block (PAPTES-*b*-PS-*b*-PAPTES) [200]. Their mesophase morphology was again characterized by SAXS and was shown to evolve from spherical to cylindrical and lamellar with increasing the PS volume fraction in the copolymer.

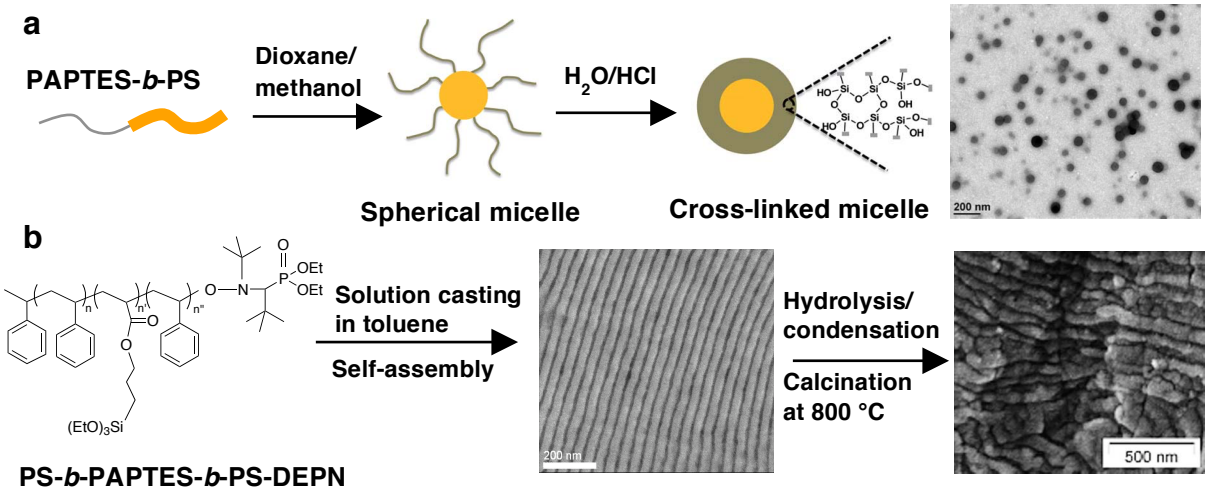

Figure 20. Illustration of the synthetic procedure used to form silicon oxide-based materials starting from a) PS-*b*-PAPTES and b) PS-*b*-PAPTES-*b*-PS di- and triblock copolymers, respectively. The copolymers were obtained by NMP and subsequently self-assembled into spherical micelles for the diblock [197] and into lamellae for the triblock copolymers [198], Copyright 2010 and 2011, respectively. Adapted with permission from Wiley Periodicals, Inc. The self-assembled structures were further consolidated by hydrolysis-condensation of the pendent triethoxysilyl moities and the polymer part removed by calcination.

3.4. Metal oxide-based functional materials

3.4.1. Titanium dioxide

Among all inorganic particles, titanium dioxide (TiO_2) displays many interesting properties such as high photocatalytic activity, transparency to visible light, UV absorption and high refractive index. In the past 15 years, several different strategies employing NMP and the grafting from method have been proposed to form stable colloidal TiO_2 suspensions in organic solutions or promote TiO_2 dispersion in polymeric matrices [201-204]. For example, Matsuno and Takahara [201, 202] utilized a phosphonic acid-terminated alkoxyamine to grow PS

chains from the surface of TiO_2 particles by SI-NMP while Abbasian et al. [204] reported the use of a TEMPO-based macroinitiator carrying a trialkoxysilyl end group. In the first case, the resulting PS-grafted TiO_2 particles were successfully redispersed in good solvents for the polymer chains such as THF, toluene or $CHCl_3$. UV-Vis spectroscopy showed that the suspension was highly transparent in the visible region as a result of the good dispersion state, and exhibited high UV-light absorption at 295 nm as expected for TiO_2 particles. The functionalized TiO_2 particles were also successfully dispersed into a PS matrix by solvent casting resulting in hybrid films with again low absorbance in the visible range and high UV absorption. Furthermore, the authors studied the tribological properties of the hybrid films and demonstrated that the presence of PS-grafted TiO_2 improved the wear resistance, with the width of the friction trace decreasing from around 147 μm for the bare PS film to 104 μm for the PS thin film containing 1 wt% of PS-grafted-TiO_2 particles [202].

3.4.2. Iron oxide

In recent years, magnetic iron oxide nanoparticles such as magnetite (Fe_3O_4) or maghemite (γ-Fe_2O_3) have attracted great interest for a wide variety of different applications, from catalysis to bioengineering. Again, in most cases, their surface need to be functionalized to protect them from the surrounding environment and promote their dispersion in organic solutions or into polymer matrices [205-208]. Taking advantage of the high affinity of phosphonic acid groups for iron oxide surfaces, Matsuno and Takahara [201, 209, 210] reported the grafting of PS and poly(3-vinylpyridine) (P3VP) polymer chains from the surface of magnetite nanoparticles. The authors showed that while unmodified magnetite formed aggregates of several hundred nanometers in $CHCl_3$, the polymer-grafted samples led to fine dispersions in either $CHCl_3$ (for PS) [209] or in aqueous acidic solution (for P3VP) [209, 210] with particle sizes of about 50 nm (Figure 21). The grafted polymer layer was shown to prevent iron oxide particles aggregation through magnetic interactions, and strongly influenced the magnetic response of the resulting colloidal suspensions that retained their ferromagnetic properties.

The grafting from strategy was also employed by Binder et al. [211] to immobilize PNIPAAm chains onto magnetic particles previously functionalized by a diol-bearing alkoxyamine initiator through ligand exchange, leading after polymerization to superparamagnetic core-shell particles with a PNIPAAm shell of controlled thickness. On the other hand, Robbes et al. [212] have devised a multistep strategy (involving charge inversion, solvent exchange followed by silane grafting and finally alkoxyamine coupling) to control the colloidal stability and surface properties of maghemite nanoparticles at all time during the grafting process, and form well-defined core-shell γ-Fe_2O_3/PS particles as assessed by scattering techniques. Finally, in two last examples, P4VP chains were grafted onto

the surface of 3-methacryloxypropyltrimethoxysilane-modified magnetite nanoparticles [213] while PSMA chains were grown from TEMPO-modified Fe_3O_4 nanoparticles [214]. In both cases, it was shown that the polymer shell did not significantly affect the magnetic properties of the Fe_3O_4 core.

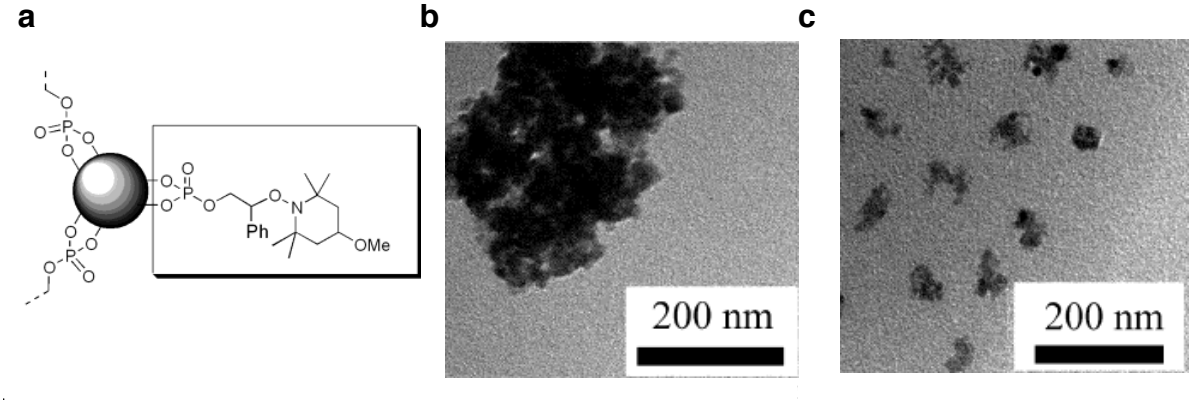

Figure 21. a) Grafting of a phosphonic acid-terminated alkoxyamine initiator onto iron oxide particles and b, c) TEM images of b) unmodified and c) PS-modified magnetite particles, dispersed in $CHCl_3$ (concentration = 0.01 g L^{-1}) [210], Copyright 2004. Adapted with permission from the American Chemical Society.

3.5. Chemical modification of metallic substrates and NMP synthesis of metallo-polymer assemblies

3.5.1. SI-NMP from planar metallic surfaces for the elaboration of surface-responsive materials and/or bio-sensors

The majority of implants consist in metals and metal alloys. To ensure long-term antibacterial protection, metallic implants need to be functionalized in order to prevent microorganisms from adherence. Hydrophilic poly(ethylene oxide) (PEO) chains and cationic polymers carrying long-alkyl-chain quaternary ammonium groups are well-known for their ability to prevent microbial growth, and have been used for this purpose.

For example, Ignatova et al. [215] reported the grafting of quaternized 2-(dimethylamino)ethyl acrylate (DMAEA)-based PS or PBA copolymers onto steel in two steps. An acrylate-terminated alkoxyamine was first attached on the surface by electrodeposition and further used to control polymer chains growth (Figure 22a). The resulting copolymers displayed antibacterial activity and were more efficient in inhibiting the growth of the Gram-positive bacteria S. aureus or the Gram-negative bacteria E. coli than PS or PBA homopolymers (Figure 22b). Such quaternary ammonium-functionalized copolymer films are promising for applications in orthopedic and dental surgery.

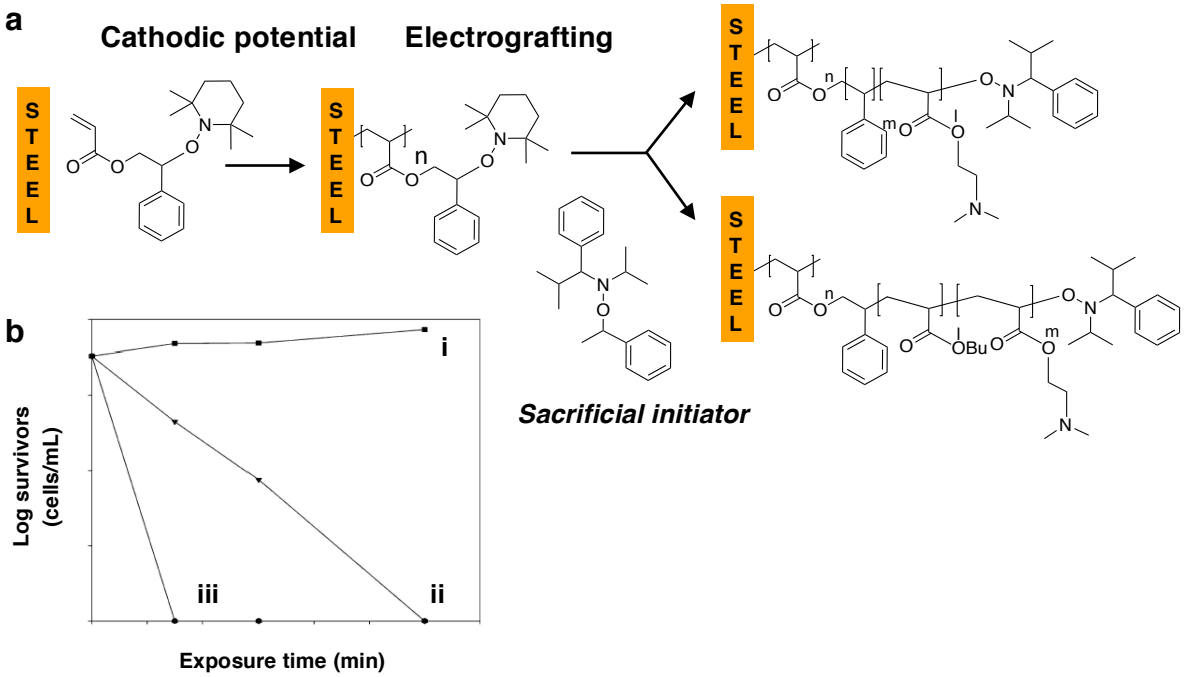

Figure 22. a) Synthetic procedure for the grafting of DMAEA-based copolymers onto steel; b) logarithmic plot of the viable cell number of E. coli *vs* the exposure time for i) blank, ii) poly(S_{62}-*co*-$DMAEA_{38}$) quaternized by 1-bromodecane and iii) poly(S_{62}-*co*-$DMAEA_{38}$) quaternized by 1-bromooctane [215], Copyright 2004. Adapted with permission from the American Chemical Society.

In another example, Borisova et al. [216] reported the NMP synthesis of pH- and electro-responsive amphiphilic poly(acrylic acid)-*b*-poly(acrylic acid-*grad*-styrene) brushes from gold-coated silicon wafers. A polymer grafting density of 0.23 chains/nm^2 was succesfully obtained under optimal experimental conditions. The presence of ionizable groups in the chains endowed the polymer brush with responsive properties giving access to multiresponsive smart materials. The authors showed that the swelling behaviour of the block copolymer layer could be fine tuned by varying the pH or the electric field. Indeed, application of an external electrical field influenced the conformation of the grafted polyelectrolyte chains and the distribution of the counterions. The polymer layer thickness increased at elevated pH (6.9) and under negative potential while it collapsed by decreasing the pH to a value of 3 and applying a positive electrical field

Finally, more recently, Guselnikova et al. [217] reported the plasmon-induced NMP of NIPAAm and 4-vinylboronic acid (VBA) from alkoxyamine-modified gold gratings. Irradiation of the gold surface with a laser beam at 785 nm generated surface plasmon polaritons propagating along the grating surface, capable to promote homolytic dissociation of the NO–C bond of the grafted alkoxyamine at

room temperature (Figure 23). The authors studied the adsorption of glycoproteins on the covalently attached PNIPAAm-*b*-PVPA block copolymers considering that the carbohydrate moieties of the glycoproteins can be entrapped by the PVBA segment while the thermoresponsive PNIPAAm block should favor glycoprotein detection by collapsing at high temperatures. As a result, Raman analysis of glycoprotein-based solutions at various temperatures showed an improved spectrum resolution and a 2.5 fold increase of the intensity of characteristic peaks at temperatures higher than the LCST of PNIPAAm (i.e. 32°C).

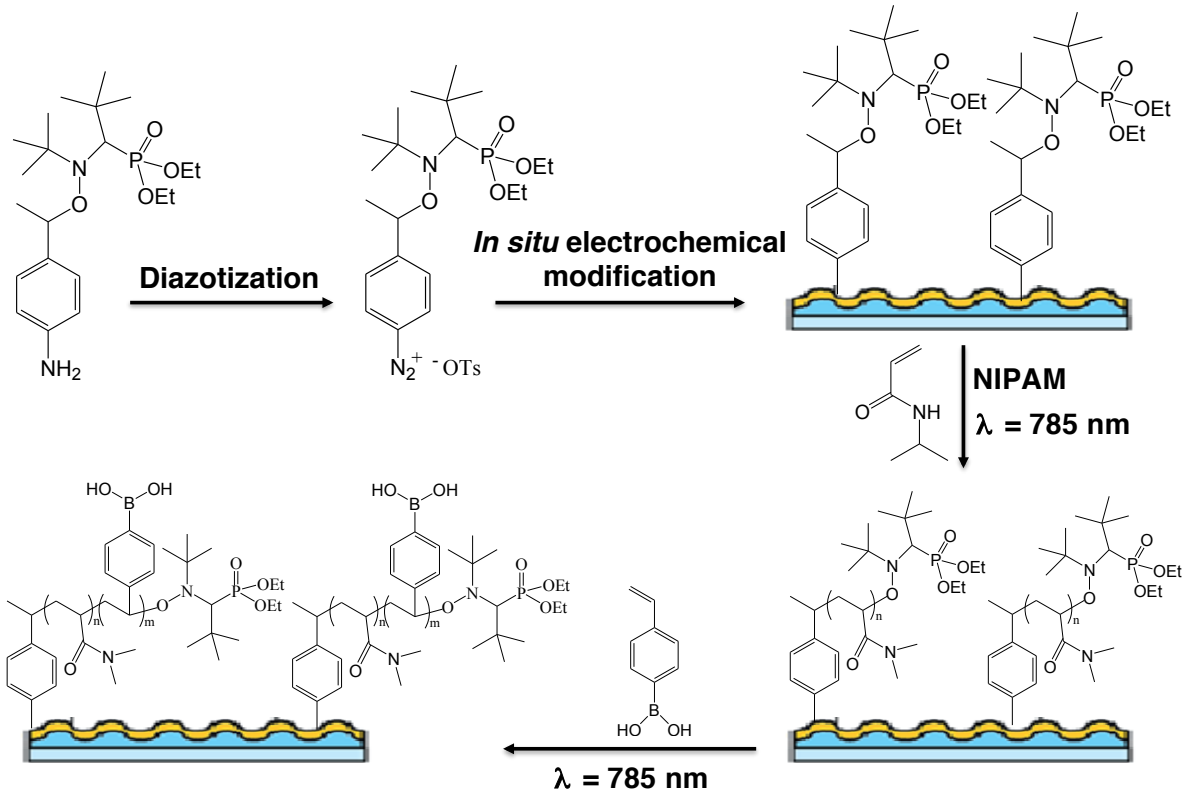

Figure 23. Plasmon-induced growth of a PNIPAAm-*b*-PVBA brush from an alkoxyamine initiator-grafted gold grating [217], Copyright 2019. Reproduced with permission from the Royal Society of Chemistry.

3.5.2. Core-shell metal-based nanoparticles and metallo-polymer assemblies for optical sensor and catalytic applications

Aside from planar surfaces, a few works have also been conducted on metallic colloidal systems. For instance, core–shell nanohybrids based on gold nanoparticles (AuNPs) were prepared by Zawada et al. [218] in order to control the gold surface plasmon resonance (SPR) and improve the thermal stability of the resulting SPR sensor (Figure 24). PS chains were grafted onto gold nanoparticles using a grafting onto-like procedure consisting in the late addition of

gold-supported TEMPO radicals to a polymerization media containing a peroxide initiator, styrene, TEMPOL and TEMPOL-terminated PS chains (Figure 24a). The obtained materials exhibited strong SPR near 520 nm. The SPR spectrum remained unchanged even after heating to 300°C contrary to the starting thiolate-coated particles (Figure 24b), making the resulting PS-grafted AuNPs valuable candidates for applications as high-temperature optical sensors. More recently, the same group used a similar approach to graft highly dense PS brushes from silver nanoparticles for antibacterial applications [219].

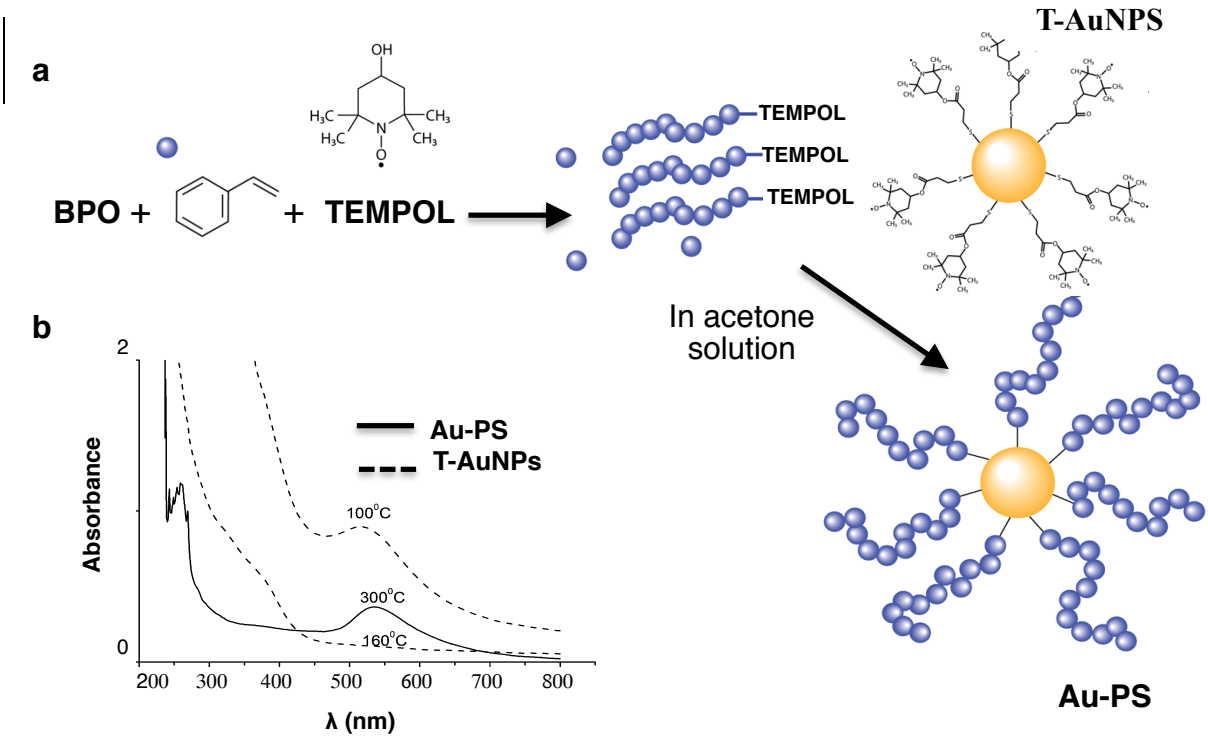

Figure 24. a) Synthetic scheme for the elaboration of PS-grafted gold nanoparticles and b) UV-Vis spectra of THF solutions of solid residues obtained after heating the PS-coated ($AuPS_4$) and thiolate-stabilized (T-AuNPs) gold nanoparticles [218], Copyright. 2014. Adapted with permission from the Royal Society of Chemistry.

In addition to metallic nanoparticles, semi-conductor cadmium selenide (CdSe) nanoparticles were also chemically modified by NMP in order to increase their dispersion in polymer matrices while maintaining their inherent fluorescence [220]. PS and poly(S-*co*-MMA) chains were grafted from the surface of CdSe nanoparticles previously covered with TEMPO-modified phospine oxide ligands. Analysis ot the fluorescence of the PS-grafted CdS particles in $CHCl_3$ solutions revealed an order of magnitude increase in intensity when compared to the initiator grafted nanoparticles.

On another topic, the group of O'Reilly et al. [221, 222] reported the NMP synthesis of non-covalently connected micelles from metallo-diblock copolymers

for applications in the field of supported catalysis (Figure 25). Well-defined block copolymers containing either terpyridine (Figure 25a) or sulfur-carbon-sulfur (SCS) pincer functionalities (Figure 25b) were firstly synthesized, and subsequently self-assembled into spherical micelles by complexation with Fe, Ru, and Cu metals for the terpyridine [221] and with Pd for the SCS pincer [222] ligands, respectively. The Cu-tethered metal complexes were shown to be active catalysts for the 1,3-dipolar cycloaddition of azide and alkynes to form 1, 2, 3 triazoles by "click" chemistry [221] while the Pd-based nanostructures could find applications as pseudo-homogeneous supported catalysts for Heck coupling reactions [222].

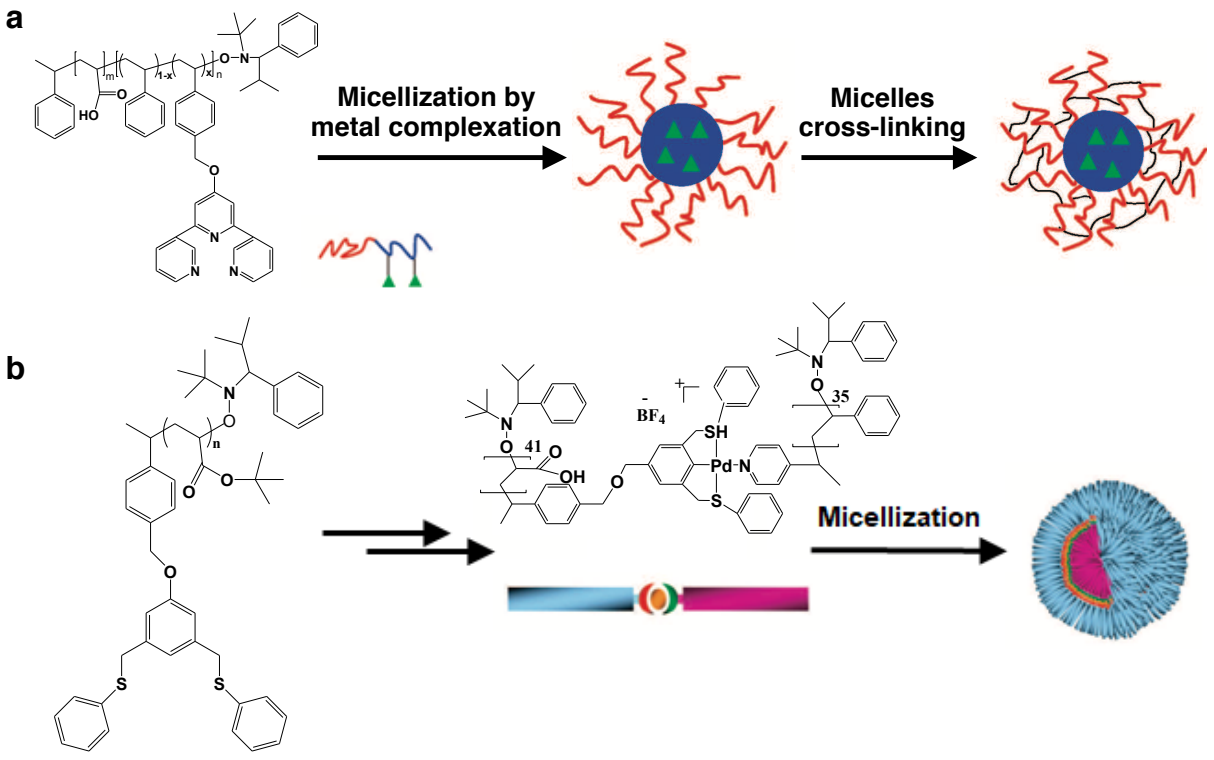

Figure 25. Preparation of metallo diblock copolymer-based micelles using functional copolymers synthesized by NMP. Panel a) illustrates the formation of the functionalized spherical micelles using the terpyridine approach [221] while Panel b) corresponds to the use of block copolymers made from the sulfur-carbon-sulfur pincer ligands [222], Copyright 2008. Adapted with permission from the American Chemical Society.

In a related example, Mugemana et al. reported the synthesis of metallo-supramolecular gels based on transition metal ions and block copolymers [223]. First, PS-*b*-P*t*BA diblock copolymers bearing terpyridine chain end groups were prepared by using NMP followed by their self assembly in ethanol to generate micelles with a PS core and a P*t*BA corona. Then, the presence of terpyridine groups on the P*t*BA chain ends allowed for the formation of micellar gels upon adding Ni(II) and Fe(II) ions in the micellar solution (Figure 26).

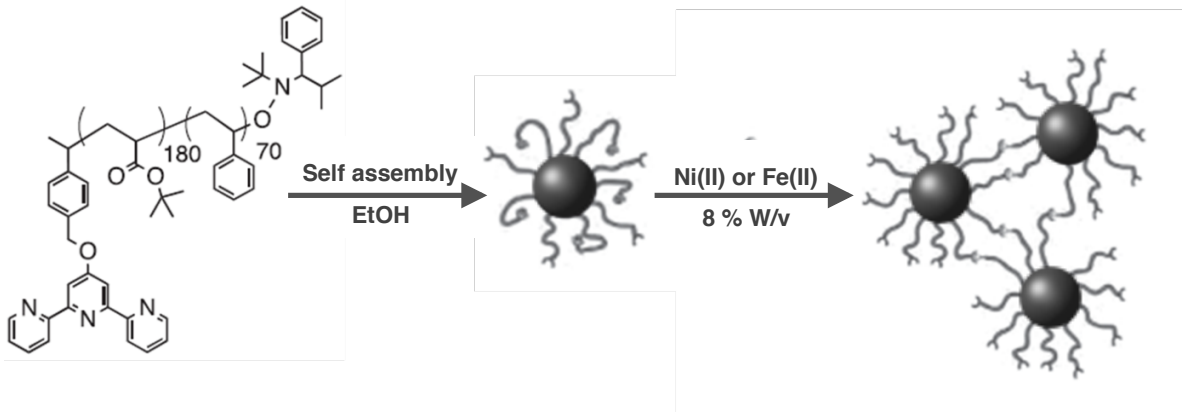

Figure 26. Formation of metallo-supramolecular gels through the addition of metal ions to self-assembled block copolymers carrying terpyridine moieties on their outer surface [223], Copyright 2013. Adapted with permission from John Wiley & Sons Inc.

3.6. Polyhedral oligomeric silsesquioxanes (POSS)

POSS molecules have a chemical composition ($RSiO_{1.5}$) intermediate between that of silica and silicone (R_2SiO). They possess a symmetrical cage-like structure with dimensions in the range of typically 1 to 3 nm, exhibiting organic functional groups on their outer surface, that can be inert or reactive. Because of their unique molecular structure and nanoscale dimensions, POSS have been considered as one of the most promising nanofillers for the enhancement of thermal, mechanical, and optical properties of polymer nanocomposites [224-228]. Moreover, the large variety of chemical groups that can be introduced into POSS makes these compounds ideally suited for the design of POSS-based materials using polymer grafting techniques [15, 224, 225, 229-232]. Many kinds of well-defined POSS-based hybrid polymers with tunable chemical compositions and physical properties have been thus synthesized by NMP. The incorporation of POSS structures with engineered polymer brushes into polymer films allows tailoring both the rheological and surface properties of the corresponding composite materials.

3.6.1. Effect of polymer grafting on the properties of POSS-based polymer composites

The first examples of NMP synthesis of POSS-based nanocomposites were reported by Miyamoto et al. [230, 231]. In their first report, the authors described the incorporation of PS-grafted POSS molecules into PS films spin-coated onto silicon wafers (Figure 27). As expected, the PS-grafted POSS-based film (with POSS content varying from 2 to 36 wt%) exhibited a smaller surface roughness than the one containing neat, un-modified octacyclopentyl POSS (CpPOSS) due to enhanced POSS dispersion in the PS matrix. Moroever, optical analysis of a polymer blend film (PS_1, M_n = 2 100 g mol^{-1}/PS_2, M_n = 44 000 g mol^{-1}, 28/72 w/w)

annealed at 423 K for 3 hours showed a complete dewetting while replacing PS_1 by PS-grafted POSS (M_n grafted PS = 2 500 g mol^{-1}) stabilized the blend film against dewetting (Figure 27c). This behaviour was attributed to POSS end groups segregation at the film–substrate interface due to favorable interactions between the POSS moiety and the silicon wafer. In a subsequent article, the authors went one step further and compared the rheological properties of PS-grafted POSS with those of PS chains of similar molar mass to that of the grafted polymer (M_n = 2 100 g mol^{-1}) [231]. While the PS sample displayed liquid-like characteristics, the PS-grafted POSS exhibited a pseudo solid like behaviour with the presence of a plateau at low frequencies, indicating that the presence of POSS decreased PS chains diffusion. The authors concluded that the increase of viscosity stabilized the film against dewetting.

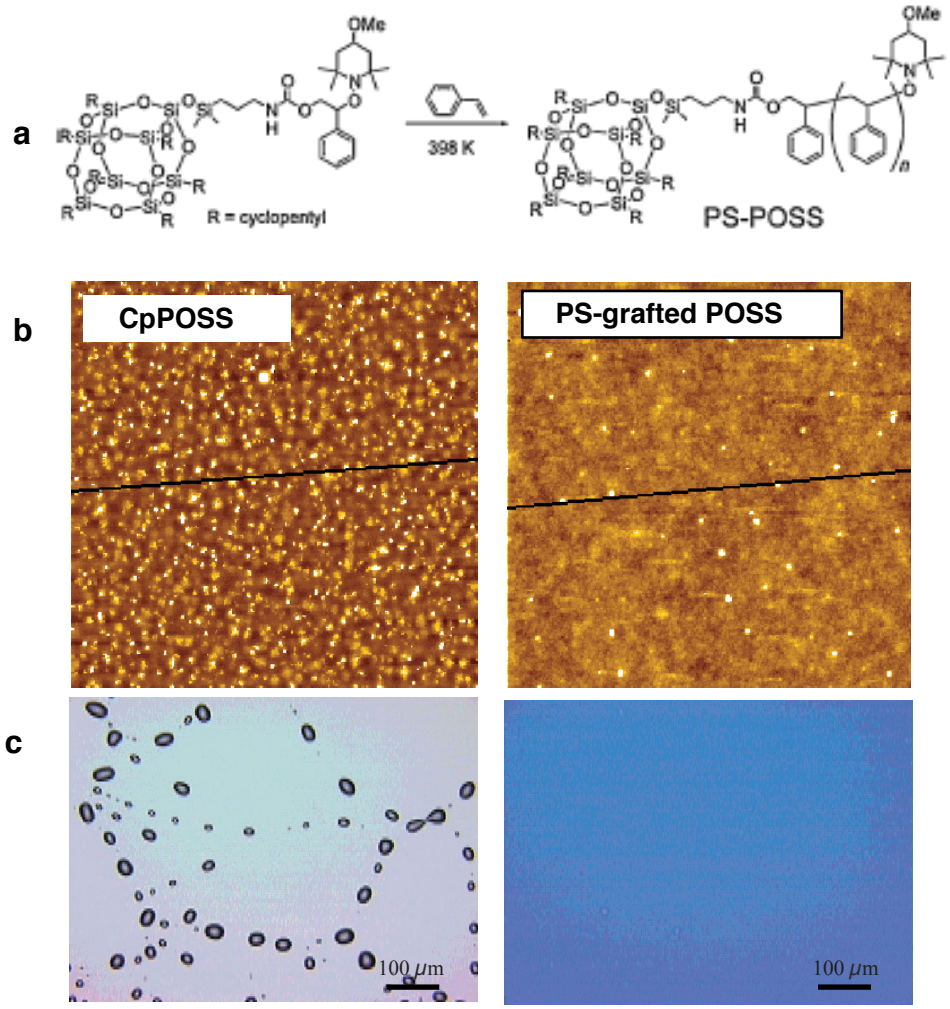

Figure 27. a) Scheme for synthesis of PS-grafted POSS by NMP, b) AFM height images and c) optical micrographs of 124 nm thick CpPOSS/PS_1/PS_2 and PS-grafted POSS/PS_2 blend films annealed at 423K for 3 h (at constant POSS weight content) [230], Copyright 2006. Adapted with permission from the Chemical Society of Japan.

3.6.2. *Preparation of nanostructured materials using a POSS-first NMP approach*

Hybrid POSS-based structures were synthesized by Lu et al. [233] using a POSS-first approach. In this strategy, octa-N-alkoxyamine-grafted POSS compounds were used as templates to grow polystyrene-*b*-poly(4-vinylpyridine) (PS-*b*-P4VP) diblock copolymer chains from their surface leading to star-like structures. Chemical incompatibility between the two blocks was evidenced by DSC with the presence of two glass transitions located at 109°C and 148°C corresponding to the PS and P4VP blocks, respectively. The increase of Tg of the PS block was attributed to a higher confinement of the PS segment in the diblock copolymer and the presence of fewer chain ends. The structure of the self-assembled $(PS\text{-}b\text{-}P4VP)_8$-grafted POSS was further confirmed by TEM that showed the formation of an alternating lamellar morphology with a lamellar period of 40 nm, consistent with SAXS analysis.

3.7. Phyllosilicates

Phyllosilicates (also called layered alumino silicates) are inorganic platelet materials built by stacking tetrahedral layers being connected to an octahedral layer occupied by different cations (Al, Mg, Fe, Ti, Li, etc.).. Clays are the most important minerals within the phyllosilicate or layered silicate family, and are commonly used as reinforcing agents in polymer nanocomposites. Indeed, their low density and their high aspect ratio allow decreasing the weight of the corresponding composite material by at least 5-10 wt% in comparison to more conventional inorganic fillers. Among them, smectite clays (such as montmorillonite (MMT), bentonite, or Laponite) and mica are the most frequently studied.

Layered silicate nanocomposites can be rarely prepared from neat, unmodified silicate layers. Indeed, the highly hydrophilic environment of clay minerals does not allow the intercalation of organic molecules, and it is therefore necessary to exchange the interlayer inorganic cations by organic cations with long alkyl chains (typically alkyl ammonium or alkyl phosphonium compounds) and/or to functionalize their inherent hydroxyl groups [234]. The incorporation of nano-scale inorganic platelets into a polymer matrix is mainly intended to confer improved mechanical properties, thermal resistance or barrier properties to the resulting hybrid materials, as described below.

3.7.1. *Elaboration of phyllosilicate-based composites with improved mechanical and barrier properties*

Several authors have reported the formation of polymer/clay nanocomposites by NMP [235-245]. Again, both bimolecular and unimolecular initiating systems have been investigated. The first example of Si-NMP using a silicate-anchored initiator was reported by Sogah et al. [235] in 1999. A TEMPO-based alkoxyamine

initiator bearing a benzyltrimethylammonium chloride moiety was first immobilized into the interlayer space of MMT by cation exchange, and further used to control the NMP of styrene. SI-NMP provided good control over molar masses and molar mass distributions allowing the originally stacked clay layers to fully delaminate in the polymer matrix leading to the formation of a dispersed nanocomposite. The same group later used a similar strategy to graft polystyrene-*b*-poly (ε–caprolactone) (PS-*b*-PCL) diblock copolymers using MMT platelets modified with a multifunctional initiator bearing a trimethyl ammonium chloride group to interact with the clay surface and groups capable to initiate the ring opening polymerization of ε-CL and the NMP of styrene (i.e., a primary alcohol and an alkoxyamine functionality, respectively) (Figure 28) [236].

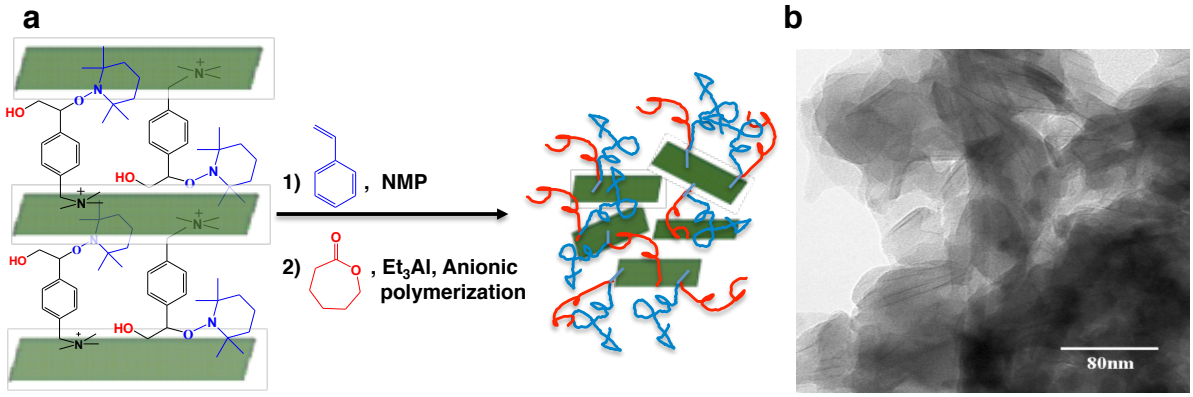

Figure 28. a) Schematic illustration and b) TEM image of PS-*b*-PCL/MMT nanocomposites obtained by NMP of styrene followed by anionic ring opening polymerization of ε-CL using a specifically designed multifonctional silicate-anchored initiator [236], Copyright 2006. Adapted with permission from the American Chemical Society.

Following a similar approach, Konn [238] and Abbasian [245] reported the formation of exfoliated nanocomposites by NMP of styrene using a cationic alkoxyamine initiator intercalated into the interlamellar space of Laponite® and MMT, respectively, while Shen et al. [242] used a 3-steps procedure for *in situ* formation of an alkoxyamine by the reaction of BPO-issued radicals with intercalated 2-methacryloyloxyethyl trimethyl ammonium chloride molecules in the presence of TEMPO. In the work of Konn et al. [238] on Laponite® clay, the PS-functionalized platelets were shown to form stable colloidal suspensions in THF as evidenced by dynamic light scattering. The hydrodynamic particle diameter first decreased with increasing the polystyrene chain length because of the presence of remaining clay agregates in THF until the molar mass of the grafted PS chains was high enough to completely destroy the aggregates resulting in an increase of particle size as the polymer chains grew (Figure 29).

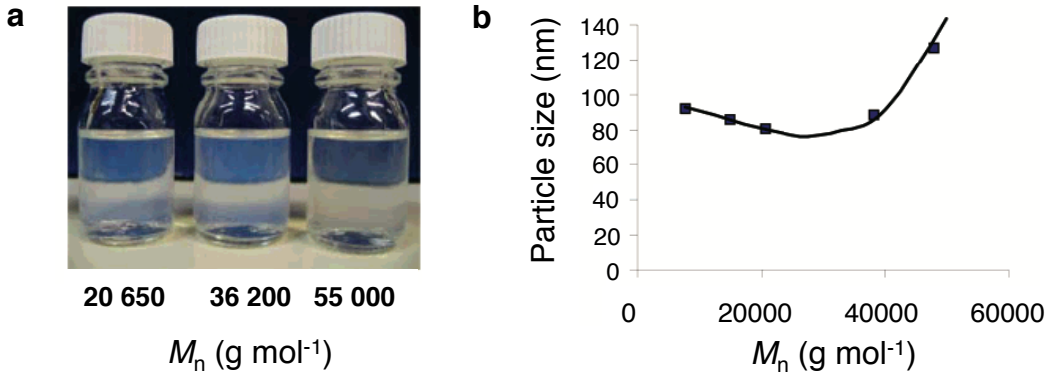

Figure 29. a) Digital photographs of PS-grafted Laponite® suspensions in THF at 2 wt% loadings and b) evolution of the hydrodynamic diameter of the hybrid particles as a function of the molar mass of the grafted PS chains determined by SEC [238], Copyright 2007. Reproduced with permission from the American Chemical Society.

In another example, Xu et al. [237] studied the viscoelastic properties of PS-modified MMT nanocomposites prepared by the grafting through technique using an intercalated vinylbenzyl ammonium chloride derivative. Linear viscoelasticity measurements revealed a liquid-to-solid transition attributed to geometrical percolation, the strongest network structure being obtained for 3.3 wt% of clay and grafted PS chains of intermediate molar mass (M_n = 12 500 g mol^{-1}). Indeed, quite surprisingly lowering the PS molar mass improved dispersability which was attributed to poor affinity of the PS chains for the clay surface. The non-linear viscoelasticity was dominated by the presence of free un-tethered shear thinning polymer chains that were inevitably present in the system.

Moreover, Mühlebach [240] studied the oxygen barrier properties of nanocomposites made of PBA-modified MMT dispersed in a polyethylene (PE) matrix using the grafting from technique. The incorporation of only 5 wt% of exfoliated PBA-grafted MMT with molar masses varying from 1 000 to 14 000 g mol^{-1} allowed a subtantial decrease of O_2 permeability (down to around 80%) whereas the O_2 permeability of the PE matrix loaded with unmodified silicate layers slightly increased due to poor compatibility between the two components resulting in void formation at the organic-inorganic interphase. This work highlights the determinant role of NMP in ensuring a good dispersion of MMT platelets in polymer matrices with complete exfoliation of the silicate layers when compared to a mixture of pure PE and unmodified MMT, resulting in better physical properties.

Finally, Cherifi et al. [243] explored the effect of clay loading and dispersion state on the thermomechanical properties of poly(BA-*co*-MMA)/MMT

nanocomposites synthesized using a bimolecular initiating system. While the presence of clay had no significance influence on the storage modulus, the incorporation of 4 wt% of MMT led to a decrease of the glass transition temperature (T_g) and enhanced thermal stability. The authors further extended the work to the synthesis of block copolymers and showed that MMT/polymer interactions played an important role in controlling the morphology and thermal properties of the resulting composite materials [244]. A similar initiator/nitroxide bimolecular initiating system was also reported by Mittal et al. for the synthesis of poly(lauryl methacrylate)/MMT composites [239].

3.7.2. Elaboration of mica-based composites with tailored optical properties

Aiming at preparing novel organic/inorganic hybrids with tunable optical properties, Ghannam et al. [246-248] reported the elaboration of polymer/mica nanocomposites using a bimolecular initiating approach similar to that reported above for MMT clay. An alizarin dye-based monomer was incorporated into the polymer chains resulting in composite materials whose color could be tuned by adjusting the (co)polymer molar mass, its grafting density and the dye content [247, 248]. The location of the pH-sensitive alizarin dye over the oxanions-based mica surface was key to tailoring the final color of the dye. Indeed, the electronic structure of the alazirin was strongly influenced by the mica substrate and the color of the copolymer varied from yellow for the P(S-*co*-A) sample in the solid state to pink for the P(S-*co*-A)-mica composite (Figure 30). The color also changed with increasing reaction time as a consequence of the increase of the distance between the dye and the mica surface [248].

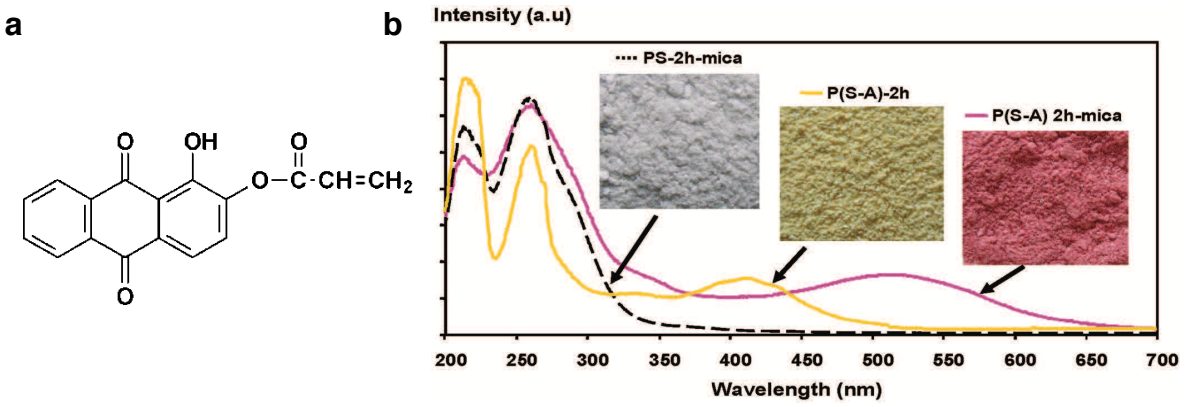

Figure 30. a) Molecular structure of the alizarin-based monomer and b) digital photographs and UV-vis diffuse reflectance spectra of the mica sheets functionalized by pure PS (in black) and P(S-*co*-A) (in pink). The yellow curve corresponds to the signal of the free P(S-*co*-A) copolymer in the solid state [248], Copyright 2008. Adapted with permission from the American Chemical Society.

Similarly, Leone et al. [249, 250] elaborated blue-emitting polymer hybrids by incorporating both rhodamine G (R6G) dye and polystyrene or a poly(styrene-*co*-styrene para substituted with π-conjugated fluorene fragment) copolymer into fluoromica layers (Figure 31).

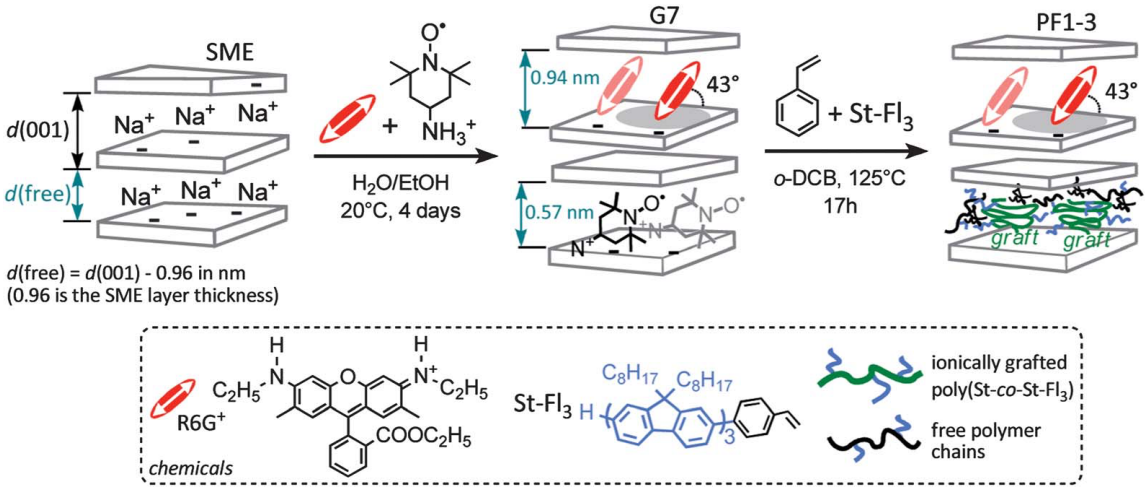

Figure 31. Synthetic scheme for the preparation of polymer dye-fluoromica clay hybrids [249], Copyright 2013. Reproduced with permission from the Royal Society of Chemistry.

The concomitant presence of rhodamine and polystyrene induced a color change from yellow-orange to red upon increasing the rhodamine content while the presence of the polystyrene layer allowed to tailor the spatial configuration of the dye in between the fluorosilicate layers thus permitting to tune the materials' photo-functions [250]. Moroever, immobilization of styrene derivatives para-substituted with (oligo)fluorene moieties onto the fluoromica interlayers surface led to a control of the conformation of the oligofluorene moieties depending on the copolymer composition. Consequently, the photoluminescence efficiency (PL-QY) increased from 0.71 to 0.90 when increasing the (oligo)fluorene content in the copolymer from 0.6 to 16.7 wt%. The obtained high PL-QY opened the route to new applications for polymer light-emitting devices.

It is worth mentioning here that similar dye-functionalized copolymer brushes were also immobilized on aluminium flakes by SI-NMP using a related approach, leading to colored pigments [251].

4. NMP synthesis of organic/inorganic hybrids in waterborne dispersed media

As reviewed in the previous sections, NMP has been extensively used to synthesize organic/inorganic materials through the covalent attachment of polymer chains on inorganic particles. These processes commonly employ organic

solvents leading to the formation of a hairy (solvated) polymer layer surrounding the inorganic colloid. Recently, and in compliance with regulations on low volatile organic compounds (VOC) emissions, a great research effort has been devoted to the formation of composite colloids from aqueous solutions or directly in aqueous dispersed media using heterophase polymerization techniques such as emulsion or miniemulsion polymerizations [4, 252]. In parallel, striking progress has been made in adapting RDRP techniques to dispersed phase systems allowing access to a wide variety of particle morphologies such as spheres, rods, fibers or vesicles using the polymerization induced self-assembly (*PISA*) process [253, 254]. As a logical extension of these achievements, RDRP has also been combined with inorganic components in heterophase systems to form organic/inorganic hybrid particles [255, 256]. Two main strategies have been reported for this purpose, which are detailed below.

4.1. Miniemulsion polymerization

One first approach relies on the use of the miniemulsion polymerization technique. In a typical process, polymer-coated inorganic particles obtained by SI-NMP are dispersed into monomers and the resulting suspension is mixed with an aqueous solution of surfactant under high shear to form inorganic-loaded monomer droplets. The surfactant stabilizes the emulsion against coalescence while a solvophobic specie is added to slow down Ostwald ripening by limiting molecular diffusion between droplets, resulting in small uniform monomer droplets that are converted in a last step into polymer latex particles. Bailly et al. [257] were the first to use this strategy to encapsulate silica particles into polystyrene latexes (Figure 32).

.

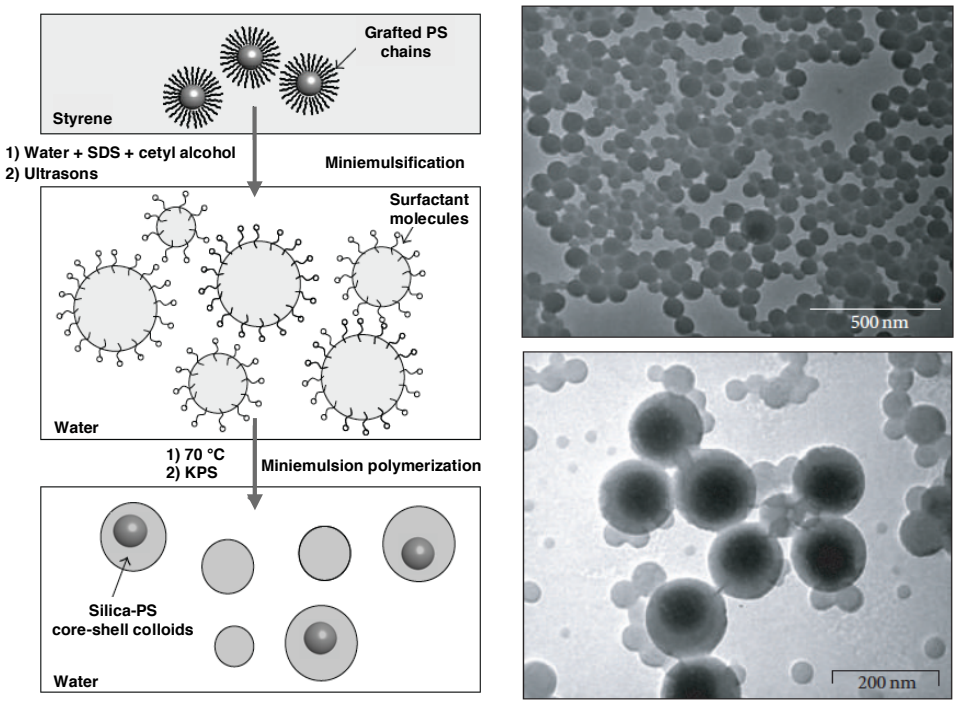

Figure 32. a) Scheme illustrating the principle of PS-grafted silica particles encapsulation through miniemulsion polymerization and b) transmission electron micrograph of the produced silica@PS core-shell latex particles [257].

The silica particles were first modified by the grafting of long polymer chains (M_n = 64 000 g mol^{-1}) affording stable colloidal suspensions in styrene. Subsequent miniemulsion polymerization of the silica-loaded droplets resulted in the formation of stable latexes containing a high proportion of pure polymer particles suggesting the occurrence of secondary nucleation, while the formation of composite particles containing only one silica bead indicated the absence of coalescence and/or coagulation.

Micusik et al. [258, 259] used a similar approach to prepare MMT/P(BA-*co*-MMA) composite latexes. A cationic macroalkoxyamine based on vinylbenzyl trimethylammonium chloride (VBTMACl), MMA, and styrene : P(VBTMACl-*co*-MMA$_7$-*co*-S$_4$), was first synthesized using a water-soluble DEPN-based alkoxyamine (MAMA-DEPN or BlocBuilder®), and subsequently exchanged with the sodium cations of MMT. Copolymerization of BA and MMA was then performed in bulk in the presence of the modified MMT with however a limited control over the molar masses, leading nevertheless to the formation of exfoliated clay sheets decorated with polymer chains. The polymer-tethered clay sheets were then dispersed in BA/MMA droplets using stearyl acrylate as the hydrophobe and Dowfax 2A1 (alkyldiphenyloxide disulfonate) as the surfactant. Miniemulsion polymerization was then initiated by the addition of KPS, yielding a stable latex able to form nanocomposite films with exfoliated clay platelets and improved adhesive properties compared with the neat polymer. In comparison, the use of MMT that had been only modified by the cationic macroalkoxyamine and without prepolymerization did not lead to a stable latex, showing the crucial role of the grafted P(BA-*co*-MMA) chains in ensuring a good dispersibility and compatibility of MMT with the polymer matrix. The authors also examined the barrier properties and showed that the water vapor transmission rate of the composite film decreased from 24.6 to 17.4 g.mm/cm^2.days in comparison to the pure copolymer, confirming the role of the exfoliated clay layers in forming a tortuous diffusion path within the polymer matrix resulting in a decreased permeability to water vapor.

4.2. Emulsion polymerization

More recently, an innovative and highly efficient strategy involving RDRP and conventional emulsion polymerization has been devised to enable the formation of composite particles in a single step, without the need for high energy mixing, such as ultrasonication, as in miniemulsion polymerization. This approach takes advantage of the recent developments in the *PISA* technique mentioned above and has the tremendous benefits of allowing access to a wide variety of hybrid particle

morphologies while eliminating the need for molecular surfactant. In brief, the method, pioneered around twelve years ago for the encapsulation of TiO_2 pigments [260], relies on the use of statistical copolymers synthesized by RDRP to stabilize inorganic nanoparticles in aqueous solution and at the same time provide reactivatable groups from which polymer chain growth can occur in a subsequent emulsion polymerization step. This generic approach, coined *REEP* for RDRP-assisted Encapsulating Emulsion Polymerization, has been initially developed using the RAFT process, and exemplified for a variety of inorganic particles [206, 261-267], opening a new route to polymer-encapsulated minerals and to composite particles with complex morphologies that were until now not accessible by conventional radical polymerization

The first example of successful implementation of this strategy using NMP as RDRP process was reported by the group of Bourgeat-Lami. In a series of papers, Qiao et al. used this approach to synthesize polymer/silica nanocomposite particles of various morphologies (Figure 33) [268-270].

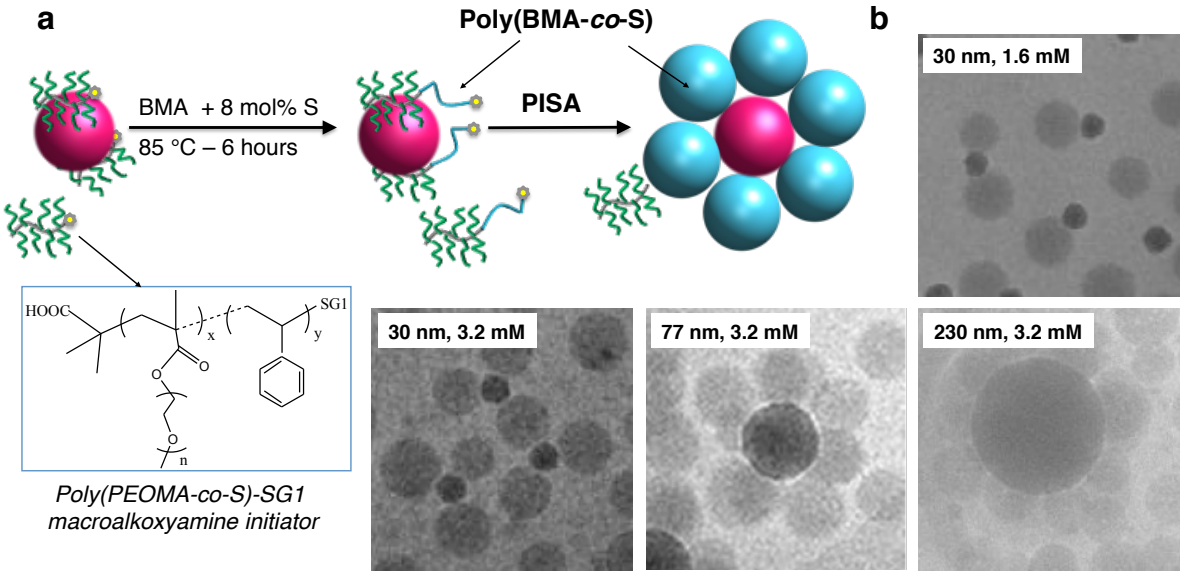

Figure 33. a) Scheme illustrating the synthesis of multipod-like silica/polymer composite particles by nitroxide-mediated polymerization-induced self-assembly of block copolymers using a physisorbed brush-like macroalkoxyamine initiator as hydrophilic block, and b) cryo-TEM images of the composite particles obtained in the presence of various silica particle sizes and initiator concentrations [268], Copyright 2015. Adapted with permission from the American Chemical Society.

A macroalkoxyamine initiator carrying PEO side chains (M_n = 950 gmol^{-1}) and a few styrene units (poly[(PEOMA$_{950}$)$_{12}$-*co*-S$_1$], M_n = 11 700 g mol^{-1}, Đ = 1.11), was first synthesized by NMP, and subsequently used to initiate the emulsion polymerization of butyl methacrylate in the presence of a small amount styrene

(Figure 33a). Strong adsorption of the hydrophilic block of the copolymer onto the colloidal silica in acidic conditions (pH ≈ 5) allowed confining the polymerization at the silica surface leading to the formation of self-assembled poly(PEOMA-*co*-S)-*b*-poly(BMA-*co*-S) block copolymer spheres uniformely distributed around the central silica beads, forming multipod-like particles. The number of polymer nodules that could be accommodated around each silica sphere increased with increasing the silica particle size leading to dumbbell-, daisy- and raspberry-shaped morphologies as the core diameter increased (Figure 33b). Furthermore, the multipod-like morphology could also be tuned by varying the initiator concentration independently from the silica particle size. Indeed increasing the macroinitiator concentration favored the formation of a larger number of latex particles influencing consequently the particle morphology which evolved from dumbbell- to daisy-like for a fixed silica particle size of 30 nm.

In a subsequent work, the authors explored the effect of pH and showed that increasing the pH led to completely new un-conventional morphologies such as "half-capped" spheres, tadpole-like and snowman-vesicles [270]. Particle morphology was again shown to strongly depend on the size of the silica nanoparticles. While large silica particles favored the formation of encapsulated (core-shell) morphologies, much smaller silica nanoparticles (~30-50 nm diameter) led to "armoured" fibres and/or vesicles (Figure 34).

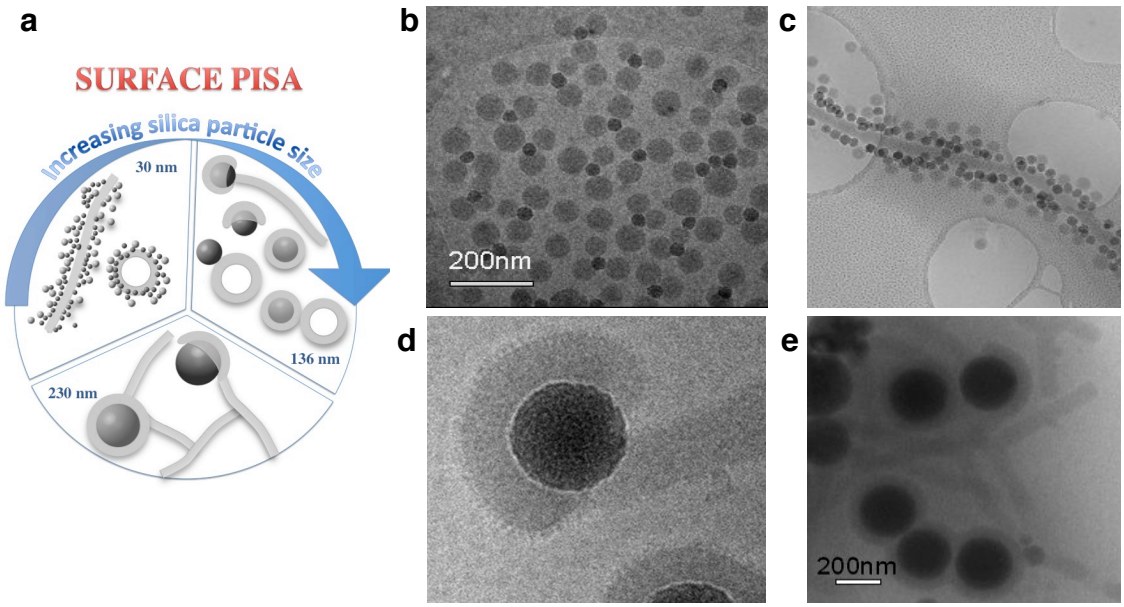

Figure 34. Effect of pH and silica particle size on the morphology of silica/polymer composite latex particles synthesized by nitroxide-mediated polymerization-induced self-assembly using a physisorbed brush-like macroalkoxyamine initiator as controlling agent [270], Copyright 2017. Adapted with permission from the American Chemical Society. a) Schematic illustration of the evolution of particle morphology with the silica particle size at pH = 8. b-e) Cryo-TEM images of the

silica/polymer composite particles for b) D_n SiO_2 = 30 nm and pH = 5, c) D_n SiO_2 = 30 nm and pH = 8, d) D_n SiO_2 = 136 nm and pH = 7.7 and e) D_n SiO_2 = 230 nm and pH = 8.2.

Finally, in a last example, hybrid nanostructures consisting of silica particles decorated by short worms of self-assembled block copolymers, were synthesized using a poly[$(PEOMA_{300})_{12}$-*co*-$MAA_{6.7}$-*co*-$S_{7.2}$] terpolymer as macroalkoxyamine initiator [269]. The later displayed a dual pH/temperature responsive behavior induced by the short PEO chain length (M_n = 300 $gmol^{-1}$) and the incorporation of methacrylic acid (MAA) units. Above pH 7, chain extension of the terpolymer with an immiscible P(BMA-*co*-S) block led to the formation of worm-like nanostructures. Worms were also formed in the presence of silica particles in similar conditions, and were composed in this case of partially coalesced spheres radially expanding from the silica core in a sea urchin-like morphology. This intringuing morphology was only observed at high pH and was presumed to result from a complex interplay between attractive forces allowing the macroinitiator to adsorb on the silica surface and repulsive electrostatic forces between the growing self-assembled block copolymers.

11. Concluding Remarks

This review article highlights the potential of the NMP technique for the synthesis of functional organic-inorganic hybrid materials with a wide range of properties. The grafting of polymer chains onto inorganic surfaces by NMP, possibly combined with (nano)lithography and patterning techniques, allows the elaboration of well-defined nanostructured materials. To achieve precise control of the polymerization occuring at the inorganic surface via the persistent radical effect, it is usually neccessary to add a sacrificial alkoxyamine initiator in solution leading to the concomitant formation of unbound polymer. Several authors have shown that the grown polymer chains have similar molar masses and dispersities than the free polymer and the later is therefore often used to evaluate the molar mass of the grafted chains. The architecture, the morphology and the thickness of the resulting polymer brush can thus be tuned on demand, and optimized for a wide range of applications such as sensing, antifouling or microfluidic.

In particular, planar and spherical silicon oxide-based surfaces can be chemically modified to produce surfaces with tailored properties such as roughness, wettability, stiffness/elasticity and hydrophobicity, depending on the nature and/or composition of the (co)polymer. On the other hand, the intercalation of polymer chains into the lamellar structure of phyllosilicates allows to confer barrier properties to the corresponding hybrid materials and/or to create colored pigments through the incorporation of dye molecules, with applications as

membranes and light emitting devices, respectively. Functionalized cage-like POSS structures have also been reported leading to hybrid materials with improved mechanical properties. In addition well-defined copolymers synthesized by NMP can act as scaffolds to guide the self-assembly of metallic particles such as gold or copper with potential use in biosensing, anti-bacterial or catalytic applications. Furthermore, macromolecular architectures incorporating sol-gel reactive groups have been shown to be promising polymeric precursors for the formation of nanomaterials and/or nano-objects by self-assembly in bulk or in solution. Finally, the modification of magnetic nanoparticles or semiconductor quantum dots by a well-defined polymer shell allows their homogeneous dispersion in polymeric matrices while maintaining their intrinsic physical properties, opening the way to biomedical applications including magnetic resonance imaging, hyperthermia, cell labelling and drug delivery.

The knowledge of the parameters guiding the homogeneous incorporation of inorganic particles into polymeric matrices and the rational design of planar substrates with controlled surface properties has improved considerably in recent years leading to a better understanding of structure-property relationships. As a result, the lab-scale development of various organic-inorganic hybrid materials has been achieved for a large variety of applications. A challenge for the future will be to translate this knowledge into industrial products, which will most likely require the development of new synthetic methodologies for larger scale production of new optimized alkoxyamine structures that will allow the synthesis of materials with the desired macroscopic properties.

As shown in the last part of the review, recent years has also seen significant progress in the use of NMP in aqueous dispersed media for the synthesis of hybrid particles. These pioneering works have benefited greatly from the recent advances in the *in situ* synthesis of block copolymer nano-objects through polymerization induced self-assembly, and are likely to be a source of inspiration in the future for the design of colloidal nanocomposites with new morphologies and functions.

Acknowledgments:

This manuscript is a tribute to the 50 year anniversary of the French Polymer Group (Groupement Français des Polymères - GFP).

Conflicts of Interest: The authors declare no conflict of interest.

References

[1] Ashby MF, Bréchet YJM. Designing hybrid materials. Acta Mater 2003;51:5801-21.

[2] Saveleva MS, Eftekhari K, Abalymov A, Douglas TEL, Volodkin D, Parakhonskiy BV, Skirtach AG. Hierarchy of Hybrid Materials - The Place of Inorganics-in-Organics in it, Their Composition and Applications. Front Chem 2019;7:179-200.
[3] Judeinstein P, Sanchez C. Hybrid organic-inorganic materials: A land of multi-disciplinarity. J Mater Chem 1996;6:511-25.
[4] Bourgeat-Lami E, Lansalot M. Organic/Inorganic Composite Latexes: The Marriage of Emulsion Polymerization and Inorganic Chemistry. Adv Polym Sci 2010;233:53-123.
[5] Kickelbick G. Hybrid Materials – Past, Present and Future. Hybrid Materials 2014;1.
[6] Kumar SK, Benicewicz BC, Vaia RA, Winey KI. 50th Anniversary Perspective: Are Polymer Nanocomposites Practical for Applications? Macromolecules 2017;50:714-31.
[7] Kroker R, Schneider M, Hamann K. Polymer reactions on powder surfaces. Prog Org Coat 1972;1:23-44.
[8] Zhao B, Brittain WJ. Polymer brushes: surface-immobilized macromolecules. Prog Polym Sci 2000;25:677-710.
[9] Jenkins AD, Jones RG, Moad G. Terminology for reversible-deactivation radical polymerization previously called "controlled" radical or "living" radical polymerization (IUPAC Recommendations 2010). Pure Appl Chem 2009;82:483-91.
[10] Pyun J, Matyjaszewski K. Synthesis of nanocomposite organic/inorganic hybrid materials using controlled/"living" radical polymerization. Chem Mater 2001;13:3436-48.
[11] Advincula RC. Surface initiated polymerization from nanoparticle surfaces. J Disper Sci Technol 2003;24:343-61.
[12] Tsujii Y, Ohno K, Yamamoto S, Goto A, Fukuda T. Structure and properties of high-density polymer brushes prepared by surface-initiated living radical polymerization. In: Jordan R, editors. Surface-Initiated Polymerization I. Berlin: Springer, 2006. p. 1-45.
[13] Barbey R, Lavanant L, Paripovic D, Schuwer N, Sugnaux C, Tugulu S, Klok HA. Polymer Brushes via Surface-Initiated Controlled Radical Polymerization: Synthesis, Characterization, Properties, and Applications. Chem Rev 2009;109:5437-527.
[14] Wu L, Glebe U, Boker A. Surface-initiated controlled radical polymerizations from silica nanoparticles, gold nanocrystals, and bionanoparticles. Polym Chem 2015;6:5143-84.
[15] Zhang ZH, Zhang PC, Wang Y, Zhang WA. Recent advances in organic-inorganic well-defined hybrid polymers using controlled living radical polymerization techniques. Polym Chem 2016;7:3950-76.

[16] Zoppe JO, Ataman NC, Mocny P, Wang J, Moraes J, Klok HA. Surface-Initiated Controlled Radical Polymerization: State-of-the-Art, Opportunities, and Challenges in Surface and Interface Engineering with Polymer Brushes. Chem Rev 2017;117:1105-318.
[17] Mocny P, Klok HA. Complex polymer topologies and polymer-nanoparticle hybrid films prepared via surface-initiated controlled radical polymerization. Prog Polym Sci 2020;100:101185.
[18] Yan J, Bockstaller MR, Matyjaszewski K. Brush-modified materials: Control of molecular architecture, assembly behavior, properties and applications. Prog Polym Sci 2020;100:101180.
[19] Park S, Cho HY, Yoon JA, Kwak Y, Srinivasan A, Hollinger JO, Paik HJ, Matyjaszewski K. Photo-Cross-Linkable Thermoresponsive Star Polymers Designed for Control of Cell-Surface Interactions. Biomacromolecules 2010;11:2647-52.
[20] Murata H, Koepsel RR, Matyjaszewski K, Russell AJ. Permanent, non-leaching antibacterial surfaces - 2: How high density cationic surfaces kill bacterial cells. Biomaterials 2007;28:4870-79.
[21] Nicolas J, Guillaneuf Y, Lefay C, Bertin D, Gigmes D, Charleux B. Nitroxide-mediated polymerization. Prog Polym Sci 2013;38:63-235.
[22] Brinks MK, Studer A. Polymer Brushes by Nitroxide-Mediated Polymerization. Macromol Rapid Commun 2009;30:1043-57.
[23] Ghannam L, Parvole J, Laruelle G, Francois J, Billon L. Surface-initiated nitroxide-mediated polymerization: a tool for hybrid inorganic/organic nanocomposites 'in situ' synthesis. Polym Int 2006;55:1199-207.
[24] Phan TNT, Jestin J, Gigmes D. Nitroxide-Mediated Polymerization from Surfaces. Adv Polym Sci 2016;270:1-27.
[25] Jaquet B, Wei D, Reck B, Reinhold F, Zhang X, Wu H, Morbidelli M. Stabilization of polymer colloid dispersions with pH-sensitive poly-acrylic acid brushes. Colloid Polym Sci 2013;291:1659-67.
[26] Mocny P, Klok H-A. Tribology of surface-grafted polymer brushes. Mol Sys Des Eng 2016;1:141-54.
[27] Yang W, Zhou F. Polymer brushes for antibiofouling and lubrication. Biosurf Biotribol 2017;3:97-114.
[28] Penelas MJ, Contreras CB, Giussi JM, Wolosiuk A, Azzaroni O, Soler Illia GJAA. Controlling dispersion, stability and polymer content on PDEGMA-functionalized core-brush silica colloids. Colloids Surf A 2019;574:12-20.
[29] Carbonell C, Valles D, Wong AM, Carlini AS, Touve MA, Korpanty J, Gianneschi NC, Braunschweig AB. Polymer brush hypersurface photolithography. Nat Commun 2020;11:1244.
[30] Fromel M, Li M, Pester CW. Surface Engineering with Polymer Brush Photolithography. Macromol Rapid Commun 2020;41:e2000177.

[31] Gal N, Schroffenegger M, Reimhult E. Stealth Nanoparticles Grafted with Dense Polymer Brushes Display Adsorption of Serum Protein Investigated by Isothermal Titration Calorimetry. J Phys Chem B 2018;122:5820-34.
[32] Edmondson S, Osborne VL, Huck WT. Polymer brushes via surface-initiated polymerizations. Chem Soc Rev 2004;33:14-22.
[33] Rühe J. Polymer Brushes: On the Way to Tailor-Made Surfaces. In: Advincula RC, Brittain WJ, Rühe J, editors. Polymer Brushes. Hoboken: John Wiley & Sons, Inc., 2004. p. 1-31.
[34] Bourgeat-Lami E, Lang J. Encapsulation of inorganic particles by dispersion polymerization in polar media 2. Effect of silica size and concentration on the morphology of silica-polystyrene composite particles. J Colloid Interface Sci 1999;210:281-89.
[35] Krenkler KP, Laible R, Hamann K. Polyreactions on pigment surfaces. 7. Reactions of polymers with chlorosilane end groups on silicon dioxide surfaces Angew Makromol Chem 1976;53:101-23.
[36] Auroy P, Auvray L, Leger L. Silica particles stabilized by long grafted polymer chains - from electrostatic to steric repulsion J Colloid Interface Sci 1992;150:187-94.
[37] Revillon A, Leroux D. Functional silica supported polymer .5. 'Onto' versus 'from' grafting processes. React Funct Polym 1995;26:105-18.
[38] Luzinov I, Tsukruk VV. Ultrathin triblock copolymer films on tailored polymer brushes. Macromolecules 2002;35:5963-73.
[39] Koutsos V, van der Vegte EW, Grim PCM, Hadziioannou G. Isolated polymer chains via mixed self-assembled monolayers: Morphology and friction studied by scanning force microscopy. Macromolecules 1998;31:116-23.
[40] Penn LS, Hunter TF, Lee Y, Quirk RP. Grafting rates of amine-functionalized polystyrenes onto epoxidized silica surfaces. Macromolecules 2000;33:1105-07.
[41] Henze M, Madge D, Prucker O, Ruhe J. "Grafting Through": Mechanistic Aspects of Radical Polymerization Reactions with Surface-Attached Monomers. Macromolecules 2014;47:2929-37.
[42] Boven G, Oosterling M, Challa G, Schouten AJ. Grafting kinetics of poly(methyl methacrylate) on microparticulate silica. Polymer 1990;31:2377-83.
[43] Prucker O, Ruhe J. Mechanism of radical chain polymerizations initiated by azo compounds covalently bound to the surface of spherical particles. Macromolecules 1998;31:602-13.
[44] Velten U, Shelden RA, Caseri WR, Suter UW, Li YZ. Polymerization of styrene with peroxide initiator ionically bound to high surface area mica. Macromolecules 1999;32:3590-97.

[45] Jordan R, Ulman A, Kang JF, Rafailovich MH, Sokolov J. Surface-initiated anionic polymerization of styrene by means of self-assembled monolayers. J Am Chem Soc 1999;121:1016-22.
[46] Milner ST. Polymer Brushes. Science 1991;251:905.
[47] Kim M, Schmitt S, Choi J, Krutty J, Gopalan P. From Self-Assembled Monolayers to Coatings: Advances in the Synthesis and Nanobio Applications of Polymer Brushes. Polymers 2015;7:1346-78.
[48] Binder K, Milchev A. Polymer brushes on flat and curved surfaces: How computer simulations can help to test theories and to interpret experiments. J Polym Sci, Part B Polym Phys 2012;50:1515-55.
[49] Choi J, Dong H, Matyjaszewski K, Bockstaller MR. Flexible Particle Array Structures by Controlling Polymer Graft Architecture. J Am Chem Soc 2010;132:12537-39.
[50] Kim SA, Mangal R, Archer LA. Relaxation Dynamics of Nanoparticle-Tethered Polymer Chains. Macromolecules 2015;48:6280-93.
[51] Spange S. Silica surface modification by cationic polymerization and carbenium intermediates. Prog Polym Sci 2000;25:781-849.
[52] Advincula R, Zhou QG, Park M, Wang SG, Mays J, Sakellariou G, Pispas S, Hadjichristidis N. Polymer brushes by living anionic surface initiated polymerization on flat silicon (SiO(x)) and gold surfaces: Homopolymers and block copolymers. Langmuir 2002;18:8672-84.
[53] Advincula R. Polymer brushes by anionic and cationic Surface-Initiated Polymerization (SIP). editors. Surface-Initiated Polymerization I. Berlin: Springer, 2006. p. 107-36.
[54] Carrot G, Rutot-Houze D, Pottier A, Degee P, Hilborn J, Dubois P. Surface-initiated ring-opening polymerization: A versatile method for nanoparticle ordering. Macromolecules 2002;35:8400-04.
[55] Mingotaud AF, Reculusa S, Mingotaud C, Keller P, Sykes C, Duguet E, Ravaine S. Ring-opening metathesis polymerization on well defined silica nanoparticles leading to hybrid core-shell particles. J Mater Chem 2003;13:1920-25.
[56] Braunecker WA, Matyjaszewski K. Controlled/living radical polymerization: Features, developments, and perspectives. Prog Polym Sci 2007;32:93-146.
[57] Shipp DA. Reversible-Deactivation Radical Polymerizations. Polym Rev 2011;51:99-103.
[58] Moad G, Rizzardo E, Thang SH. Living Radical Polymerization by the RAFT Process – A Third Update. Aust J Chem 2012;65:985-1076.
[59] Destarac M. Industrial development of reversible-deactivation radical polymerization: is the induction period over? Polym Chem 2018;9:4947-67.

[60] Kreutzer J, Yagci Y. Metal Free Reversible-Deactivation Radical Polymerizations: Advances, Challenges, and Opportunities. Polymers 2018;10:35.
[61] Shanmugam S, Matyjaszewski K. Reversible Deactivation Radical Polymerization: State-of-the-Art in 2017. In: Matyjaszewski K, Gao H, Sumerlin BS, Tsarevsky NV, editors. Reversible Deactivation Radical Polymerization: Mechanisms and Synthetic Methodologies. ACS Symposium Series: American Chemical Society, 2018. p. 1-39.
[62] Gaynor SG, Wang J-S, Matyjaszewski K. Controlled Radical Polymerization by Degenerative Transfer: Effect of the Structure of the Transfer Agent. Macromolecules 1995;28:8051-56.
[63] Tsujii Y, Ejaz M, Sato K, Goto A, Fukuda T. Mechanism and kinetics of RAFT-mediated graft polymerization of styrene on a solid surface. 1. Experimental evidence of surface radical migration. Macromolecules 2001;34:8872-78.
[64] Baum M, Brittain WJ. Synthesis of polymer brushes on silicate substrates via reversible addition fragmentation chain transfer technique. Macromolecules 2002;35:610-15.
[65] Li C, Han J, Ryu CY, Benicewicz BC. A versatile method to prepare RAFT agent anchored substrates and the preparation of PMMA grafted nanoparticles. Macromolecules 2006;39:3175-83.
[66] Ranjan R, Brittain WJ. Synthesis of high density polymer brushes on nanoparticles by combined RAFT polymerization and click chemistry. Macromol Rapid Commun 2008;29:1104-10.
[67] Ohno K, Ma Y, Huang Y, Mori C, Yahata Y, Tsujii Y, Maschmeyer T, Moraes J, Perrier S. Surface-Initiated Reversible Addition–Fragmentation Chain Transfer (RAFT) Polymerization from Fine Particles Functionalized with Trithiocarbonates. Macromolecules 2011;44:8944-53.
[68] Zhao YL, Perrier S. Reversible Addition-Fragmentation Chain Transfer Polymerization from Surfaces. In: Vana P, editors. Controlled Radical Polymerization at and from Solid Surfaces. New York: Springer, 2016. p. 77-106.
[69] Banerjee S, Paira TK, Mandal TK. Surface confined atom transfer radical polymerization: access to custom library of polymer-based hybrid materials for speciality applications. Polym Chem 2014;5:4153-67.
[70] Hui CM, Pietrasik J, Schmitt M, Mahoney C, Choi J, Bockstaller MR, Matyjaszewski K. Surface-Initiated Polymerization as an Enabling Tool for Multifunctional (Nano-)Engineered Hybrid Materials. Chem Mater 2014;26:745-62.
[71] Khabibullin A, Mastan E, Matyjaszewski K, Zhu SP. Surface-Initiated Atom Transfer Radical Polymerization. In: Vana P, editors. Controlled Radical

Polymerization at and from Solid Surfaces. New York: Springer, 2016. p. 29-76.
[72] Moad G, Solomon D. The Chemistry of radical polymerization, 2nd Edition, Elsevier Ltd. editors. 2006. p.
[73] Beckwith ALJ, Bowry VW, Oleary M, Moad G, Rizzardo E, Solomon DH. Kinetic data for coupling of primary alkyl radicals with a stable nitroxide. J Chem Soc Chem Commun 1986;1003-04.
[74] Johnson CHJ, Moad G, Solomon DH, Spurling TH, Vearing DJ. The application of supercomputers in modeling chemical reaction kinetics: kinetic simulation of 'quasi-living' radical polymerization. Aust J Chem 1990;43:1215-30.
[75] Georges MK, Veregin RPN, Kazmaier PM, Hamer GK. Narrow molecular-weight resins by a free-radical polymerization process. Macromolecules 1993;26:2987-88.
[76] Grimaldi S, Finet JP, Le Moigne F, Zeghdaoui A, Tordo P, Benoit D, Fontanille M, Gnanou Y. Acyclic beta-phosphonylated nitroxides: A new series of counter-radicals for "living"/controlled free radical polymerization. Macromolecules 2000;33:1141-47.
[77] Benoit D, Grimaldi S, Robin S, Finet JP, Tordo P, Gnanou Y. Kinetics and mechanism of controlled free-radical polymerization of styrene and n-butyl acrylate in the presence of an acyclic beta-phosphonylated nitroxide. J Am Chem Soc 2000;122:5929-39.
[78] Benoit D, Chaplinski V, Braslau R, Hawker CJ. Development of a universal alkoxyamine for "living" free radical polymerizations. J Am Chem Soc 1999;121:3904-20.
[79] Maric M. Application of Nitroxide Mediated Polymerization in Different Monomer Systems. Curr Org Chem 2018;22:1264-84.
[80] Zaremski MY. Kinetic features of pseudoliving radical polymerization under conditions of reversible inhibition by nitroxide radicals. Polym Sci Ser C 2015;57:65-85.
[81] Bertin D, Gigmes D, Marque SRA, Tordo P. Kinetic subtleties of nitroxide mediated polymerization. Chem Soc Rev 2011;40:2189-98.
[82] Grubbs RB. Nitroxide-Mediated Radical Polymerization: Limitations and Versatility. Polym Rev 2011;51:104-37.
[83] Sciannamea V, Jerome R, Detrembleur C. In-situ nitroxide-mediated radical polymerization (NMP) processes: Their understanding and optimization. Chem Rev 2008;108:1104-26.
[84] Hawker CJ, Bosman AW, Harth E. New polymer synthesis by nitroxide mediated living radical polymerizations. Chem Rev 2001;101:3661-88.
[85] Guégain E, Guillaneuf Y, Nicolas J. Nitroxide-Mediated Polymerization of Methacrylic Esters: Insights and Solutions to a Long-Standing Problem. Macromol Rapid Commun 2015;36:1227-47.

[86] Charleux B, Nicolas J, Guerret O. Theoretical expression of the average activation-deactivation equilibrium constant in controlled/living free-radical copolymerization operating via reversible termination. Application to a strongly improved control in nitroxide-mediated polymerization of methyl methacrylate. Macromolecules 2005;38:5485-92.

[87] Nicolas J, Dire C, Mueller L, Belleney J, Charleux B, Marque SRA, Bertin D, Magnet S, Couvreur L. Living character of polymer chains prepared via nitroxide-mediated controlled free-radical polymerization of methyl methacrylate in the presence of a small amount of styrene at low temperature. Macromolecules 2006;39:8274-82.

[88] Qiao XG, Lansalot M, Bourgeat-Lami E, Charleux B. Nitroxide-Mediated Polymerization-Induced Self-Assembly of Poly(poly(ethylene oxide) methyl ether methacrylate-co-styrene)-b-poly(n-butyl methacrylate-co-styrene) Amphiphilic Block Copolymers. Macromolecules 2013;46:4285-95.

[89] Qiao XG, Zhou Z, Pang XC, Lansalot M, Bourgeat-Lami E. Nitroxide-mediated polymerization of methacrylates in the presence of 4-vinyl pyridine as controlling comonomer. Polymer 2019;172:330-38.

[90] Brusseau S, Belleney J, Magnet S, Couvreur L, Charleux B. Nitroxide-mediated copolymerization of methacrylic acid with sodium 4-styrene sulfonate: towards new water-soluble macroalkoxyamines for the synthesis of amphiphilic block copolymers and nanoparticles. Polym Chem 2010;1:720-9.

[91] Lessard BH, Ling EJY, Marić M. Fluorescent, Thermoresponsive Oligo(ethylene glycol) Methacrylate/9-(4-Vinylbenzyl)-9H-carbazole Copolymers Designed with Multiple LCSTs via Nitroxide Mediated Controlled Radical Polymerization. Macromolecules 2012;45:1879-91.

[92] Schmidt AC, Turgut H, Le D, Beloqui A, Delaittre G. Making the best of it: nitroxide-mediated polymerization of methacrylates via the copolymerization approach with functional styrenics. Polym Chem 2020;11:593-604.

[93] Guillaneuf Y, Gigmes D, Marque SRA, Astolfi P, Greci L, Tordo P, Bertin D. First Effective Nitroxide-Mediated Polymerization of Methyl Methacrylate. Macromolecules 2007;40:3108-14.

[94] Greene AC, Grubbs RB. Nitroxide-Mediated Polymerization of Methyl Methacrylate and Styrene with New Alkoxyamines from 4-Nitrophenyl 2-Methylpropionat-2-yl Radicals. Macromolecules 2010;43:10320-25.

[95] Astolfi P, Greci L, Stipa P, Rizzoli C, Ysacco C, Rollet M, Autissier L, Tardy A, Guillaneuf Y, Gigmes D. Indolinic nitroxides: evaluation of their potential as universal control agents for nitroxide mediated polymerization. Polym Chem 2013;4:3694-704.

[96] Ballard N, Aguirre M, Simula A, Agirre A, Leiza JR, Asua JM, van Es S. New Class of Alkoxyamines for Efficient Controlled Homopolymerization of Methacrylates. ACS Macro Lett 2016;5:1019-22.
[97] Simula A, Aguirre M, Ballard N, Veloso A, Leiza JR, van Es S, Asua JM. Novel alkoxyamines for the successful controlled polymerization of styrene and methacrylates. Polym Chem 2017;8:1728-36.
[98] Fischer H. The Persistent Radical Effect: A Principle for Selective Radical Reactions and Living Radical Polymerizations. Chem Rev 2001;101:3581-610.
[99] Husseman M, Malmstrom EE, McNamara M, Mate M, Mecerreyes D, Benoit DG, Hedrick JL, Mansky P, Huang E, Russell TP, Hawker CJ. Controlled synthesis of polymer brushes by "Living" free radical polymerization techniques. Macromolecules 1999;32:1424-31.
[100] Chevigny C, Gigmes D, Bertin D, Schweins R, Jestin J, Boué F. Controlled grafting of polystyrene on silicananoparticles using NMP: a new route without free initiator to tune the grafted chain length. Polym Chem 2011;2:567-71.
[101] Halperin A, Tirrell M, Lodge TP. Tethered chains in polymer microstructures Adv Polym Sci 1992;100:31-71.
[102] Wang JG, Mao GP, Ober CK, Kramer EJ. Liquid crystalline, semifluorinated side group block copolymers with stable low energy surfaces: Synthesis, liquid crystalline structure, and critical surface tension. Macromolecules 1997;30:1906-14.
[103] Chaki NK, Vijayamohanan K. Self-assembled monolayers as a tunable platform for biosensor applications. Biosens Bioelectron 2002;17:1-12.
[104] Lamping S, Buten C, Ravoo BJ. Functionalization and Patterning of Self-Assembled Monolayers and Polymer Brushes Using Microcontact Chemistry. Acc Chem Res 2019;52:1336-46.
[105] Mansky P, Liu Y, Huang E, Russell TP, Hawker CJ. Controlling polymer-surface interactions with random copolymer brushes. Science 1997;275:1458-60.
[106] Devaux C, Chapel JP, Beyou E, Chaumont P. Controlled structure and density of "living" polystyrene brushes on flat silica surfaces. Eur Phys J E 2002;7:345-52.
[107] Zhao B. Synthesis of binary mixed homopolymer brushes by combining atom transfer radical polymerization and nitroxide-mediated radical polymerization. Polymer 2003;44:4079-83.
[108] Zhao B, He T. Synthesis of Well-Defined Mixed Poly(methyl methacrylate)/Polystyrene Brushes from an Asymmetric Difunctional Initiator-Terminated Self-Assembled Monolayer. Macromolecules 2003;36:8599-602.
[109] Andruzzi L, Hexemer A, Li XF, Ober CK, Kramer EJ, Galli G, Chiellini E, Fischer DA. Control of surface properties using fluorinated polymer

brushes produced by surface-initiated controlled radical polymerization. Langmuir 2004;20:10498-506.
[110] Zhao B, Haasch RT, MacLaren S. Solvent-Induced Self-Assembly of Mixed Poly(methyl methacrylate)/Polystyrene Brushes on Planar Silica Substrates: Molecular Weight Effect. J Am Chem Soc 2004;126:6124-34.
[111] Zhao B, Haasch RT, MacLaren S. Self-reorganization of mixed poly(methyl methacrylate)/polystyrene brushes on planar silica substrates in response to combined selective solvent treatments and thermal annealing. Polymer 2004;45:7979-88.
[112] Devaux C, Cousin F, Beyou E, Chapel JP. Low swelling capacity of highly stretched polystyrene brushes. Macromolecules 2005;38:4296-300.
[113] Li J, Chen XR, Chang YC. Preparation of end-grafted polymer brushes by nitroxide-mediated free radical polymerization of vaporized vinyl monomers. Langmuir 2005;21:9562-67.
[114] Parvole J, Montfort JP, Reiter G, Borisov O, Billon L. Elastomer polymer brushes on flat surface by bimolecular surface-initiated nitroxide mediated polymerization. Polymer 2006;47:972-81.
[115] Lewis GT, Cohen Y. Controlled Nitroxide-Mediated Styrene Surface Graft Polymerization with Atmospheric Plasma Surface Activation. Langmuir 2008;24:13102-12.
[116] Ostaci RV, Celle C, Seytre G, Beyou E, Chapel JP, Drockenmuller E. Influence of nitroxide structure on polystyrene brushes "Grafted-from" silicon wafers. J Polym Sci Part A Polym Chem 2008;46:3367-74.
[117] Yang W, He X, Gao J, Guo H, He X, Wan F, Zhao X, Yu Y, Pei B. Synthesis, characterization, and tunable wettability of poly(ionic liquid) brushes via nitroxide-mediated radical polymerization (NMP). Chinese Sci Bull 2010;55:3562-68.
[118] Thiessen W, Wolff T. NMRP and ATRP Double Initiators for the Formation of Binary Polymer Brushes via Grafting-From Methods. Des Monomers Polym 2012;14:287-302.
[119] Zhou SK, Xu YJ, Fang SM. Controlled/Living Free Radical Polymerization of PS-b-P4-VP Brush Initiated from the Alkoxyamine-Functionalized Silicon Surface. Polym Plast Technol Eng 2012;51:1377-81.
[120] Long SJ, Wan F, Yang W, Guo H, He XY, Ren J, Gao JZ. Fabrication and characterization of tunable wettability surface on copper substrate by poly(ionic liquid) modification via surface-initiated nitroxide-mediated radical polymerization. J Appl Polym Sci 2013;128:2687-93.
[121] Thompson CV. Solid-State Dewetting of Thin Films. Annu Rev Mater Res 2012;42:399-434.
[122] Zhao B. A Combinatorial Approach to Study Solvent-Induced Self-Assembly of Mixed Poly(methyl methacrylate)/Polystyrene Brushes on

Planar Silica Substrates: Effect of Relative Grafting Density. Langmuir 2004;20:11748-55.
[123] Wang Y, Brittain WJ. Simultaneous Binary Mixed Homopolymer Brush Formation by Combining Nitroxide-Mediated Radical Polymerization and Living Cationic Ring-Opening Polymerization. Macromol Rapid Commun 2007;28:811-15.
[124] Weimer MW, Scherman OA, Sogah DY. Multifunctional Initiators Containing Orthogonal Sites. One-Pot, One-Step Block Copolymerization by Simultaneous Free Radical and Either Cationic Ring-Opening or Anionic Ring-Opening Polymerization. Macromolecules 1998;31:8425-28.
[125] Li M, Pester CW. Mixed Polymer Brushes for "Smart" Surfaces. Polymers 2020;12:1553.
[126] Yu Q, Ista LK, Gu R, Zauscher S, Lopez GP. Nanopatterned polymer brushes: conformation, fabrication and applications. Nanoscale 2016;8:680-700.
[127] Husemann M, Morrison M, Benoit D, Frommer KJ, Mate CM, Hinsberg WD, Hedrick JL, Hawker CJ. Manipulation of surface properties by patterning of covalently bound polymer brushes. J Am Chem Soc 2000;122:1844-45.
[128] Xu FJ, Song Y, Cheng ZP, Zhu XL, Zhu CX, Kang ET, Neoh KG. Controlled micropatterning of a Si(100) surface by combined nitroxide-mediated and atom transfer radical polymerizations. Macromolecules 2005;38:6254-58.
[129] Brinks MK, Hirtz M, Chi L, Fuchs H, Studer A. Site-selective surface-initiated polymerization by Langmuir-Blodgett lithography. Angew Chem Int Ed 2007;46:5231-33.
[130] Andruzzi L, Senaratne W, Hexemer A, Sheets ED, Ilic B, Kramer EJ, Baird B, Ober CK. Oligo(ethylene glycol) containing polymer brushes as bioselective surfaces. Langmuir 2005;21:2495-504.
[131] Hirtz M, Brinks MK, Miele S, Studer A, Fuchs H, Chi L. Structured polymer brushes by AFM lithography. Small 2009;5:919-23.
[132] Wagner H, Li Y, Hirtz M, Chi L, Fuchs H, Studer A. Site specific protein immobilization into structured polymer brushes prepared by AFM lithography. Soft Matter 2011;7:9854-58.
[133] Mardyukov A, Li Y, Dickschat A, Schafer AH, Studer A. Chemical Modification of Polymer Brushes via Nitroxide Photoclick Trapping. Langmuir 2013;29:6369-76.
[134] Roling O, Mardyukov A, Krings JA, Studer A, Ravoo BJ. Polymer Brushes Exhibiting Versatile Supramolecular Interactions Grown by Nitroxide-Mediated Polymerization and Structured via Microcontact Chemistry. Macromolecules 2014;47:2411-19.
[135] Buhl M, Tesch M, Lamping S, Moratz J, Studer A, Ravoo BJ. Preparation of Functional Alternating Polymer Brushes and Their Orthogonal Surface Modification through Microcontact Printing. Chem Eur J 2017;23:6042-47.

[136] Radhakrishnan B, Ranjan R, Brittain WJ. Surface initiated polymerizations from silica nanoparticles. Soft Matter 2006;2:386-96.
[137] Zou H, Wu S, Shen J. Polymer/Silica Nanocomposites: Preparation, Characterization, Properties, and Applications. Chem Rev 2008;108:3893-957.
[138] Parvole J, Billon L, Montfort JP. Formation of polyacrylate brushes on silica surfaces. Polym Int 2002;51:1111-16.
[139] Kasseh A, Ait-Kadi A, Riedl B, Pierson JF. Organic/inorganic hybrid composites prepared by polymerization compounding and controlled free radical polymerization. Polymer 2003;44:1367-75.
[140] Parvole J, Laruelle G, Guimon C, Francois J, Billon L. Initiator-Grafted Silica Particles for Controlled Free Radical Polymerization: Influence of the Initiator Structure on the Grafting Density. Macromol Rapid Commun 2003;24:1074-78.
[141] Parvole J, Montfort JP, Billon L. Formation of inorganic/organic nanocomposites by nitroxide-mediated polymerization in bulk using a bimolecular system. Macromol Chem Phys 2004;205:1369-78.
[142] Bartholome C, Beyou E, Bourgeat-Lami E, Chaumont P, Zydowicz N. Nitroxide-mediated polymerizations from silica nanoparticle surfaces: "Graft from" polymerization of styrene using a triethoxysilyl-terminated alkoxyamine initiator. Macromolecules 2003;36:7946-52.
[143] Laruelle G, Parvole J, Francois J, Billon L. Block copolymer grafted-silica particles: a core/double shell hybrid inorganic/organic material. Polymer 2004;45:5013-20.
[144] Bartholome C, Beyou E, Bourgeat-Lami E, Cassagnau P, Chaumont P, David L, Zydowicz N. Viscoelastic properties and morphological characterization of silica/polystyrene nanocomposites synthesized by nitroxide-mediated polymerization. Polymer 2005;46:9965-73.
[145] Bartholome C, Beyou E, Bourgeat-Lami E, Chaumont P, Zydowicz N. Nitroxide-mediated polymerization of styrene initiated from the surface of fumed silica. Comparison of two synthetic routes. Polymer 2005;46:8502-10.
[146] Parvole J, Laruelle G, Khoukh A, Billon L. Surface Initiated Polymerization of Poly(butyl acrylate) by Nitroxide Mediated Polymerization: First Comparative Polymerization of a Bimolecular and a Unimolecular Initiator-Grafted Silica Particles. Macromol Chem Phys 2005;206:372-82.
[147] Bartholome C, Beyou E, Bourgeat-Lami E, Chaumont P, Lefebvre F, Zydowicz N. Nitroxide-mediated polymerization of styrene initiated from the surface of silica nanoparticles. In situ generation and grafting of alkoxyamine initiators. Macromolecules 2005;38:1099-106.
[148] Inoubli R, Dagréou S, Khoukh A, Roby F, Peyrelasse J, Billon L. 'Graft from' polymerization on colloidal silica particles: elaboration of alkoxyamine

grafted surface by in situ trapping of carbon radicals. Polymer 2005;46:2486-96.
[149] Inoubli R, Dagréou S, Delville M-H, Lapp A, Peyrelasse J, Billon L. In situ thermo-dependant trapping of carbon radicals: a versatile route to well-defined polymer-grafted silica nanoparticles. Soft Matter 2007;3:1014-24.
[150] Chevigny C, Gigmes D, Bertin D, Jestin J, Boué F. Polystyrene grafting from silica nanoparticles via nitroxide-mediated polymerization (NMP): synthesis and SANS analysis with the contrast variation method. Soft Matter 2009;5:3741-53.
[151] Wang YP, Shen YJ, Pei XW, Zhang WJ, Wei YL, Yang C. In Situ Synthesis of Polystyrene/SiO2 Hybrid Composites via a 'Grafting Through' Strategy Based on Nitroxide-mediated Radical Polymerisation. Polym Polym Compos 2008;16:621-26.
[152] Wang YP, Shen YQ, Pei XW, Zhang SC, Liu HG, Ren JM. In situ synthesis of poly(styrene-co-maleic anhydride)/SiO2 hybrid composites via "grafting onto" strategy based on nitroxide-mediated radical polymerization. React Funct Polym 2008;68:1225-30.
[153] Yin QY, Charlot A, Portinha D, Beyou E. Nitroxide-mediated polymerization of pentafluorostyrene initiated by PS-DEPN through the surface of APTMS modified fumed silica: towards functional nanohybrids. RSC Adv 2016;6:58260-67.
[154] Li DJ, Sheng X, Zhao B. Environmentally responsive "Hairy" nanoparticles: Mixed homopolymer brushes on silica nanoparticles synthesized by living radical polymerization techniques. J Am Chem Soc 2005;127:6248-56.
[155] Zhao B, Zhu L. Nanoscale Phase Separation in Mixed Poly(tert-butyl acrylate)/Polystyrene Brushes on Silica Nanoparticles under Equilibrium Melt Conditions. J Am Chem Soc 2006;128:4574-75.
[156] Jiang XM, Zhao B, Zhong GJ, Jin NX, Horton JM, Zhu L, Hafner RS, Lodge TP. Microphase Separation of High Grafting Density Asymmetric Mixed Homopolymer Brushes on Silica Particles. Macromolecules 2010;43:8209-17.
[157] Jiang XM, Zhong GJ, Horton JM, Jin NX, Zhu L, Zhao B. Evolution of Phase Morphology of Mixed Poly(tert-butyl acrylate)/Polystyrene Brushes Grafted on Silica Particles with the Change of Chain Length Disparity. Macromolecules 2010;43:5387-95.
[158] Bao CH, Tang SD, Horton JM, Jiang XM, Tang P, Qiu F, Zhu L, Zhao B. Effect of Overall Grafting Density on Microphase Separation of Mixed Homopolymer Brushes Synthesized from Y-Initiator-Functionalized Silica Particles. Macromolecules 2012;45:8027-36.
[159] Horton JM, Tang SD, Bao CH, Tang P, Qiu F, Zhu L, Zhao B. Truncated Wedge-Shaped Nanostructures Formed from Lateral Microphase Separation of Mixed Homopolymer Brushes Grafted on 67 nm Silica Nanoparticles:

Evidence of the Effect of Substrate Curvature. ACS Macro Lett 2012;1:1061-65.
[160] Bao CH, Tang SD, Wright RAE, Tang P, Qiu F, Zhu L, Zhao B. Effect of Molecular Weight on Lateral Microphase Separation of Mixed Homopolymer Brushes Grafted on Silica Particles. Macromolecules 2014;47:6824-35.
[161] Li WK, Bao CH, Wright RAE, Zhao B. Synthesis of mixed poly(epsilon-caprolactone)/polystyrene brushes from Y-initiator-functionalized silica particles by surface-initiated ring-opening polymerization and nitroxide-mediated radical polymerization. RSC Adv 2014;4:18772-81.
[162] Tang S, Lo T-Y, Horton JM, Bao C, Tang P, Qiu F, Ho R-M, Zhao B, Zhu L. Direct Visualization of Three-Dimensional Morphology in Hierarchically Self-Assembled Mixed Poly(tert-butyl acrylate)/Polystyrene Brush-Grafted Silica Nanoparticles. Macromolecules 2013;46:6575-84.
[163] Zhu L, Zhao B. Transmission Electron Microscopy Study of Solvent-Induced Phase Morphologies of Environmentally Responsive Mixed Homopolymer Brushes on Silica Particles. J Phys Chem B 2008;112:11529-36.
[164] Fox TL, Tang S, Horton JM, Holdaway HA, Zhao B, Zhu L, Stewart PL. In Situ Characterization of Binary Mixed Polymer Brush-Grafted Silica Nanoparticles in Aqueous and Organic Solvents by Cryo-Electron Tomography. Langmuir 2015;31:8680-8.
[165] Tang S, Fox TL, Lo TY, Horton JM, Ho RM, Zhao B, Stewart PL, Zhu L. Environmentally responsive self-assembly of mixed poly(tert-butyl acrylate)-polystyrene brush-grafted silica nanoparticles in selective polymer matrices. Soft Matter 2015;11:5501-12.
[166] Wichaita W, Polpanich D, Tangboriboonrat P. Review on Synthesis of Colloidal Hollow Particles and Their Applications. Ind Eng Chem Res 2019;58:20880-901.
[167] Bourgeat-Lami E. Hollow particles: Synthetic pathways and potential applications. In: A E, editors. Colloidal Polymers: Synthesis and Characterization Surfactant Science Series Vol 115. New York: Marcel Dekker, Inc., 2003. p.
[168] Blomberg S, Ostberg S, Harth E, Bosman AW, Van Horn B, Hawker CJ. Production of crosslinked, hollow nanoparticles by surface-initiated living free-radical polymerization. J Polym Sci Part A Polym Chem 2002;40:1309-20.
[169] Ladmiral V, Morinaga T, Ohno K, Fukuda T, Tsujii Y. Synthesis of monodisperse zinc sulfide particles grafted with concentrated polystyrene brush by surface-initiated nitroxide-mediated polymerization. Eur Polym J 2009;45:2788-96.

[170] Lenarda M, Chessa G, Moretti E, Polizzi S, Storaro L, Talon A. Toward the preparation of a nanocomposite material through surface initiated controlled/"living" radical polymerization of styrene inside the channels of MCM-41 silica. J Mater Sci 2006;41:6305-12.
[171] Blas H, Save M, Boissiere C, Sanchez C, Charleux B. Surface-Initiated Nitroxide-Mediated Polymerization from Ordered Mesoporous Silica. Macromolecules 2011;44:2577-88.
[172] Kumar SK, Krishnamoorti R. Nanocomposites: structure, phase behavior, and properties. Annu Rev Chem Biomol Eng 2010;1:37-58.
[173] Choi J, Hui CM, Schmitt M, Pietrasik J, Margel S, Matyjazsewski K, Bockstaller MR. Effect of Polymer-Graft Modification on the Order Formation in Particle Assembly Structures. Langmuir 2013;29:6452-59.
[174] Midya J, Cang Y, Egorov SA, Matyjaszewski K, Bockstaller MR, Nikoubashman A, Fytas G. Disentangling the Role of Chain Conformation on the Mechanics of Polymer Tethered Particle Materials. Nano Lett 2019;19:2715-22.
[175] Ohno K, Morinaga T, Takeno S, Tsujii Y, Fukuda T. Suspensions of Silica Particles Grafted with Concentrated Polymer Brush: Effects of Graft Chain Length on Brush Layer Thickness and Colloidal Crystallization. Macromolecules 2007;40:9143-50.
[176] Dukes D, Li Y, Lewis S, Benicewicz B, Schadler L, Kumar SK. Conformational Transitions of Spherical Polymer Brushes: Synthesis, Characterization, and Theory. Macromolecules 2010;43:1564-70.
[177] Kumar SK, Jouault N, Benicewicz B, Neely T. Nanocomposites with Polymer Grafted Nanoparticles. Macromolecules 2013;46:3199-214.
[178] Song Y, Zheng Q. Linear rheology of nanofilled polymers. J Rheol 2015;59:155-91.
[179] Choi J, Hui CM, Pietrasik J, Dong H, Matyjaszewski K, Bockstaller MR. Toughening fragile matter: mechanical properties of particle solids assembled from polymer-grafted hybrid particles synthesized by ATRP. Soft Matter 2012;8:4072-82.
[180] Fernandes NJ, Koerner H, Giannelis EP, Vaia RA. Hairy nanoparticle assemblies as one-component functional polymer nanocomposites: opportunities and challenges. MRS Commun 2013;3:13-29.
[181] Song Y, Zheng Q. Concepts and conflicts in nanoparticles reinforcement to polymers beyond hydrodynamics. Prog Mater Sci 2016;84:1-58.
[182] Goel V, Pietrasik J, Dong H, Sharma J, Matyjaszewski K, Krishnamoorti R. Structure of Polymer Tethered Highly Grafted Nanoparticles. Macromolecules 2011;44:8129-35.
[183] Cassagnau P. Melt rheology of organoclay and fumed silica nanocomposites. Polymer 2008;49:2183-96.

[184] Inoubli R, Dagréou S, Lapp A, Billon L, Peyrelasse J. Nanostructure and Mechanical Properties of Polybutylacrylate Filled with Grafted Silica Particles. Langmuir 2006;22:6683-89.
[185] Chen Q, Gong S, Moll J, Zhao D, Kumar SK, Colby RH. Mechanical Reinforcement of Polymer Nanocomposites from Percolation of a Nanoparticle Network. ACS Macro Lett 2015;4:398-402.
[186] Chevigny C, Jouault N, Dalmas F, Boué F, Jestin J. Tuning the mechanical properties in model nanocomposites: Influence of the polymer-filler interfacial interactions. J Polym Sci B Polym Phys 2011;49:781-91.
[187] Chevigny C, Dalmas F, Di Cola E, Gigmes D, Bertin D, Boué Fo, Jestin J. Polymer-Grafted-Nanoparticles Nanocomposites: Dispersion, Grafted Chain Conformation, and Rheological Behavior. Macromolecules 2011;44:122-33.
[188] Shen J, Liu J, Gao Y, Cao D, Zhang L. Revisiting the Dispersion Mechanism of Grafted Nanoparticles in Polymer Matrix: A Detailed Molecular Dynamics Simulation. Langmuir 2011;27:15213-22.
[189] Du J, Chen Y, Zhang Y, Han CC, Fischer K, Schmidt M. Organic/Inorganic Hybrid Vesicles Based on A Reactive Block Copolymer. J Am Chem Soc 2003;125:14710-11.
[190] Du J, Chen Y. Atom-Transfer Radical Polymerization of a Reactive Monomer: 3-(Trimethoxysilyl)propyl Methacrylate. Macromolecules 2004;37:6322-28.
[191] Mellon W, Rinaldi D, Bourgeat-Lami E, D'Agosto F. Block copolymers of gamma-methacryloxypropyltrimethoxysilane and methyl methacrylate by RAFT polymerization. A new class of polymeric precursors for the sol-gel process. Macromolecules 2005;38:1591-98.
[192] Chang C, Wei H, Feng J, Wang Z-C, Wu X-J, Wu D-Q, Cheng S-X, Zhang X-Z, Zhuo R-X. Temperature and pH Double Responsive Hybrid Cross-Linked Micelles Based on P(NIPAAm-co-MPMA)-b-P(DEA): RAFT Synthesis and "Schizophrenic" Micellization. Macromolecules 2009;42:4838-44.
[193] Chung JJ, Jones JR, Georgiou TK. Toward Hybrid Materials: Group Transfer Polymerization of 3-(Trimethoxysilyl)propyl Methacrylate. Macromol Rapid Commun 2015;36:1806-9.
[194] Teo GH, Zetterlund PB, Thickett SC. Interfacial crosslinking of self-assembled triblock copolymer nanoparticles via alkoxysilane hydrolysis and condensation. J Polym Sci Part A Polym Chem 2018;57:1897-907.
[195] Kickelbick G. Concepts for the incorporation of inorganic building blocks into organic polymers on a nanoscale. Prog Polym Sci 2003;28:83-114.
[196] Czarnecki S, Bertin A. Hybrid Silicon-Based Organic/Inorganic Block Copolymers with Sol-Gel Active Moieties: Synthetic Advances,

Self-Assembly and Applications in Biomedicine and Materials Science. Chem Eur J 2018;24:3354-73.

[197] Gamys CG, Beyou E, Bourgeat-Lami E. Micellar Behavior of Well-Defined Polystyrene-Based Block Copolymers with Triethoxysilyl Reactive Groups and Their Hydrolysis-Condensation. J Polym Sci Part A Polym Chem 2010;48:784-93.

[198] Gamys CG, Beyou E, Bourgeat-Lami E, Alcouffe P, David L. Nanostructured Organic-Inorganic Hybrid Films Prepared by the Sol-Gel Method from Self-Assemblies of PS-b-PAPTES-b-PS Triblock Copolymers. J Polym Sci Part A Polym Chem 2011;49:4193-203.

[199] Gamys CG, Beyou E, Bourgeat-Lami E, David L, Oberdisse J. SAXS and SANS characterization of gelable polystyrene-b-poly(acryloxy propyl triethoxysilane) (PS-b-PAPTES) diblock copolymer micelles before and after hydrolysis-condensation. Soft Matter 2012;8:6564-72.

[200] Gamys CG, Beyou E, Bourgeat-Lami E, David L, Alcouffe P. Tunable Morphologies From Bulk Self-Assemblies of Poly(acryloxypropyl triethoxysilane)-b-poly (styrene)-b poly (acryloxypropyl triethoxysilane) Triblock Copolymers. Macromol Chem Phys 2012;213:10-18.

[201] Kobayashi M, Matsuno R, Otsuka H, Takahara A. Precise surface structure control of inorganic solid and metal oxide nanoparticles through surface-initiated radical polymerization. Sci Technol Adv Mat 2006;7:617-28.

[202] Matsuno R, Otsuka H, Takahara A. Polystyrene-grafted titanium oxide nanoparticles prepared through surface-initiated nitroxide-mediated radical polymerization and their application to polymer hybrid thin films. Soft Matter 2006;2:415-21.

[203] Jaymand M. Synthesis and characterization of novel type poly (4-chloromethyl styrene-grft-4-vinylpyridine)/TiO2 nanocomposite via nitroxide-mediated radical polymerization. Polymer 2011;52:4760-69.

[204] Abbasian M, Aali NK. Nitroxide-Mediated Radical Polymerization of Styrene Initiated from the Surface of Titanium Oxide Nanoparticles. J Nanostruct 2016;6:38-45.

[205] Flesch C, Unterfinger Y, Bourgeat-Lami E, Duguet E, Delaite C, Dumas P. Poly(ethylene glycol) surface coated magnetic particles. Macromol Rapid Commun 2005;26:1494-98.

[206] Li K, Dugas P-Y, Bourgeat-Lami E, Lansalot M. Polymer-encapsulated γ-Fe2O3 nanoparticles prepared via RAFT-mediated emulsion polymerization. Polymer 2016;106:249-60.

[207] Guimarães TR, Lansalot M, Bourgeat-Lami E. Synthesis of double-responsive magnetic latex particles via seeded emulsion polymerization using macroRAFT block copolymers as stabilizers. Polym Chem 2020;11:648-52.

[208] Guimaraes TR, Lansalot M, Bourgeat-Lami E. Polymer-encapsulation of iron oxide clusters using macroRAFT block copolymers as stabilizers: tuning of the particle morphology and surface functionalization. J Mater Chem B 2020;8:4917-29.
[209] Matsuno R, Yamamoto K, Otsuka H, Takahara A. Polystyrene-Grafted Magnetite Nanoparticles Prepared through Surface-Initiated Nitroxyl-Mediated Radical Polymerization. Chem Mater 2003;15:3-5.
[210] Matsuno R, Yamamoto K, Otsuka H, Takahara A. Polystyrene- and poly(3-vinylpyridine)-grafted magnetite nanoparticles prepared through surface-initiated nitroxide-mediated radical polymerization. Macromolecules 2004;37:2203-09.
[211] Binder WH, Gloger D, Weinstabl H, Allmaier G, Pittenauer E. Telechelic poly(N-isopropylacrylamides) via nitroxide-mediated controlled polymerization and "click" chemistry: Livingness and "grafting-from" methodology. Macromolecules 2007;40:3097-107.
[212] Robbes A-S, Cousin F, Meneau F, Chevigny C, Gigmes D, Fresnais J, Schweins R, Jestin J. Controlled grafted brushes of polystyrene on magnetic γ-Fe2O3 nanoparticles via nitroxide-mediated polymerization. Soft Matter 2012;8:3407-18.
[213] Chen ZJ, Yang QX, Peng K, Guo YB. Surface-Initiated Nitroxide-Mediated Radical Polymerization of 4-Vinylpyridine on Magnetite Nanoparticles. J Appl Polym Sci 2011;119:3582-90.
[214] Chen F, Cai ZW, Huang Y, Luo WQ, Chen JC. Synthesis and characterization of copolymer grafted magnetic nanoparticles via surface-initiated nitroxide-mediated radical polymerization. Polym Eng Sci 2013;53:956-62.
[215] Ignatova M, Voccia S, Gilbert B, Markova N, Mercuri PS, Galleni M, Sciannamea V, Lenoir S, Cossement D, Gouttebaron R, Jerome R, Jerome C. Synthesis of copolymer brushes endowed with adhesion to stainless steel surfaces and antibacterial properties by controlled nitroxide-mediated radical polymerization. Langmuir 2004;20:10718-26.
[216] Borisova OV, Billon L, Richter RP, Reimhult E, Borisov OV. pH- and Electro-Responsive Properties of Poly(acrylic acid) and Poly(acrylic acid)-block-poly(acrylic acid-grad-styrene) Brushes Studied by Quartz Crystal Microbalance with Dissipation Monitoring. Langmuir 2015;31:7684-94.
[217] Guselnikova O, Marque SRA, Tretyakov EV, Mares D, Jerabek V, Audran G, Joly JP, Trusova M, Svorcik V, Lyutakov O, Postnikov P. Unprecedented plasmon-induced nitroxide-mediated polymerization (PI-NMP): a method for preparation of functional surfaces. J Mater Chem 2019;7:12414-19.

[218] Zawada K, Tomaszewski W, Megiel E. A smart synthesis of gold/polystyrene core-shell nanohybrids using TEMPO coated nanoparticles. RSC Adv 2014;4:23876-85.
[219] Krystosiak P, Tomaszewski W, Megiel E. High-density polystyrene-grafted silver nanoparticles and their use in the preparation of nanocomposites with antibacterial properties. J Colloid Interface Sci 2017;498:9-21.
[220] Sill K, Emrick T. Nitroxide-Mediated Radical Polymerization from CdSe Nanoparticles. Chem Mater 2004;16:1240-43.
[221] Ievins AD, Wang XF, Moughton AO, Skey J, O'Reilly RK. Synthesis of core functionalized polymer micelles and shell cross-linked nanoparticles. Macromolecules 2008;41:2998-3006.
[222] Moughton AO, O'Reilly RK. Noncovalently connected micelles, nanoparticles, and metal-functionalized nanocages using supramolecular self-assembly. J Am Chem Soc 2008;130:8714-25.
[223] Mugemana C, Joset A, Guillet P, Appavou M-S, De Souza N, Fustin C-A, Leyh B, Gohy J-F. Structure of Metallo-Supramolecular Micellar Gels. Macromol Chem Phys 2013;214:1699-709.
[224] Zhang W, Camino G, Yang R. Polymer/polyhedral oligomeric silsesquioxane (POSS) nanocomposites: An overview of fire retardance. Prog Polym Sci 2017;67:77-125.
[225] Chen F, Lin F, Zhang Q, Cai R, Wu Y, Ma X. Polyhedral Oligomeric Silsesquioxane Hybrid Polymers: Well-Defined Architectural Design and Potential Functional Applications. Macromol Rapid Commun 2019;40:1900101.
[226] Dong F, Lu L, Ha CS. Silsesquioxane-Containing Hybrid Nanomaterials: Fascinating Platforms for Advanced Applications. Macromol Chem Phys 2019;220:1800324-45.
[227] Wang M, Chi H, K SJ, Wang F. Progress in the Synthesis of Bifunctionalized Polyhedral Oligomeric Silsesquioxane. Polymers 2019;11:2098-118.
[228] Zhou H, Chua MH, Xu J. 6 - Functionalized POSS-Based Hybrid Composites. In: Pielichowski K, Majka TM, editors. Polymer Composites with Functionalized Nanoparticles. Amsterdam: Elsevier, Ltd., 2019. p.
[229] Hussain H, Shah SM. Recent developments in nanostructured polyhedral oligomeric silsesquioxane-based materials via 'controlled' radical polymerization. Polym Int 2014;63:835-47.
[230] Miyamoto K, Hosaka N, Otsuka H, Takahara A. Stabilization of Polystyrene Thin Films against Dewetting by Silsesquioxane-terminated Polystyrene Additives. Chem Lett 2006;35:1098-99.
[231] Miyamoto K, Hosaka N, Kobayashi M, Otsuka H, Yamada N, Torikai N, Takahara A. Dewetting Inhibition and Interfacial Structures of Silsesquioxane-terminated Polystyrene Thin Films. Polym J 2007;39:1247-52.

[232] Sinirlioglu D, Muftuoglu AE. Synthesis of an Inorganic–Organic Hybrid Material Based on Polyhedral Oligomeric Silsesquioxane and Polystyrene via Nitroxide-Mediated Polymerization and Click Reactions. Des Monomers Polym 2012;14:273-86.
[233] Lu C-H, Wang J-H, Chang F-C, Kuo S-W. Star Block Copolymers Through Nitroxide-Mediated Radical Polymerization From Polyhedral Oligomeric Silsesquioxane (POSS) Core. Macromol Chem Phys 2010;211:1339-47.
[234] Chiu CW, Huang TK, Wang YC, Alamani BG, Lin JJ. Intercalation strategies in clay/polymer hybrids. Prog Polym Sci 2014;39:443-85.
[235] Weimer MW, Chen H, Giannelis EP, Sogah DY. Direct synthesis of dispersed nanocomposites by in situ living free radical polymerization using a silicate-anchored initiator. J Am Chem Soc 1999;121:1615-16.
[236] Di JB, Sogah DY. Exfoliated block copolymer/silicate nanocomposites by one-pot, one-step in-situ living polymerization from silicate-anchored multifunctional initiator. Macromolecules 2006;39:5052-57.
[237] Xu L, Reeder S, Thopasridharan M, Ren J, Shipp DA, Krishnamoorti R. Structure and melt rheology of polystyrene-based layered silicate nanocomposites. Nanotechnology 2005;16:S514-21.
[238] Konn C, Morel F, Beyou E, Chaumont P, Bourgeat-Lami E. Nitroxide-mediated polymerization of styrene initiated from the surface of laponite clay platelets. Macromolecules 2007;40:7464-72.
[239] Mittal V. Polymer chains grafted "to" and "from" layered silicate clay platelets. J Colloid Interface Sci 2007;314:141-51.
[240] Muhlebach A, Nesvadba P, Rime F, Bugnon L. Exfoliation of Sheet Silicates by Nitroxide Mediated Polymerization. Chimia 2008;62:799-804.
[241] Jaymand M. Synthesis and characterization of an exfoliated modified syndiotactic polystyrene/Mg–Al-layered double-hydroxide nanocomposite. Polym J 2010;43:186-93.
[242] Shen Y, Wang Y, Chen J, Li H, Li Z, Li C. Nitroxide-mediated polymerization of styrene initiated from the surface of montmorillonite clay platelets. J Appl Polym Sci 2010;118:1198-203.
[243] Cherifi N, BenAboura A, Save M, Billon L. Filler effect on properties of "All-Acrylic" copolymer/clay elastomeric materials synthesized by "in situ" nitroxide mediated polymerization. J Polym Sci Part A Polym Chem 2012;50:3976-85.
[244] Cherifi N, BenAboura A, Save M, Billon L. Acrylic Diblock Copolymers/Clay Nanocomposites Via In Situ Nitroxide Mediated Polymerization. Macromol Chem Phys 2015;216:1462-71.
[245] Abbasian M, Mahi R. In-situ synthesis of polymer - silica nanocomposites by living radical polymerisation using TEMPO initiator. J Exp Nanosci 2014;9:785-98.

[246] Ghannam L, Bacou M, Garay H, Shanahan MER, Francois J, Billon L. Elastomer monolayers adsorbed on mica surfaces by nitroxide-mediated polymerisation. Polymer 2004;45:7035-45.
[247] Ghannam L, Garay H, Shanahan MER, Francois J, Billon L. A new pigment type: Colored diblock copolymer-mica composites. Chem Mater 2005;17:3837-43.
[248] Ghannam L, Garay H, Billon L. Sensitive Colored Hybrid Inorganic/Organic Pigments Based on Polymer-Coated Microsized Particles. Macromolecules 2008;41:7374-82.
[249] Leone G, Giovanella U, Bertini F, Hoseinkhani S, Porzio W, Ricci G, Botta C, Galeotti F. Hierarchically structured, blue-emitting polymer hybrids through surface-initiated nitroxide-mediated polymerization and water templated assembly. J Mater Chem C 2013;1:6585-93.
[250] Leone G, Giovanella U, Bertini F, Porzio W, Meinardi F, Botta C, Ricci G. Poly(styrene)-graft-/rhodamine 6G-fluoromica hybrids: synthesis, characterization and photophysical properties. J Mater Chem C 2013;1:1450-60.
[251] Joubert M, Khoukh A, Tranchant J-F, Morvan F, Billon L. Hybrid Aluminum Colored Pigments Based on Gradient Copolymers Design. Macromol Chem Phys 2009;210:1544-55.
[252] Thickett SC, Teo GH. Recent advances in colloidal nanocomposite design via heterogeneous polymerization techniques. Polym Chem 2019;10:2906-24.
[253] Zetterlund PB, Thickett SC, Perrier S, Lansalot M, Bourgeat-Lami E. Controlled/Living Radical Polymerization in Dispersed Systems: An Update. Chem Rev 2015;115:9745-800.
[254] Penfold NJW, Yeow J, Boyer C, Armes SP. Emerging Trends in Polymerization-Induced Self-Assembly. ACS Macro Lett 2019;8:1029-54.
[255] Cenacchi-Pereira A, Grant E, D'Agosto F, Lansalot M, Bourgeat-Lami E. Encapsulation with the Use of Controlled Radical Polymerization. In: Kobayashi S, Müllen K, editors. Encyclopedia of Polymeric Nanomaterials. Berlin: Springer, 2015. p. 718-729.
[256] Bourgeat-Lami E, D'Agosto F, Lansalot M. Synthesis of Nanocapsules and Polymer/Inorganic Nanoparticles Through Controlled Radical Polymerization At and Near Interfaces in Heterogeneous Media. Adv Polym Sci 2016;270:123-61.
[257] Bailly B, Donnenwirth AC, Bartholome C, Beyou E, Bourgeat-Lami E. Silica-polystyrene nanocomposite particles synthesized by nitroxide-mediated polymerization and their encapsulation through miniemulsion polymerization. J Nanomater 2006;2006:076371.
[258] Micusik M, Bonnefond A, Paulis M, Leiza JR. Synthesis of waterborne acrylic/clay nanocomposites by controlled surface initiation from macroinitiator modified montmorillonite. Eur Polym J 2012;48:896-905.

[259] Diaconu G, Micusik M, Bonnefond A, Paulis M, Leiza JR. Macroinitiator and Macromonomer Modified Montmorillonite for the Synthesis of Acrylic/MMT Nanocomposite Latexes. Macromolecules 2009;42:3316-25.
[260] Nguyen D, Zondanos HS, Farrugia JM, Serelis AK, Such CH, Hawkett BS. Pigment Encapsulation by Emulsion Polymerization Using Macro-RAFT Copolymers. Langmuir 2008;24:2140-50.
[261] Zgheib N, Putaux J-L, Thill A, Bourgeat-Lami E, D'Agosto F, Lansalot M. Cerium oxide encapsulation by emulsion polymerization using hydrophilic macroRAFT agents. Polym Chem 2013;4:607-14.
[262] Rodrigues Guimaraes T, de Camargo Chaparro T, D'Agosto F, Lansalot M, Martins Dos Santos A, Bourgeat-Lami E. Synthesis of multi-hollow clay-armored latexes by surfactant-free emulsion polymerization of styrene mediated by poly(ethylene oxide)-based macroRAFT/Laponite complexes. Polym Chem 2014;5:6611-22.
[263] Bourgeat-Lami E, França AJPG, Chaparro TC, Silva RD, Dugas PY, Alves GM, Santos AM. Synthesis of Polymer/Silica Hybrid Latexes by Surfactant-Free RAFT-Mediated Emulsion Polymerization. Macromolecules 2016;49:4431-40.
[264] Cenacchi A, Pearson S, Kostadinova D, Leroux F, D'Agosto F, Lansalot M, Bourgeat-Lami E, Prevot V. Nanocomposite latexes containing layered double hydroxides via RAFT-assisted encapsulating emulsion polymerization. Polym Chem 2017;8:1233-43.
[265] Pearson S, Pavlovic M, Augé T, Torregrossa V, Szilagyi I, D'Agosto F, Lansalot M, Bourgeat-Lami E, Prévot V. Controlling the Morphology of Film-Forming, Nanocomposite Latexes Containing Layered Double Hydroxide by RAFT-Mediated Emulsion Polymerization. Macromolecules 2018;51:3953-66.
[266] Silva RD, Chaparro TdC, Monteiro IS, Dugas P-Y, D'Agosto F, Lansalot M, Martins dos Santos A, Bourgeat-Lami E. Tailoring the Morphology of Polymer/Montmorillonite Hybrid Latexes by Surfactant-Free Emulsion Polymerization Mediated by Amphipathic MacroRAFT Agents. Macromolecules 2019;52:4979-88.
[267] Chaparro TC, Silva RD, Dugas P-Y, D'Agosto F, Lansalot M, Martins dos Santos A, Bourgeat-Lami E. Laponite®-based colloidal nanocomposites prepared by RAFT-mediated surfactant-free emulsion polymerization: the role of non-ionic and anionic macroRAFT polymers in stability and morphology control. Polym Chem 2021;12:69-81.
[268] Qiao XG, Dugas PY, Charleux B, Lansalot M, Bourgeat-Lami E. Synthesis of Multipod-like Silica/Polymer Latex Particles via Nitroxide-Mediated Polymerization-Induced Self-Assembly of Amphiphilic Block Copolymers. Macromolecules 2015;48:545-56.

[269] Qiao XG, Dugas PY, Charleux B, Lansalot M, Bourgeat-Lami E. Nitroxide-mediated polymerization-induced self-assembly of amphiphilic block copolymers with a pH/temperature dual sensitive stabilizer block. Polym Chem 2017;8:4014-29.

[270] Qiao XG, Lambert O, Taveau JC, Dugas PY, Charleux B, Lansalot M, Bourgeat-Lami E. Nitroxide-Mediated Polymerization-Induced Self-Assembly of Block Copolymers at the Surface of Silica Particles: Toward New Hybrid Morphologies. Macromolecules 2017;50:3797-807.